OCEANOGRAPHIC AND ENGINEERING ANALYSIS OF SEAWATER AIR-CONDITIONING SYSTEM FEASIBILITY FOR THE BLACK SEA

by

Margarita Pozhidaeva

Ed.S., Industrial and Civil Engineering, Moscow State University of Civil Engineering, 2013

Submitted to the Institute for Graduate Studies in
Science and Engineering in partial fulfillment of
the requirements for the degree of
Master of Science

Graduate Program in Civil Engineering
Boğaziçi University
2017

ABSTRACT

OCEANOGRAPHIC AND ENGINEERING ANALYSIS OF SEAWATER AIR-CONDITIONING SYSTEM FEASIBILITY FOR THE BLACK SEA

Conventional air-conditioning systems constitute a large portion of the building energy consumption and operating cost. To reduce the carbon footprint of the air cooling system in buildings, cost and energy efficient technologies based on renewable energy are needed. Naturally-occurred cold seawater can serve as a working fluid in the seawater air-conditioning (SWAC) system by absorbing the heat from the building and transferring it to the ocean. SWAC technology is widely used in the world, however, it still has not been applied at the Black Sea coast.

The Black Sea has a unique layered water structure with year-round cold seawater available at relatively shallow depths. Low seawater temperatures in the cold intermediate layer of the Black Sea are suitable for effective use of SWAC in coastal communities. The relatively high initial cost of SWAC can be offset by large electricity savings. Cost-benefit analysis of a SWAC system based on a hybrid seawater-cooled chiller for a university campus at the Black Sea coast of Istanbul shows that SWAC is 60% more efficient than conventional air-conditioning systems.

ÖZET

DENİZ SUYU İKLİMLENDİRME SİSTEM FİZİBİLİTESİNİN KARADENİZ İÇİN OŞİNOGRAFİK VE MÜHENDİSLİK ANALİZİ

Binaların toplam işletim maliyetinin büyük bir kısmı geleneksel iklimlendirme sistemlerinden kaynaklanmaktadır. Bu da daha verimli, yenilenebilir ve daha az karbon ayak izi bırakan enerji teknolojilerinin araştırılmasına ve uygulanmasına olan ihtiyacı arttırmakdır. Deniz suyu iklimlendirme sistemi (DSİS) doğal ortamında yeterli sıcaklıkta olan deniz suyunu bina iklimlendirme sisteminde ısı transferi aracı akışkanı olarak kullanan bir yenilenebilir enerji teknolojisidir. Dünyada yaygın olarak kullanılmasına rağmen Karadeniz kıyılarında henüz uygulaması bulunmamaktadır.

Karadeniz'in katmanlı su yapısı ve yıl boyunca sığ derinliklerdeki düşük su sıcaklığı, deniz suyu soğutma sistemlerinin verimli bir şekilde bölgede uygulanmasına imkan vermektedir. DSİS'nin yüksek kuruluş maliyeti elektrik enerjisi tasarrufuyla dengelenmektedir. İstanbul'un Karadeniz kıyısındaki bir üniversite kampüsünde kurulacak bir DSİS geleneksel soğutma sistemlerine göre %60 daha ekonomik bir çözüm sunmaktadır.

TABLE OF CONTENTS

LIST OF FIGURES

LIST OF TABLES

LIST OF SYMBOLS

A	Yearly payment amount
A_h	Effective heat transfer surface area
C	Cost
C_i	Specific heat of material i
CO_2	Carbon dioxide
D	Inside pipe diameter
D_o	Outside pipe diameter
f	Friction factor
g	Gravitational acceleration
H	Wave height
h_c	Depth of closure
h_i	Convective heat transfer coefficient of material i
h	Total head loss
h_m	Minor head loss
h_f	Frictional head loss
i	Interest rate
k	Minor loss coefficient
k_p	Thermal conductivity of the pipe
k_s	Seawater thermal conductivity
L	Length
$\dot{m}$	Mass flow rate
N	Empirical exponent
Nu	Nusselt Number
P	Present value
P_i	Absolute pressure at a point i
ppm	Parts per million
ppt	Parts per thousand
Pr	Prandtl Number
q	Volumetric flow rate
$\dot{Q}_{\text{load}}$	Heat transfer load

R	Thermal resistance to heat transfer
Re	Reynold’s Number
T	Temperature
U	Heat transfer coefficient
W	Power
Z	Elevation
γ	Specific weight of water
η	Effciency
ν	Seawater kinematic viscosity
ρ	Density

LIST OF ACRONYMS/ABBREVIATIONS

ACCA	Air Conditioning Contractors of America
ASHRAE	American Society of Heating and Air-Conditioning Engineers
BTU	British Thermal Unit
CIL	Cold Intermediate Layer
CLTD	Cooling Load Temperature Difference
CO_2	Carbon Dioxide
COP	Coefficient of Performance
CTD	Conductivity, Temperature, Depth
EER	Energy Efficiency Ratio
GPS	Global Positioning System
HDPE	High Density Polyethylene
HVAC	Heating, Cooling, Ventilating and Air-Conditioning
IPLV	Integrated Part-Load Value
LMTD	Log Mean Temperature Difference
NPLV	Nonstandard Part-Load Value
SWAC	Seawater Air-Conditioning

1. INTRODUCTION

Fossil fuels are unsustainable both as an energy resource but also for climate change. This creates an increasing need for energy production from renewables and development of new energy efficient technologies. Heating, ventilating and air conditioning (HVAC) systems account for roughly one-sixth of global energy consumption. It has high initial cost and due to the high electrical power demand of the system, it is expensive to operate especially in warm, humid climate. In Europe, the cooling market is still undeveloped with significantly lower saturation of cooling demand than in U.S.A. and Japan. However, the intense growth of the demand is predicted and it will require the increase of electricity production and development of energy efficient technologies for cooling. One of the efficient alternatives to the conventional cooling system is seawater air-conditioning (SWAC) that utilizes a naturally cold water bodies as a thermal sink for heat rejection.

Decades of research have shown that SWAC can be a cost-effective low-energy technology. SWAC can fully replace or augment the conventional cooling. It has been successfully applied both to new buildings and as a retrofitting measure for existing buildings. The scale of SWAC also varies from the dedicated cooling system for an individual building to the district cooling application for multiple buildings. Examples of the most successful application of SWAC systems are usually located in regions, where the distance to cold seawater is minimal, and air-conditioning demand is very high. At places with ideal conditions power savings can approach 90% compared to conventional chillers. One of the largest SWAC application examples is located at Honolulu, U.S.A. SWAC provides cooling to commercial and residential buildings in the downtown of the island. The system with the capacity of 87.5 MW saves more than 77 million kWh/year which results in approximately 70% of energy savings. It also minimizes the carbon footprint of the cooling system by avoiding 84,000 tons of carbon dioxide/ year, which is equivalent to carbon emission of 15,000 cars.

There many factors influencing SWAC system’s feasibility. One of the most important once is the presence of sufficiently cold seawater in close proximity that primarily affects system configuration and pipelines costs. Another factor is the size of the air-conditioning load. The smaller the system the more difficult to economically justify it. Besides that, the utilization percentage, local electrical cost and complexity of distribution system on shore also affect the feasibility.

The main objective of this thesis is to evaluate the energy potential of cold seawater from the Black Sea to air condition indoor spaces and identify applicable SWAC system configurations for this region.

The present thesis engages several areas of science: civil, oceanographic and mechanical engineering. The scope of the thesis consists of literature review, technical assessments of SWAC systems for the Black Sea in general and a case study in Istanbul. The selected site for the case study is the Boğaziçi University Sarıtepe Campus, for which a feasibility analysis is conducted including field measurements, computer modelings and economic evaluation.

The literature survey includes the state-of-art review of SWAC, describes different design concepts and work principles, compares it to the conventional chillers and provides successful real-world examples. Special attention was paid to the Black Sea oceanography and environmental barriers to the application of SWAC technology in the region.

A computer model developed by the European Earth Observation Programme Copernicus was used for estimation of oceanographic parameters in the Black Sea. The large-scale bathymetry of the Black Sea was taken from Navionics SonarChart. Coastal field surveys were conducted during the study to validate the seawater potential temperature and bathymetry for the case study application in Istanbul. Field surveys included measurement of temperature and salinity profiles, coastal topography and bathymetry. The oceanographic data helped to understand the seawater temperature fluctuation in the Black Sea and to determine the optimum offshore distance to reach the sufficiently cold seawater for SWAC.

Technical and economic analyses examine the Black Sea seawater temperature fluctuation, heat exchanger and pipeline design, determination of electricity consumption and greenhouse gas emission as well as methods for the capital and operating costs evaluation. Finally, the applicability of SWAC for the Boğaziçi University Sarıtepe Campus was determined.

Different SWAC configurations were analyzed in comparison to conventional air-conditioning systems. The analysis included seawater intake and discharge lines, building demand, heat exchanger and chiller when present, but excluded distribution of chilled water from the central cooling station to individual buildings. The reason is that the remaining part of the air-conditioning system, including pipe network from the central cooling station and return pipes, air handling units and fan coils inside buildings would be the same for all types of the system and should be designed by mechanical engineers.

2. BACKGROUND

This chapter gives basic principles of conventional air cooling and describes various SWAC system configurations and requirements, associated environmental concerns and restrictions, compares SWAC with conventional cooling systems, provides examples of the successful application of SWAC and gives an overview oceanographic characteristics in the Black Sea.

2.1. Conventional Air-Conditioning

Air-conditioning is a process of supplying and maintaining desirable internal atmosphere conditions for human comfort. The basic concept of the air-conditioning system is to generate a constant cold fresh water flow that circulates throughout the building for heat removal. The most commonly used way of cooling is the conventional AC system, which usually consists of a chiller unit, a piping system, an air handling unit and a cooling tower in a case if the condenser is cooled by water. The refrigerant inside the chiller is a working fluid that absorbs (in evaporator) and releases (in the condenser) the heat while changing its state between gas and liquid forms, then the heat is rejected to air or water.

Summer indoor design conditions are defined as the dry-bulb temperature at 23.9 – 25.6ºC and 50% of relative humidity [1]. Chillers usually operate with chilled water supply temperature of 6-7ºC. After the heat is absorbed from the building, chilled water with the temperature raised by 5-6 degrees is returned to the chiller unit. These conditions are recommended and most commonly used since they take the refrigeration cost into account and eliminate freezing of the coil surface if the return water temperature is below the required value. If a lower temperature is still required, antifreeze solutions can be used. Room dew point temperature sets the upper limit for the chilled water temperature in the coil of air handling unit. The water temperature in the coil should not exceed the dew point value of the air in the room at its design conditions to be able to remove the moisture from it. Recommended limit is set to 13ºC with accordance to the psychometric chart (Figure A.1). If the chilled water temperature is higher than the dew point value, no latent cooling will occur. Even though air-handling unit can operate at chilled water temperatures ranging from

4.4 to 12.8ºC, its cooling capacity at 12ºC of supply and 18ºC of return is 50% lower than at supplied 7ºC and returned 12ºC. That results in ineffective operation with high capital and operating costs [2].

The chiller unit uses electrical power for transferring heat between the water returned from the building and the air. A large air-conditioning system requires a significant amount of energy and may become a major electrical load of the building. The energy load primarily depends on the cooling system type, the age of the system and building's climatologic location. Typically, the power requirement for the conventional air-conditioning system is 0.9 – 1.3 kW/ton [3]. Its operation is associated with fossil fuels combustion which consequently leads to high greenhouse gas emission and significant impact on global warming problem.

2.2. Seawater Air-Conditioning

The seawater in most coastal regions is as cold as or even colder than the water used in conventional air-conditioning systems. In tropical regions, the deep ocean seawater with 7ºC or lower can be reached approximately at depths of 700 meters in summer with small seasonal variation. At northern coasts, the cold seawater can be found at shallower depths. And therefore it can serve as a heat sink with an unlimited cooling capacity. In some regions, SWAC may be an effective technology that saves up to 90% of electrical use compared to the conventional system [3]. Alternative configurations of this technology may utilize cold freshwater from rivers or lakes.

The pioneering research on the use of a seawater for cooling buildings was conducted by Physical Oceanographic Laboratory of Nova University in Florida, U.S.A. in 1975 [4]. The idea belonged to Dr. William S. Richardson and was further investigated by his colleagues at the university. The study proposed several configurations of SWAC system and proved that it could technically be feasible to apply it in coastal communities. The amount of electrical savings reached 70-80% along with significant capital cost reduction. It was also discovered that in-situ, long-term time series temperature measurements of the cold source waters at the pipeline intake are fundamental for system performance.

The first prototype of modern SWAC system was built in 1983 in the U.S. to air condition a small research van at NELHA (Natural Energy Laboratory of Hawaii Authority). It consisted of small seawater intake, radiator and a box fan from the hardware store. The system had operated for nine months before the radiator failed [5]. SWAC has evolved since then, and today it is applied in various locations around the world (Figure 2.1).

The smallest currently operating SWAC system is located at Prudy's Warf in Halifax, Canada. It provides 25 tons of cooling using 228 meters intake pipe. The system with the largest intake is also located in Canada and provides air cooling for the city of Toronto using cold lake water. The system capacity is 75,000 tons supplied by three 1.6 meter diameter intake pipes with the length of 5 kilometers each. The lake freshwater is additionally used for drinking. One of the world's largest SWAC systems is located in Stockholm providing 60 MW of cooling to the city since 1995 [6].

Usually, SWAC is applied in the form of a district cooling system, rather than for a single building. All equipment, such as heat exchangers, pumps, and optionally chillers are consolidated in one location, whereas the chilled water is delivered to buildings through a pipe network. Such projects serving as district cooling required high capital cost and large size equipment. However, district cooling simplifies equipment maintenance and electrical power distribution and results in cost savings when compared to multiple individual house systems.

Key factors affecting SWAC system efficiency are:

- The amount of the air-conditioning load;
- Offshore distance to the depth of required seawater temperature;
- Duration of air-conditioning system usage during the year;
- Local electricity cost;
- Availability of ready marine infrastructure.
- Secondary use of effluent.

Figure 2.1. SWAC Systems around the World.

Benefits of SWAC system:

- Large energy savings;
- Reduction in greenhouse gas emission;
- Renewable energy use;
- Reduced potable water use;
- Short economic payback period;
- Availability of seawater for additional applications.

2.2.1. Standalone Seawater Air-Conditioning

The basic concept of a standalone SWAC system is to use sufficiently cold seawater to cool down the fresh water that circulates throughout the buildings for heat removal. The chilled water circulates through the buildings with the same temperatures and flows as it is in the conventional system. The interior of the air-conditioning system inside the building remains unchanged, but in SWAC facility the chiller unit is replaced by the heat exchanger, seawater pump and seawater intake/discharge piping system (Figure 2.2).

Cold seawater is pumped to the shore through the intake structure and pipeline, where it is passed through a heat exchanger to absorb the heat from the fresh water returned from the building. The warm seawater then is discharged back to the source to the location with similar water characteristics. The return water from SWAC unit can also be used for secondary applications, such as desalination, aquaculture or secondary cooling where humidity control is not necessary.

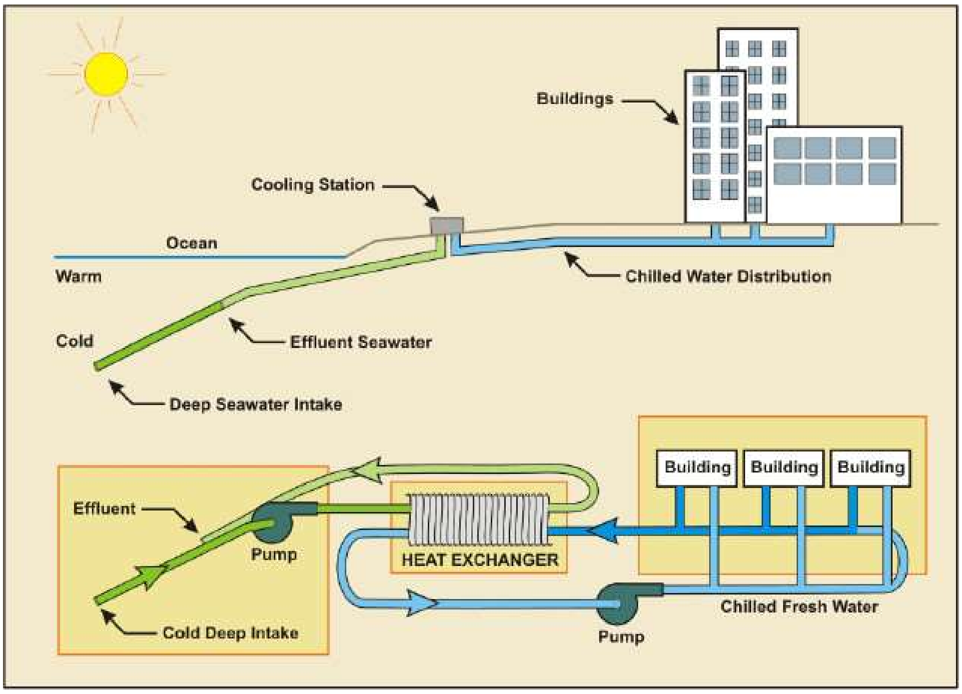

Figure 2.2. Sketch of a Standalone SWAC System [3].

Performance and configuration of SWAC system are highly dependent on site characteristics and cooling demand; it has to be optimized for each specific location. If it is too costly to supply sufficiently cold seawater required for full fresh water cooling in the chilled loop, the use of a hybrid SWAC system or an additional chiller unit is necessary.

2.2.2. Hybrid Seawater Air-Conditioning

In a case, if the intake seawater temperature is not sufficiently cold for direct air cooling but still has a lower temperature than the fresh water returned from the building, the hybrid SWAC system can be considered for the use. In that configuration, fresh water is cooled by the seawater in a heat exchanger unit as in the stand-alone system, but then an auxiliary chiller provides the remaining cooling, to reach a sufficient temperature for proper air dehumidification. The condenser in the chiller unit is also cooled down by the seawater return flow. Hybrid SWAC can be twice more efficient than the conventional air-cooled systems (Figure 2.3) [3].

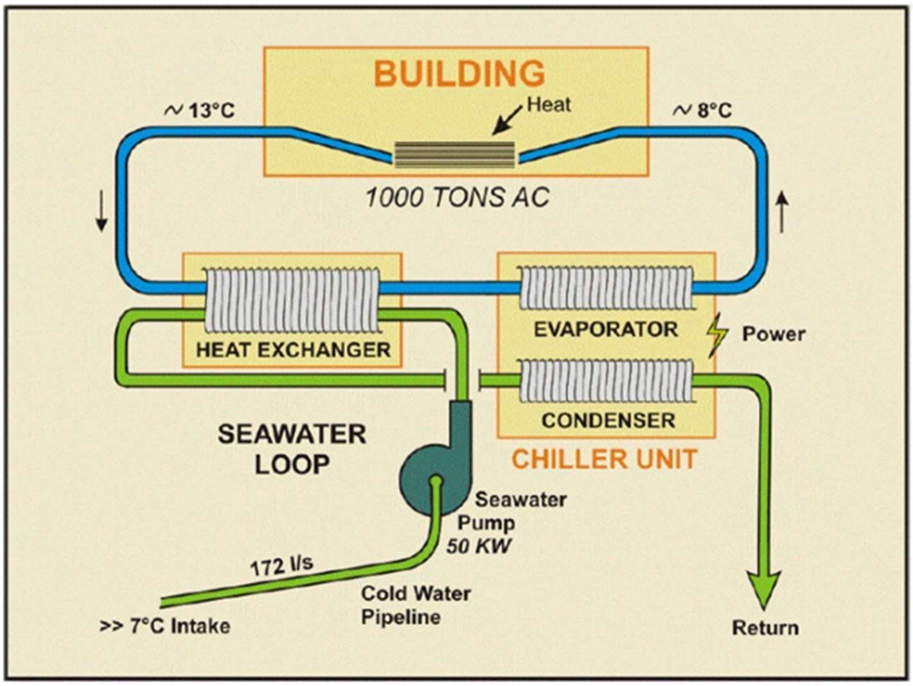

Figure 2.3. Sketch of Hybrid SWAC System [3].

2.2.3. Seawater-Cooled Chiller Units

If the available seawater is not cold enough neither to provide the primary cooling nor for the use in the hybrid SWAC system, the use of seawater-cooled chiller units is another SWAC configuration available to reduce the energy costs associated with air-conditioning.

Cooling fans and cooling tower can be replaced by alternative systems that utilize seawater for condenser cooling. There are two sub-types of seawater-cooled chiller units with direct and indirect cooling. In the directly cooled chiller unit, the heat exchanger can be eliminated from the system and the heat from the condenser is rejected to the seawater (Figure 2.4). It not only utilizes less equipment but also uses the seawater for the condenser cooling. However, the cost associated with such units is usually much higher than in the fresh water-cooled chiller case, since all system components require using corrosion resistant materials and extra bio-fouling measures.

The indirectly cooled chillers utilize fresh water for the heat elimination which is rejected to the seawater at a later stage in the heat exchanger. The main working principle of such systems involves seawater, which is drawn in through the intake pipe to the heat exchanger facility, where it accepts the heat from the fresh water of the condenser circuit and then it is returned to the sea (Figure 2.5). In the second loop, the fresh water circulates between the condenser of the chiller and the heat exchanger, absorbs heat eliminated from the building and then rejects it to the seawater. Even though the system is more complex and requires more complicated engineering design, expensive corrosion resistant materials in the chiller can be avoided, and bio-fouling is localized in the seawater circulation loop.

In summer, shallow seawater is typically cooler than the air and can provide enough cooling to eliminate the heat from water that cools down the condenser. The seawater cooled chiller system can achieve more than 25% energy savings [3].

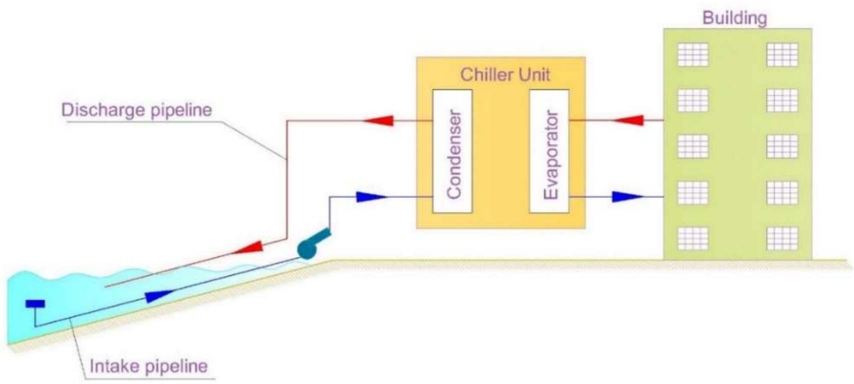

Figure 2.4. Sketch of Directly Cooled Chiller Unit.

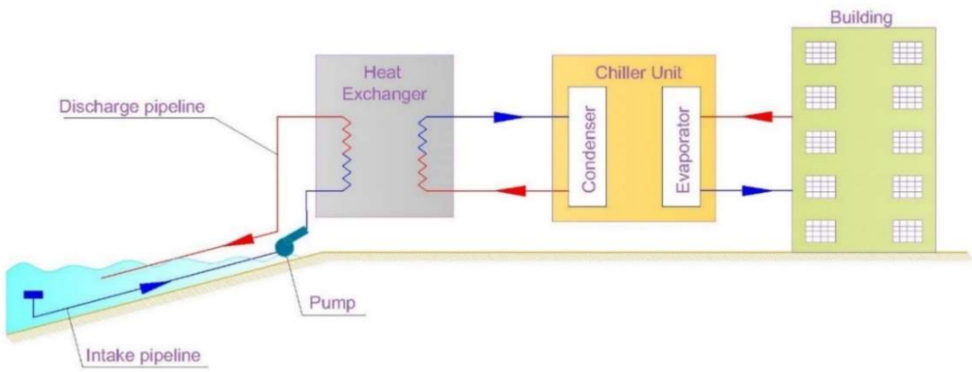

Figure 2.5. Sketch of Indirectly Cooled Chiller Unit.

2.3. Oceanographic Characteristics of the Black Sea

The Black Sea is the world's largest land-locked sea basin remarkable for its unique marine environment. It drains through the Mediterranean Sea into the Atlantic Ocean, via the Strait of Istanbul, Marmara Sea, Dardanelles, Aegean Sea and Gibraltar Strait. About 24% of the total basin area is a shelf zone whose outer edge can be traced along the 100-150 meters depth contours. The geological structure of the Black Sea consists of the West and the East basins separated by north-south oriented Andrusov and Arkhangelsky ridges [7]. The sea thermocline is highly affected by regional climates, currents, upwelling, downwelling and water exchange with the Marmara Sea and the Azov Sea.

Water circulation in the Black Sea consists of two main wind-driven circulations that influence both the upper layer (mixed layer) and the upper part of the deep water mass. The first driving force is a rim current, formed by West winds from the Caucasus Mountains. It cyclonically moves along the continental slope and completes one full cycle around the whole basin in a few months. Secondly, permanent cyclonic and anticyclonic eddies in western and eastern basins provide mixing in the upper 200 meters of the water column. Water circulation driven by eddies is unstable and shows big changes throughout the year (Figure 2.6) [7].

The water of the Black Sea characterized by a distinct vertical stratification: the low salinity surface water is followed by the cold intermediate layer (CIL) and the deep dense water. Clear permanent halocline, formed due to a weak water exchange of the Black Sea with the adjacent basins and large fresh water inflow, restricts active vertical mixing to the upper 150 meters of the sea [8].

The top layer due to its small thickness (30 meters) is exposed to a significant influence from the atmosphere. The water temperature varies seasonally, and its density is highly affected by the rivers inflow. The main fresh water discharge occurs in the northwestern part of the sea where the Danube, Dnepr and Dniester rivers fall into it; that results in the decrease of the mean salinity value at the sea surface from 18 ppt to 16-17 ppt. The diluted low-salinity seawater travels with the rim current to the southwestern Black Sea [9].

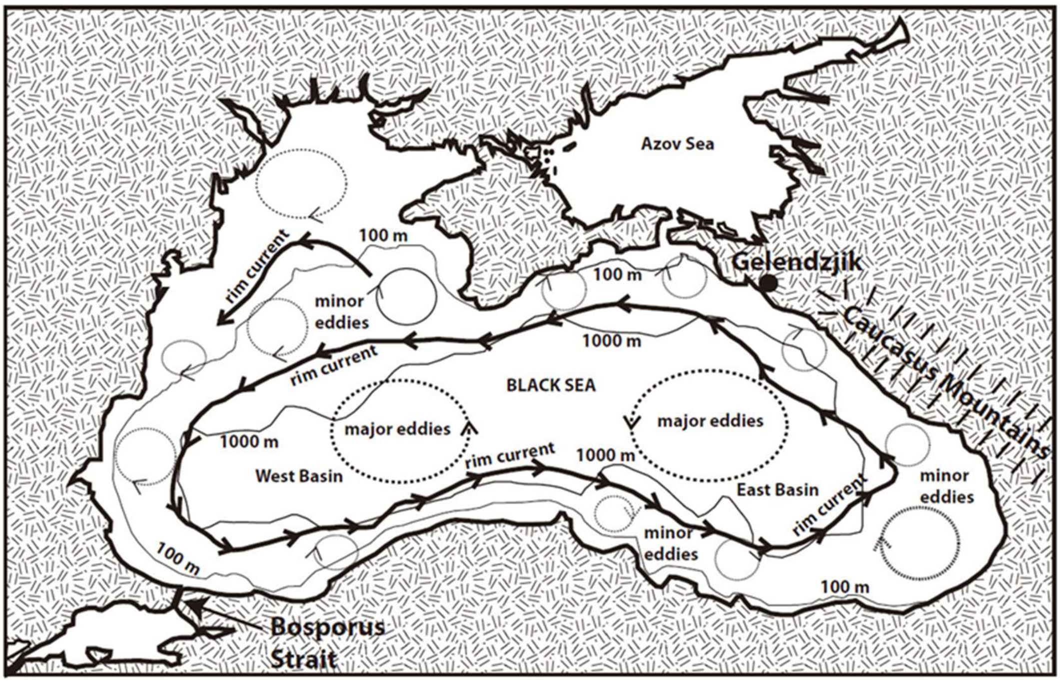

Figure 2.6. Overall Circulation Patterns of the Black Sea [8].

CIL is an example of a dicothermal layer, which is a cold water layer sandwiched between warmer surface, and warmer deeper water. There are many theories about the nature of CIL in the Black Sea, but the exact mechanism of its formation remains unclear. It seems to be the result of complex convective processes and is closely related to the atmospheric conditions, currents, and topography. CIL can be the remnant of cool surface water colder than 8ºC. In winter, the reduced freshwater discharge into the northwestern Black Sea coincides with the cold atmospheric conditions in this region and results in the formation of the denser cold water mass which is after driven southward along the shoreline by the rim current and spread over the entire sea. The second region of CIL formation is in the northern part of the central basin, where an outcropping of the deep isopycnal water together with winter rim current intensification allows the cold water to penetrate to CIL density level. CIL can usually be found at 50 -180 meters depth with the temperature of 8ºC limiting isotherms and the minimum temperature at the core can reach 6ºC. CIL is capped by warm surface water in summer and forms a subsurface with minimum temperature. In winter, the upper layer of the Black Sea up to 80 meters depth becomes almost isothermal with the temperature of 7ºC. CIL properties are uniform across the whole basin and do not change with meteorological conditions [8-9].

With the depth, seasonal variations of temperature and salinity diminished. Physical and chemical properties water below 500 meters are stagnant. The mean salinity value rises up to 22 ppt, and the average temperature becomes uniform at 8-9ºC. Dense warm Mediterranean water sinks to the intermediate layer after exiting the Strait of Istanbul and spreads along the continental shelf towards the East basin following a steep bottom. After mixing with the CIL, the Mediterranean water cools down from 14.5ºC to 8ºC, and similarly, it gets diluted and the salinity decreases from 37 to 22 ppt (Figure 2.7) [9].

As a result of a clear salinity stratification, vertical mixing and heat exchange between the layers is much less compared to other similar semi-closed basins [10]. This fact makes upwelling and downwelling primary reasons for the vertical water exchange. In the northern hemisphere, the water transport is at a 90 degree angle to the right of the direction of the wind due to Coriolis effect (Figure 2.8). As the result, the upwelling causes the rise of the CIL water to the surface and consequently temperature decrease, and the downwelling causes the process in the opposite direction, when the wan surface water sinks down to CIL. These events are observed in the central and in the periphery parts of the Black Sea [11]. Winter cooling has maximum intensity in the central part of the sea, because of a relatively small depth of mixed layer. It is limited by the upwelling of dense deep water, and strong density gradient [12]. Cold dense surface water formed in winter sinks into the CIL following the salinity gradient. In the northwestern part, upwelling driven by the wind forces and rim current lasts for only a few hours [13]. Whereas in the southwestern part and along the Anatolian coast due to the interaction with the shore, upwelling patterns from CIL to surface waters are observed every summer during the entire month [9]. In contrast, downwelling is observed in the shelf zone almost of the whole basin with particular strength in the northwestern part of continental shelf slope [12]. The cold dense water formed in winter there sinks to the CIL and travels toward the south [14].

The Black Sea is also exposed to the effect of various large-scale atmospheric modes, leading to significant changes in the weather conditions. The North Atlantic Oscillation along with the east Atlantic/West Russia pattern have a strong impact on the Mediterranean and the Black Sea hydrodynamics and sea surface temperature during some years. The El Niño southern Oscillation promotes the occurrence of extreme sea surface temperature values during some years [8].

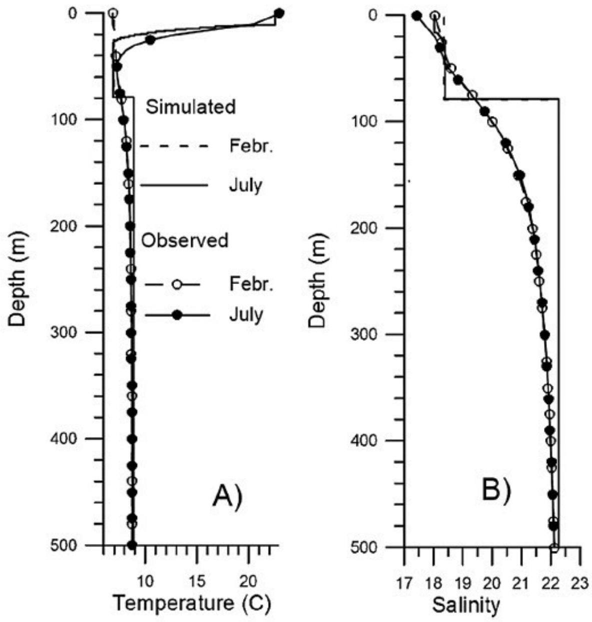

Figure 2.7. Simulated and Observed Temperature and Salinity Profiles at the Black Sea [15].

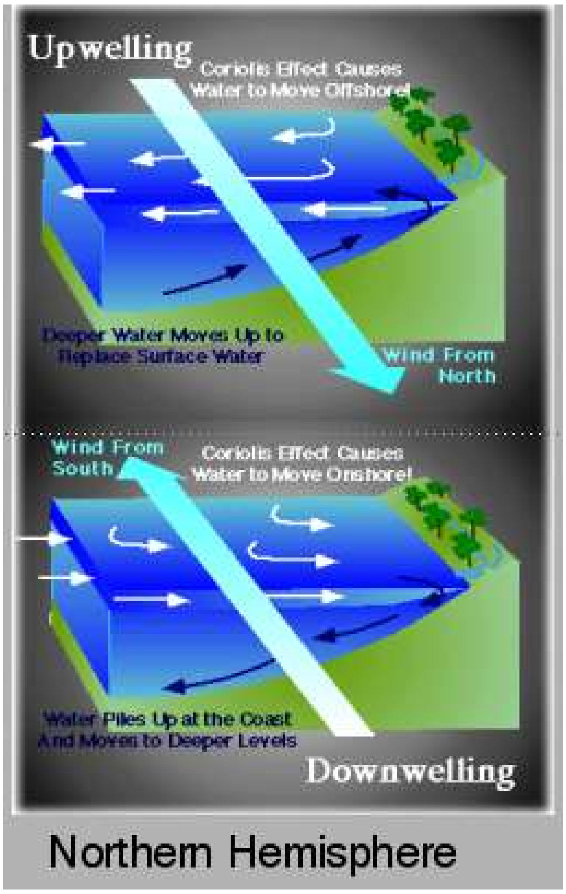

Figure 2.8. Upwelling and Downwelling in the Northern Hemisphere [16].

2.4. Environmental Aspects

From an environmental point of view, one of the main concerns of a direct seawater intake is the entering of marine life and other debris into the system. Section 316 (b) of the Clean Water Act through the National Pollution Discharge Elimination System establishes measures to avoid impingement and entrainment and mitigate the impact to the environment. The use of the fine screen filters at the seawater intake structure prevents intrusion of foreign objects and organisms to the system. Impingement occurs when organisms sufficiently large to avoid going through the screens are still trapped by the flowing water force. Therefore, the opening size in the intake structure should be designed to control the local velocity of the intake water to avoid the impingement. It can be ensured by designing the intake head cross section area large enough to reduce inflow velocities. The appropriate velocity of water entering thresholds should be based on the maximum current velocities of which the local fish species can tolerate without getting forced into the intake pipes. The velocity threshold of 0.15 m/s is recommended [17].

Other major challenges encountered in the SWAC systems are marine growth and corrosion. Superior corrosion resistant materials have to be used in the seawater operating facilities of the cooling plant. Measures, used to prevent the marine growth, must be environmentally friendly, as far as possible, to minimize the impact on the seawater quality in the basin. Mechanical or chemical treatment can reduce bio-fouling. Also, stagnant system condition should be avoided. Although the system is well protected from entering of macro-organisms by filtering, microscopic bacteria and fungi still can penetrate through screens. Chemical treatment is necessary for all parts of the system where seawater is used. For environmental friendliness, continuous chlorine dosing, generated from electrolysis of seawater using electro-chlorinators and injected at the seawater intake, would minimize bio-fouling. The optimal dosage at the intake is about 1.5 ppm and the residual concentration at the discharge should not exceed 0.09 ppm (due to losses and chemical degradation) [18].

If the SWAC return water is warmer than ambient water temperature at the discharge location, it may have a severe effect on habitats' life. The temperature difference of 3-4°C increases death among corals and fishes [19]. According to [20] the seawater discharge should be located in the open sea, away from the shoreline as well as away from areas of special biological significance. The maximum temperature fluctuation from the ambient temperature at discharge location should not exceed 2^{o}C.

3. TECHNICAL ANALYSIS

The technical analysis involves a detailed investigation of seawater temperature fluctuations and bathymetric characteristics of the Black Sea. Engineering calculations are conducted to evaluate the potential of SWAC use in the Black Sea region. SWAC system configurations which are applicable for the Black Sea SWAC are defined.

3.1. Climatic and Oceanographic Analysis of Seawater Air-Conditioning Potential in the Black Sea

Hot and humid summer in the Black Sea coastal region creates a significant energy demand for air-conditioning. SWAC system efficiency is highly dependent on the supply cold water temperature and the distance to reach that temperature. Summer seawater temperatures at the sea floor around the Europeans coast obtained from the Copernicus model vary drastically from 4ºC in the Atlantic Ocean to 29ºC in the Azov Sea (Figure 3.1). Even though the Atlantic Ocean is considerably colder than the Mediterranean basin, the SWAC viability in the Atlantic coast is questionable due to the long distance of cold water from the shore. The Black Sea waters have a high potential for SWAC system since cold seawater of around 8ºC can be reached near the coast.

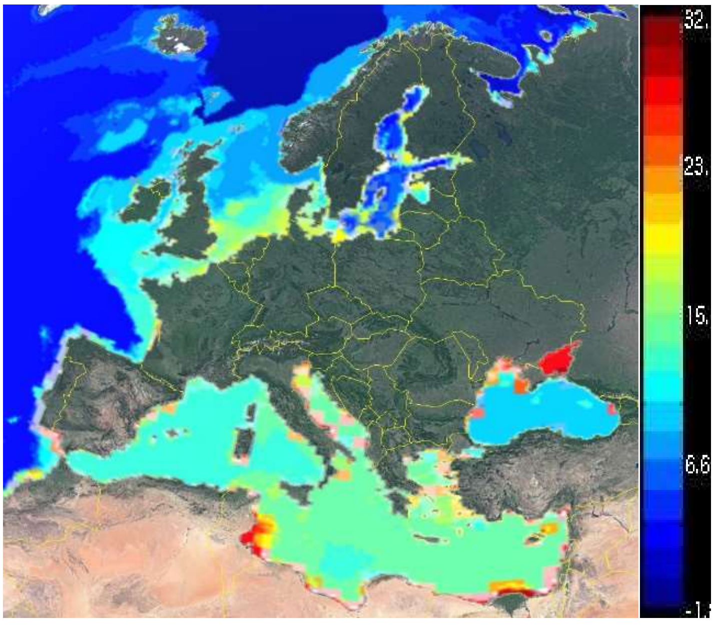

Figure 3.1. European Seawater Temperatures at the Seafloor.

3.1.1. Climate around the Black Sea Coast

The population of the Black Sea towns and cities ranges from a few dozens to millions of people. Population of the biggest cities around the Black Sea coast are given in Table 3.1. The mean summer air temperature in the Black Sea region varies between 22°C and 27°C (Figure 3.2), which is one of the hottest regions of Europe. Maximum values are observed in Istanbul, Turkey and in Krasnodar Krai, Russia. Large populations living in the hot and humid coastal cities increase the air-conditioning demand around the Black Sea.

Table 3.1. Population Size at the Black Sea Coastal Communities [22].

Place	**Population**
Istanbul	14,163,989 (2015)
Odessa	2,388,297 (2012)
Samsun	1,269,989 (2015)
Trabzon	766,789 (2015)
Sochi	389,946 (2015)
Sevastopol	398,973 (2015)
Varna	330,486 (2012)
Batumi	336,500 (2015)
Novorossiysk	260,704 (2015)
Yalta	76,746 (2014)

3.1.2. Oceanography around the Black Sea Coast

Availability of the sufficiently cold seawater close to facilities is the most critical factor that affects the SWAC system performance. It is necessary to base the analysis on accurate water temperature data to minimize the possibility of system failure. This chapter provides the investigation and statistical analysis of the summer seawater temperature fluctuations in the Black Sea.

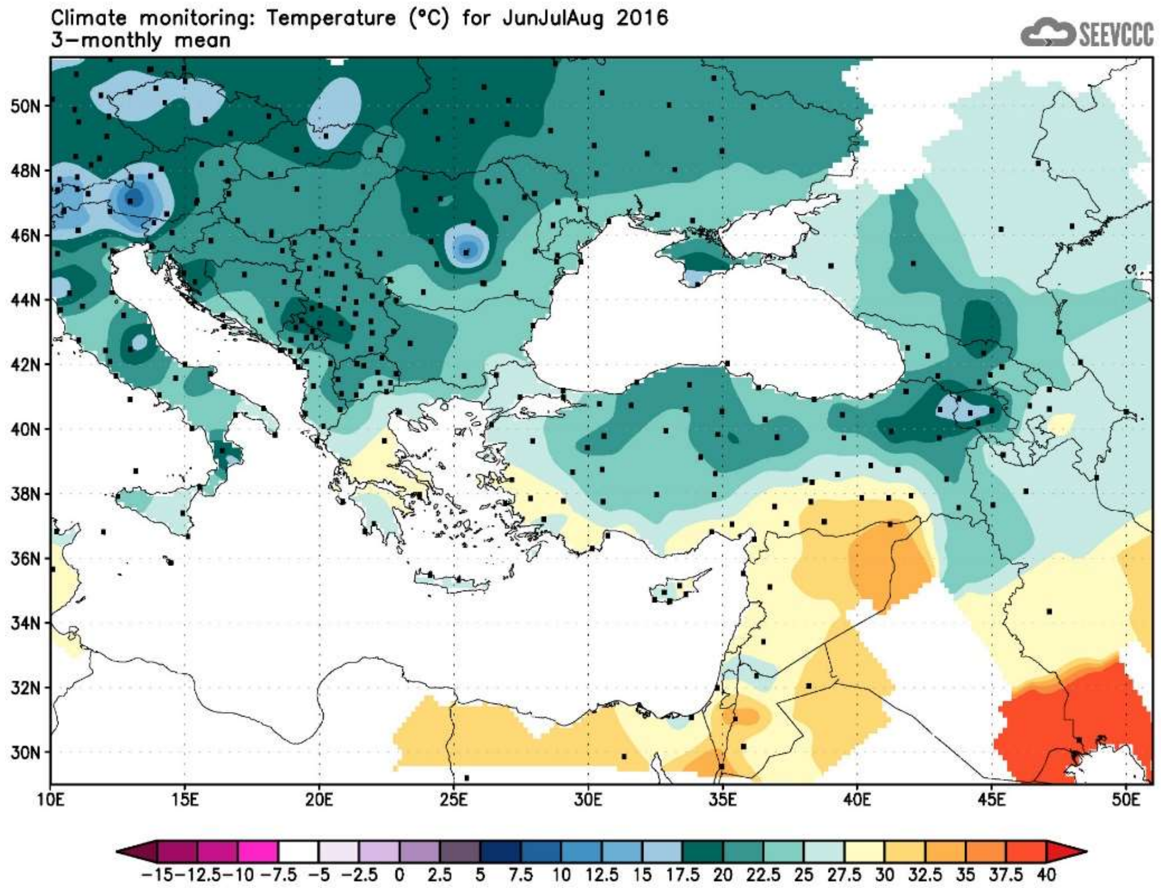

Figure 3.2. Mean Summer Air Temperature [21].

The Operational Mercator Global Ocean Analysis and Forecast System (Copernicus model) operated under the European Earth Observation Programme Copernicus provides daily mean seawater potential temperature and salinity for the Black Sea for past years and 10 days forecast updated daily. The data were obtained with 1/12 degrees (9.2 km) horizontal resolution and 50 vertical levels ranging from 0 to 5500 meters of depth. Temperature and salinity advection is modeled with a total variance diminishing advection scheme. In situ temperature and salinity vertical profiles together with the satellite sea surface temperature are jointly assimilated to estimate the initial conditions for numerical ocean forecasting model.

Although low water temperatures can be reached at relatively shallow depths in the Black Sea, the stability of their occurrence strongly affects the system performance.

Therefore, statistical analysis of seawater temperature fluctuations at different depths is crucial for the choice of the intake location.

Comparison of annual surface water, CIL and deep water temperature variations in the Black Sea (Figure 3.3) showed stable thermal stratification in the entire basin. Here, the depths of CIL and the deep water are defined at 77 and 220 meters respectively. The sea surface is highly exposed to seasonal temperature variation with the mean annual value of 19^{o}C and fluctuation amplitude of 8^{o}C. The probability density functions of sea surface temperatures in all four parts of the Black Sea (eastern, western, northern and southern) indicate a double peak distribution. The most frequent sea surface temperatures are 10^{o}C and 24^{o}C (Figure C.1). The CIL and deep water temperatures do not vary significantly throughout the year and have similar values almost everywhere in the basin (Figure C.2). The only exception is the southern part of the Black Sea, where warm Mediterranean water, driven by the rim current, causes 1-3 ^{o}C occasional increase. In general, CIL is slightly colder than the deep water with a mean value around 8.4^{o}C. The deep water temperature is stagnant at 8.8^{o}C (Figure C.3).

The availability of cold water in CIL and stable water stratification make the Black Sea a favorable environment for SWAC. Seawater from the CIL can serve as an excellent source for efficient work of the SWAC system if it can be reached with a sufficiently short pipeline. Although it is more distant to reach, the deep water of the Black Sea can also be used for the SWAC application. However, its anoxic nature may create undesirable environmental issues at the discharge location. Thus, further chemical and physical composition analyses are required.

For the further analysis of SWAC application to a particular site, the fluctuation of the temperature difference between the selected intake and discharge depths has to be examined, since temperature variations at different depths are not in line with each other. The difference between intake and discharge water temperatures strongly affects the configuration, performance and stable operation of the heat exchanger which are the measures of SWAC's system success.

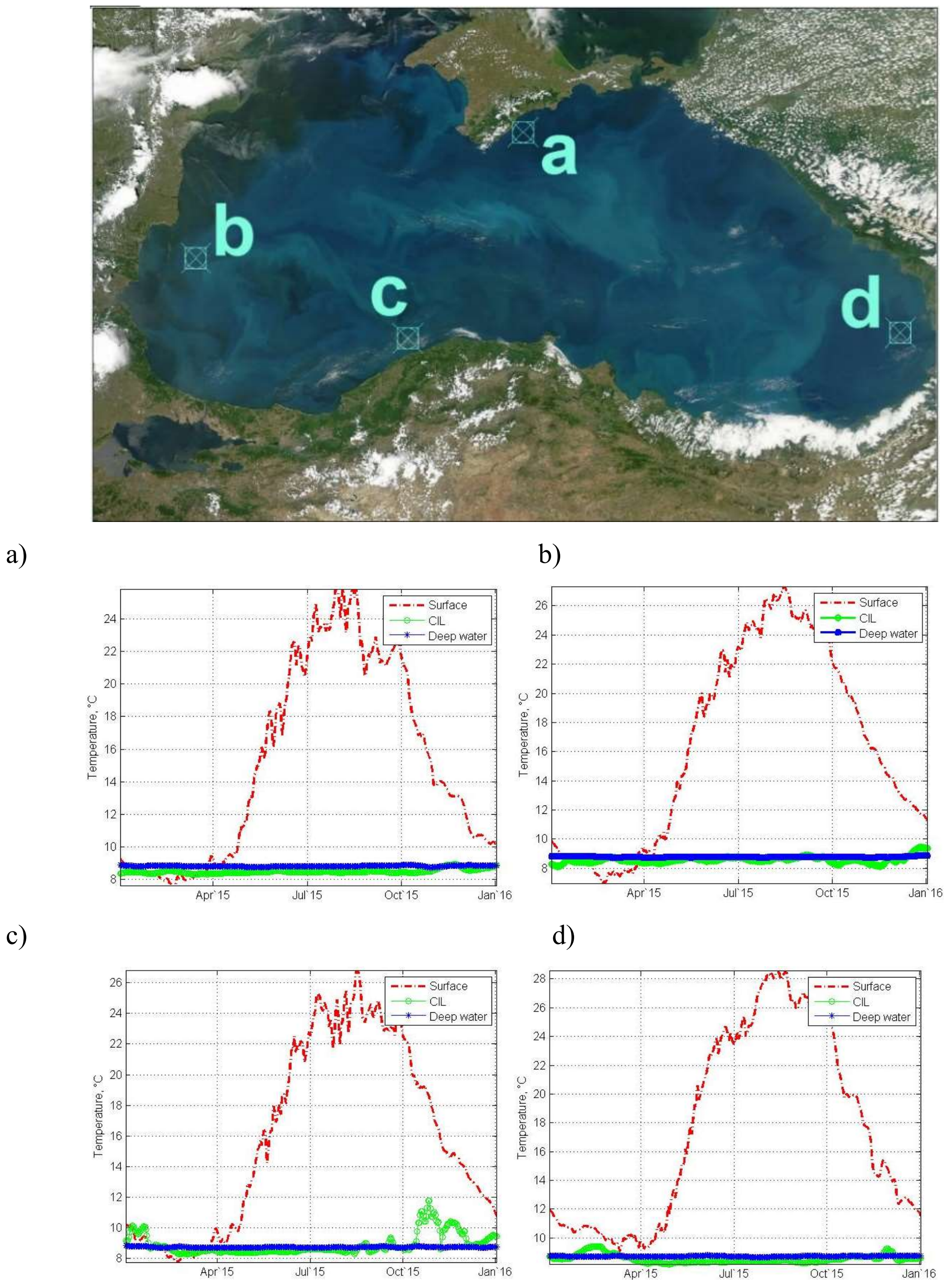

Figure 3.3. Annual Variation of Seawater Temperature at Sea Surface, Cold Intermediate Layer and Deep Water for a) Northern, b) Western, c) Southern and d) Eastern Black Sea.

3.1.3. Verification of Modeled Oceanographic Parameters with Field Measurements

To ensure the accuracy of computed oceanographic parameters, two sea surveys were conducted in the Black Sea territorial waters of the Boğaziçi University Sarıtepe Campus. During the December 7, 2015 and April 16, 2016 measurements, temperature, conductivity, and depth (CTD) data were collected. An area of 1 km (long-shore) by 1.8 km (cross-shore) was covered by the the survey boat measuring at water depths from 1 and 20 meters. Measurements were done with the help of a Topcon Real Time Kinematic (RTK) GPS survey set and an Airmar P66 transducer sonar. Bathymetry contour lines are defined after filtering out the wave induced boat motion, and sonar calibration. It was found that the average bottom slope in the cross-shore direction is approximately 0.01. During the surveys, multiple shots of seawater conductivity and temperature between the surface and 20 meters depth were taken by using a CTD device AML Minos. (Figure 3.4, Figure B.1). The seawater temperature (Figure B.2, Figure B.3) was almost uniform at the examined depths in December, with a mean value of 13.8^{o}C. Temperatures in April survey, showed a variation between 9^{o}C and 14^{o}C due to spring conditions.

PSS 1978 (Practical Salinity Scale) method was used to obtain the water salinity level from conductivity and temperature values for corresponding depths. In the surface layer, the salinity in December was uniform over the depth at 18,1 ppt. In April, it dropped to 17 ppt (Figure B.4, Figure B.5). These salinity results support previously stated oceanographic findings that the seasonal salinity fluctuation in the upper layer is due to the large freshwater inflow from rivers in the northwestern Black Sea in the spring. For further analysis, an average salinity value of 18 ppt for depths below 10 meters was be assumed.

Comparing the measurements with the model results, daily average temperature profiles at the same locations of 20 meters depth at given dates show a maximum deviation of less than 1^{o}C (Figure 3.5). This deviation is assumed as acceptable for using the Operational Mercator global ocean model in the engineering analysis.

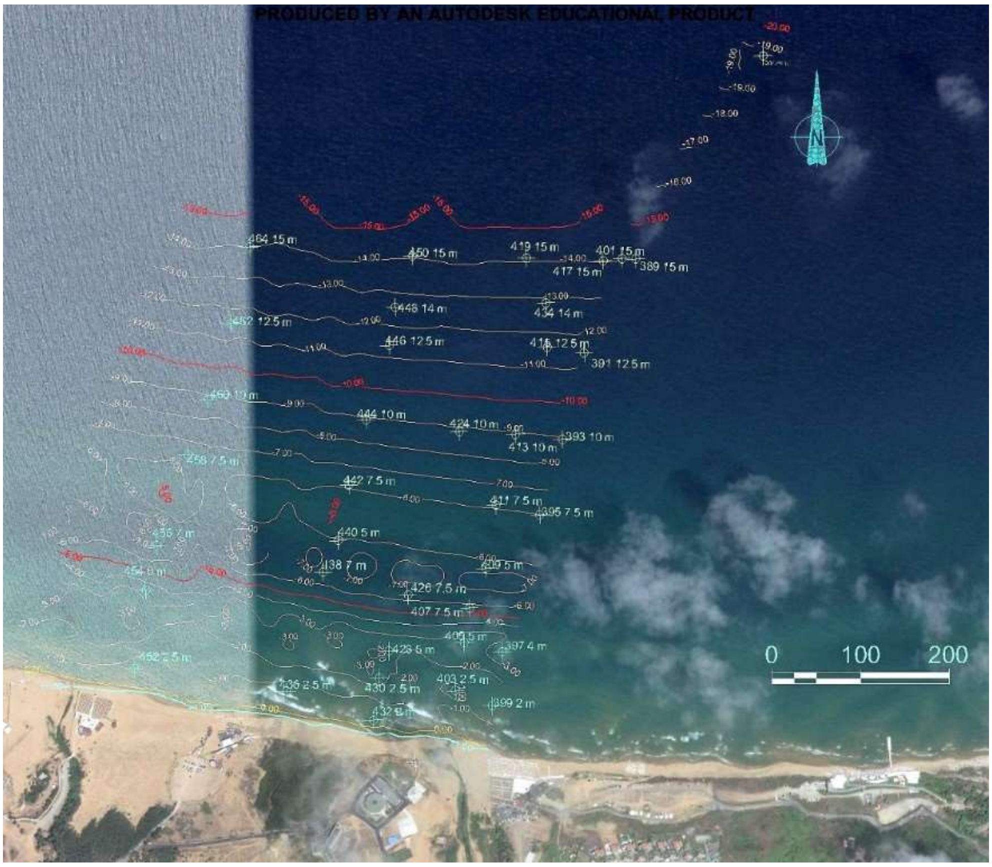

Figure 3.4. CTD Locations and Bathymetry Contours of the Covered Area (December 7, 2015).

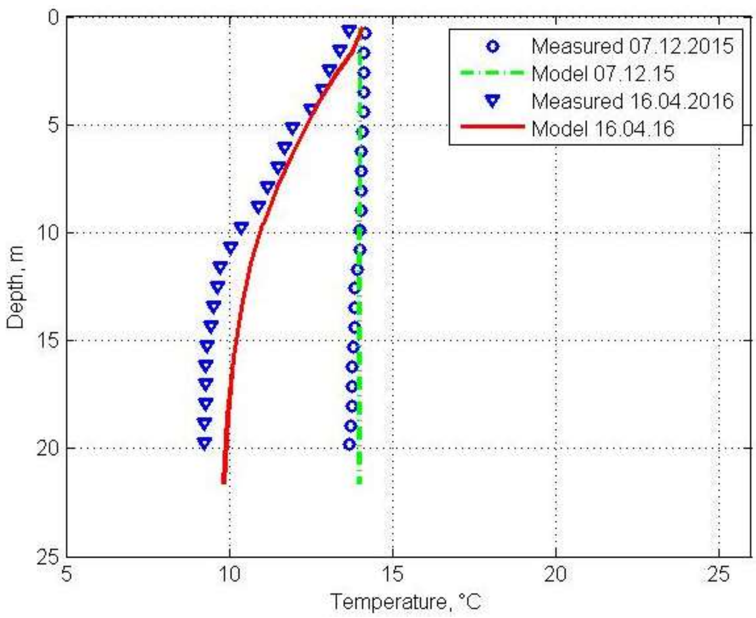

Figure 3.5. Measured vs. Modeled Temperature Profiles.

3.1.4. Nearshore Bathymetry and Hydrodynamics of the Coastal Black Sea

Oceanographic studies and model results of temperature distribution reveal that the required cold water of 6-7°C, for a standalone SWAC system, does not permanently exist in the Black Sea. Analysis of summer water temperature profiles near large coastal cities in the Black Sea showed, that water temperatures of 8-9°C can be found at the upper boundary of the CIL located at around 50-60 meters depth almost all over the entire basin. Istanbul is the only exception where the water temperature at the Black Sea coast is 3 degrees higher compared to other Black Sea cities due to the warm Mediterranean water influx from the Strait of Istanbul (Figure 3.6, Figure D.1). Although the presence of a cold seawater at shallow depth is the necessary condition, it alone does not guarantee the feasible application of SWAC. The feasibility is highly dependent on the length of the offshore pipeline and the associated costs. The intake pipeline length at a depth of 50 meters may vary from 150 meters in the eastern part of the sea to 150 kilometers in the northwestern part of the Black Sea (Figure 3.7).

The discharge seawater temperature of SWAC outfall is defined by the system configuration. However, the ambient temperature at the discharge location cannot be controlled therefore it should be taken into account to avoid the harmful effect on marine habitats. According to the Turkish environmental law, the temperature difference between the returned water and the ambient seawater at the discharge point should not exceed 1 or 2°C in summer and winter respectively. This condition heavily influences the system configuration, cost, and performance.

The discharge seawater temperature of SWAC outfall is defined by the system configuration. However, the ambient temperature at the discharge location cannot be controlled therefore it should be taken into account to avoid the harmful effect on marine habitats. According to the Turkish environmental law, the temperature difference between the returned water and the ambient seawater at the discharge point should not exceed 1 or 2°C in summer and winter respectively. This condition heavily influences the system configuration, cost, and performance.

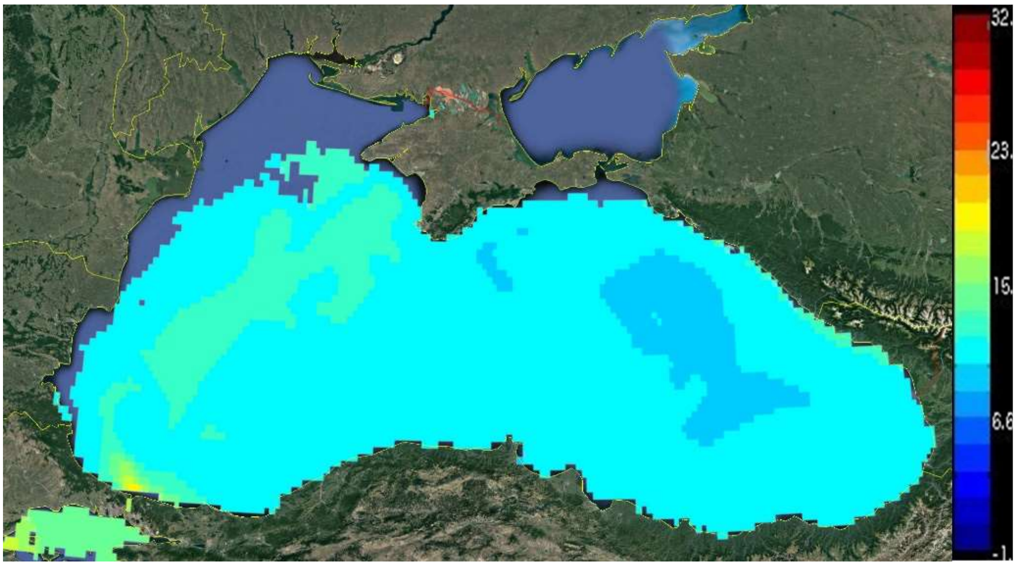

Figure 3.6. Seawater Temperature at 50 m Depth in the Black Sea (Modeling, July 25, 2016).

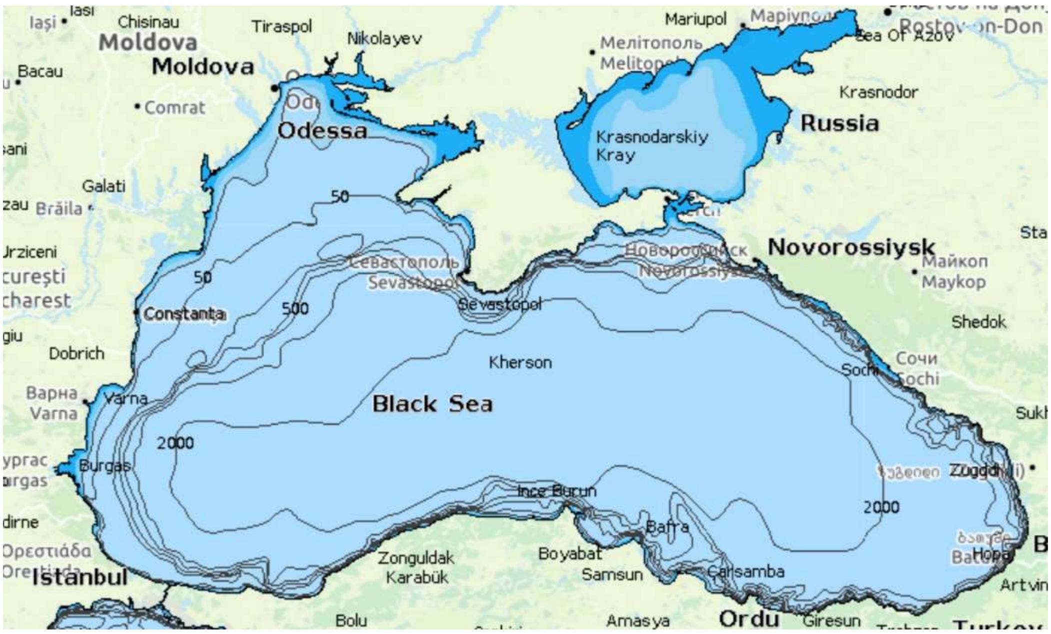

Figure 3.7. Bathymetric Contour Map of the Black Sea [23].

The intense nearshore hydrodynamics adds another constraint to the location of the SWAC outfall. From the economical point of view, it is desirable to make pipelines as short as it possible, but the wave motion in shallow water may destroy or pollute SWAC facilities with sediments on sandy coasts. It also may cause scouring or depositional effects of the seabed around intake and discharge structures. To avoid that, SWAC intake and outfall have to be located deeper than the depth of closure.

The depth of closure, h_c, describes the seaward limit of appreciable depth change due to sediment motion induced by waves at sandy beaches. It may be regarded as the absolute depth beyond which there is no cross-shore sediment transport due to waves at the sea bottom. Beach profiles of sandy coasts show that the seasonal or episodic variations in the sea bed decreases with increasing depth. The closure depth corresponds to a depth below which the vertical bottom changes become small. The analytical method that provides an accurate estimation of the closure depth has been proposed by Hallermeier (1981). The method is based on the extreme wave conditions: with significant wave height that is exceeded only 12 hours a year, $H_{S,12}$, and the associated wave period, $T_{S,12}$:

$$h_c = 2{,}28 H_{s,12} - 68.5\ H_{s,12}^2 / g T_{s,12}^2 \tag{3.1}$$

For water basins that are not exposed to the open ocean conditions, closure depth can also be linearly approximated as [24]:

$$h_c \cong q_1 H_{s,12} \cong q_2 H_{s,mean} \tag{3.2}$$

Where $H_{s,mean}$ is the annual mean significant wave height, q_1 is usually in the range of 1.5-1.57, and q_2 is 8.25. Based on the mean annual significant wave height conditions at the Black Sea (Figure 3.8), the closure depth is in the range of 5-7 meters across the basin.

Taking into account all thermal, bathymetric and hydrodynamic specifics of the Black Sea, the nearshore zone between the 5 m and 150 m depth contours is suitable for the seawater intake location of SWAC system facilities. The most feasible solution for the seawater intake location is below the depth of 50 meters to ensure stable operation of the system.

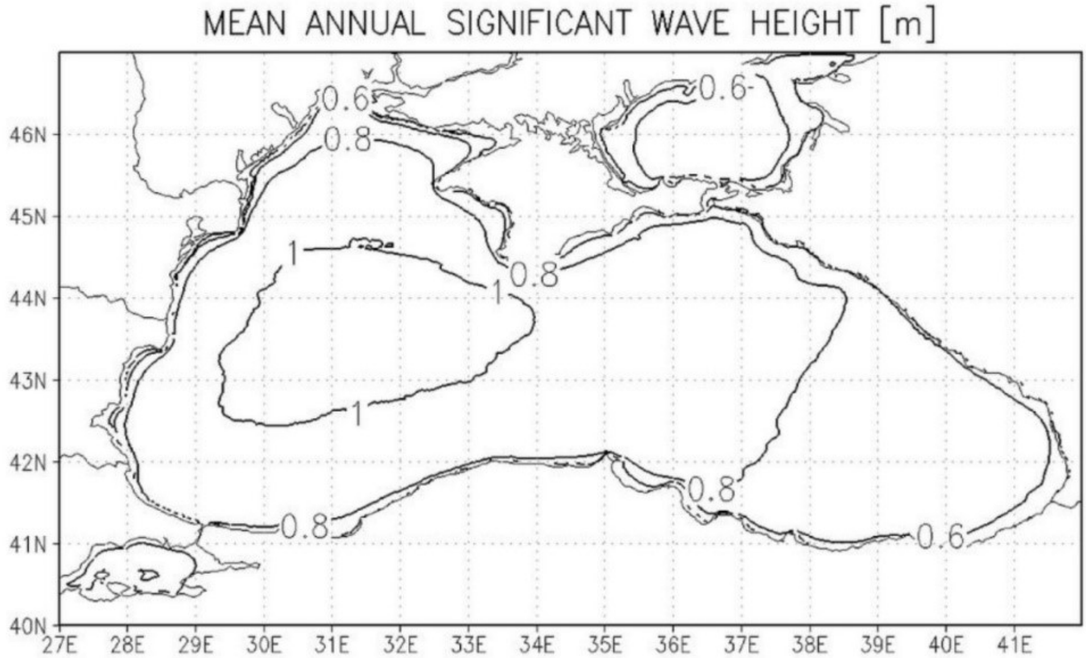

Figure 3.8. Mean Annual Significant Wave Height in the Black Sea [25].

3.2. Engineering Analysis of Seawater Air-Conditioning System

For the engineering analysis of land side units, first the air-conditioning demand of buildings is calculated to determine the energy load of the SWAC system. For the calculated demand, an appropriate system is configured. Since the use of a standalone SWAC system is technically not possible for the Black Sea due to the absence of sufficiently cold seawater temperatures, the use of a hybrid system or seawater-cooled chiller unit has to be considered. Operational properties of chillers from top HVAC equipment manufacturers: YORK and Carrier, are used in the analysis. Their products comply with the current energy standards in Turkey and achieve good efficiencies at true operating conditions without compromising the environment.

3.2.1. Air-Conditioning Demand

The first step in any HVAC system design is the estimation of the air-conditioning load which is the required capacity of the cooling system. Cooling load dictates the equipment selection. Its accurate calculation will have a direct impact on the system efficiency, capital costs, and occupant comfort. A variety of methods different in their complexity is used in practice in cooling load calculations. The rule of thumb is the simplest method that specifies the required load based on the cooling area. The age-old rule of thumb assumes one ton of refrigeration for every 400 square feet of space and usually results in an oversized HVAC equipment. With the improvement of building insulation techniques and windows specifications, new rules of thumb have been developed. The required cooling can be found from the relation of one ton per 600 square feet or even one ton per 1000 square feet [26]. The rule of thumb may give a rough estimation of the cooling load to get an idea about HVAC size at the preliminary design stage.

Because of the complicity of cooling load calculation, it is best performed a computer software. There are several methods used in the software engines, the most commonly used once are Manual J developed by Air Conditioning Contractors of America (ACCA) and VDI 2078 provided by Association of German Engineers. Both methods are based on the approach developed by ASHRAE, the Cooling Load Temperature Difference (CLTD).

LiNear GmbH Building is a software suite for heating and cooling load calculation. Estimation of the cooling demand is in line with VDI 2078. The software calculates room-by-room cooling load on daily progression basis, meaning that cooling load of every following hour depends on the load at the previous hour and thermal envelope of the building. Predetermined target temperature and humidity defined by comfort zone conditions which are 24ºC dry-bulb temperature and 50% relative humidity. The outdoor design conditions are location dependent and can be obtained from the ASHRAE Handbook.

External cooling load comes from the heat originated from outside the building and primarily depends on the ambient temperature. At the same time the heat from the inside forms internal load (people, lightning, equipment) which usually constitutes from 40% to 60% of the total cooling energy demand. The heat transfer happens whenever there is a temperature gradient between outside and inside conditions. The total heat that has to be removed consist of sensible and latent heat loads. Sensible heat is gained due to the total temperature difference, while latent heat is responsible for the air dehumidification since the water latent heat capacity is 1000 BTU per pound it results in the additional cooling load.

A cooling load calculation is usually made for a day during the hottest month of the year, and the air-conditioning demand is expected to reach its peak in one of afternoon hours (Figure 3.9). The air-conditioning system is sized correctly if it runs at its full capacity at the hottest hour of the day. Also, continuously running air-conditioning system has the lowest peak performance. It is advised to consider continuous system operation (24/7) to reduce the maximum of required air-conditioning load.

Design data necessary for cooling load calculation:

- Comfort-based indoor design conditions (dry bulb temperature and relative humidity);
- Outdoor design conditions;
- Orientation of the building;
- Building envelope and U-values;
- Specific characteristics of the air-conditioned space (occupancy, function, use schedule, equipment and lightning use).

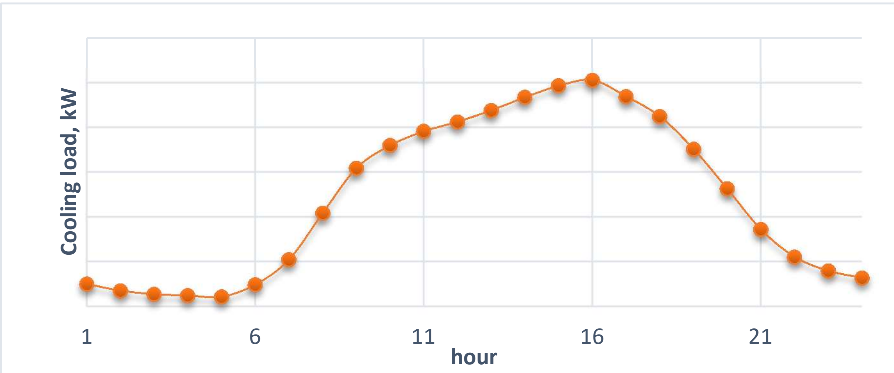

Figure 3.9. Typical Daily Cooling Load Distribution.

3.2.2. Heat Exchanger

A heat exchanger is a device that helps to transfer heat between mediums without a direct contact. The basic concept is that the heat loss on the hot side of the exchanger equals to the heat gain on the cold side. There is a variety of types, sizes and materials for heat exchangers, but counter flow plate-type titanium heat exchangers are the best option for SWAC application. Titanium is a high corrosion resistant material and titanium plates are very durable and well proven for heat transfer in SWAC systems. In the plate type heat exchanger, water flows through baffles that separate fluids, that results in larger heat transfer area and higher efficiency than in the shell and tube exchangers. In the counter-flow heat exchanger, fluids enter from opposite sides of the element and reach a higher heat transfer efficiency compared to the parallel-flow and cross-flow exchangers. Moreover, the plate type heat exchanger requires less space than other units and the number of the plate can be easily manipulated in case of a change in cooling load in the future.

The log mean temperature difference (*LMTD*) method can be used for selecting a heat exchanger that meets system heat transfer requirements when all inlet and outlet temperatures are specified (Figure 3.10). The size and cost of the heat exchanger are determined by the surface area of heat transfer.

The overall heat transfer rate is represented by:

$$\dot{Q}_{load} = U_h A_h (LMTD) \tag{3.3}$$

Where $\dot{Q}_{load}$ is the heat transfer rate, U_h is the overall heat transfer coefficient, A_h is the effective heat transfer surface area and *LMTD* is the log mean temperature difference.

LMTD is defined by the temperature differences at inlet and outlet of heat exchanger divided by their logarithmic ratio:

$$LMTD = \frac{\Delta T_2 - \Delta T_1}{ln\frac{\Delta T_2}{\Delta T_1}} \tag{3.4}$$

Where $T^s_{HE,in}$ is the seawater temperature at the inlet of the heat exchanger, $T^s_{HE,out}$ is the seawater temperature at the outlet of the heat exchanger, $T^f_{HE,in}$ is the fresh water temperature at the inlet of the heat exchanger and $T^f_{HE,out}$ is the fresh water temperature at the outlet of the heat exchanger.

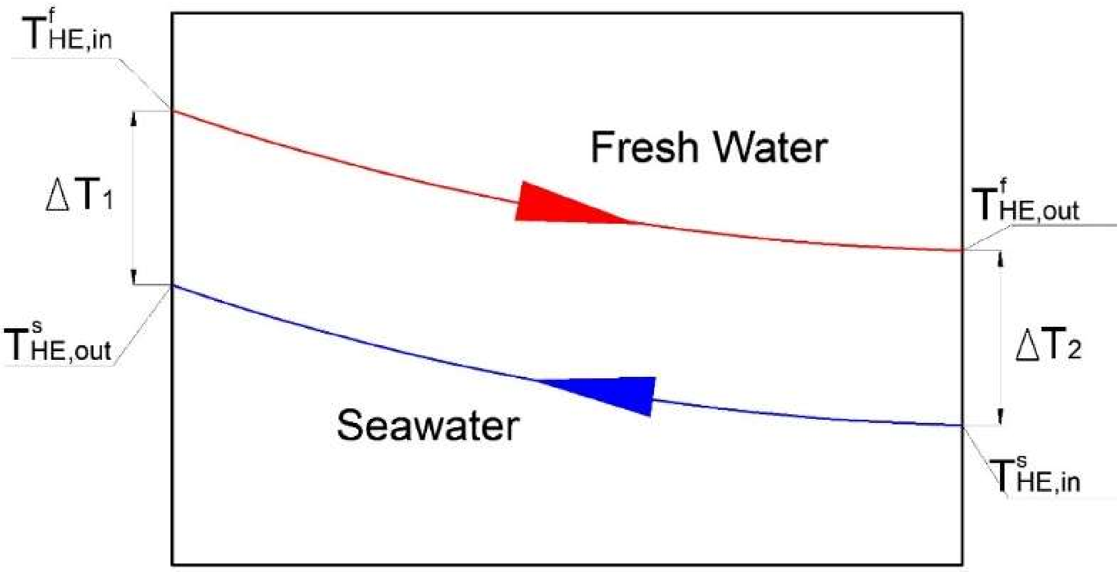

Figure 3.10. Temperature Profile in the Counter Flow Heat Exchanger.

The overall heat transfer coefficient, U_h, represents the resistance to heat transfer between fluids. It is a function of fluid properties, the material of a heat exchanger and flow geometry and for titanium heat exchanger its value can be expected to be 7166.4 W/m^2 ^{o}C [27].

Inlet and outlet temperatures on the seawater side of the heat exchanger are defined by the SWAC intake temperature and the required outfall temperature at the discharge depth. For indirectly seawater-cooled chiller units, the characteristics of the fresh water side are specified by the chiller unit manufacturer. For the hybrid systems, the fresh water temperature at the inlet of the heat exchanger can be assumed 12^{o}C which is the typical temperature of water returned from the air handling unit. The fresh water temperature at the outlet depends on the amount of heat that seawater can accept in the heat exchanger.

The total temperature rise of water circulating through buildings can be assumed 6-7^{o}C after it absorbs heat from spaces and experiences heat gain due to friction and conduction in the pipe network.

In the hybrid SWAC system, the total heat absorbed by the fresh water, $\dot{Q}_{load}$, has to be balanced by the heat transferred to seawater in the heat exchanger, $\dot{Q}_{HE}$, and in water-cooled chiller, $\dot{Q}_c^w$:

$$\dot{Q}_{load} = \dot{Q}_{HE} + \dot{Q}_c^w \tag{3.5}$$

The heat transfer equation:

$$\dot{Q}_{load} = \dot{m}_f C_{pf}\ \Delta T_f \tag{3.6}$$

Where total temperature change on the fresh water side, ΔT_f, can be split into temperature drop in the heat exchanger, ΔT_{HE}^f, and in the chiller unit, ΔT_c^f . The mass flow rate in the fresh water loop, $\dot{m}_f$, is the same for every component, as well as the specific heat value for the fresh water, C_{pf}, can be assumed constant with the value of 4186 J/kg ºC, since the temperature change is relatively small [28]. Therefore,

$$\Delta T_f = \Delta T_{HE}^f + \Delta T_c^f \tag{3.7}$$

Energy balance inside the heat exchanger can be similarly expressed as:

$$\dot{Q}_{HE} = \dot{m}_f C_{pf}\ (T_{HE,in}^f - T_{HE,out}^f) \tag{3.8}$$

Where $T_{HE,in}^f$ and $T_{HE,out}^f$ are fresh water temperatures at the entrance and exit of the heat exchanger correspondingly. The temperature at the heat exchanger exit tends to approach the entrance seawater temperature with some constant tolerance, δT_{f-s}^{HE}, that can be assumed as 1ºC [28]. Therefore,

$$\dot{Q}_{HE} = \dot{m}_f C_{pf}\ (T_{HE,in}^f - T_{HE,in}^s + \delta T_{f-s}^{HE} + \Delta T_{s,pipe}) \tag{3.9}$$

The remaining cooling has to be provided by the chiller unit.

There is a wide range of heat exchanger design software available, and Aspen Exchanger Design and Rating is one of the leaders on the market. It allows to evaluate the optimum heat exchanger configuration for given initial conditions and a fouling factor based on *LMTD* method. It specifies the size, cost and flow rate, required for further design and system evaluation.

3.2.3. Intake and Discharge Pipelines

High density polyethylene (HDPE) has significant advantages for seawater intake pipelines since it is inert and will neither corrode nor contaminate the water. Polyethylene also has excellent strength and flexibility and is buoyant. Before the deployment, polyethylene lengths are heat fused together onshore. They form a long continuous pipeline with joints that are as strong as the pipe itself and then are later submerged. These characteristics allow a large amount of design flexibility and deployment ease. The pipe wall thickness varies depending on strength requirements for deployment and operating suction over the lifetime of the pipe.

The pipeline length is dependent on the topography of the sea bottom and can be approximated using the rule of Pythagoras, as the square root of the sum squared horizontal distance and corresponding depth. 10% safety factor should be applied to account modulation of the pipe on the seabed [2].

Noise, erosion, installation and operation costs limit the value of maximum and minimum velocities at the pipe. The too small size of the pipe leads to noise, erosion and high pumping cost when the too large pipe size leads to the high installation costs. Therefore, to minimize the initial cost and negative effect of velocity it is recommended that the maximum velocity of cold liquid flow in pipes should not exceed 2.4 m/s [29].

To estimate the intake pipe diameter the heat transfer equation is used:

$$\dot{Q}_{load} = \dot{m}_s C_{ps}\, \Delta T_{HE}^{s} \tag{3.10}$$

Where $\dot{m}_s$ is the mass flow rate of seawater inside the intake pipeline, $\dot{Q}_{load}$ is the heat transfer rate, ΔT_{HE}^{s} is the change in seawater temperature across the heat exchanger and C_{ps} is the specific heat capacity of seawater at constant pressure.

Seawater mass flow rate, as well as the change in seawater temperature across the heat exchanger, are defined from the heat exchanger modeling.

Volumetric flow rate:

$$Q = \dot{m}_s/\rho \tag{3.11}$$

And finally, average velocity inside the pipe:

$$V = 4Q/\pi D^2 \tag{3.12}$$

where D is the inside pipe diameter.

The intake pipe diameter has to be adjusted to the average flow velocity. The major requirement is that velocity should not exceed 2.4 m/s and the flow rate has to stay on the level required by the heat exchanger. If the flow velocity exceeds 2.4 m/s the pipe diameter has to be increased.

3.2.4. Heat Gain in the Intake Pipeline

While cold seawater travels to the shore, it tends to gain some heat due to the non-constant ambient water temperature outside the pipe, which is typically higher than the seawater temperature at the intake location.

To evaluate the seawater temperature rise in the intake line, the pipeline should be divided into a number of sections. The temperature gain in each section can be depending on the average ambient water temperature in the relevant section. The final temperature that arrives at the heat exchanger is determined by the cumulative sum of the initial intake temperature and the heat gains along the pipe [27].

The heat transferred across the seawater supply line is absorbed by the seawater inside the pipe:

$$\dot{m}_s C_{ps} \Delta T_{s,pipe} = U\left[T_a - \left(T_m + \Delta T_{s,pipe}/2\right)\right] \tag{3.13}$$

Where U is the overall heat transfer coefficient of the pipe, T_m is the average water temperature in the intake pipe and T_a is the average ambient water temperature on the external surface of the pipe.

The seawater temperature change, $\Delta T_{s,pipe}$, in the supply line:

$$\Delta T_{s,pipe} = 2U(T_a - T_m)/\left(2mC_{ps} + U\right) \tag{3.14}$$

The final exit temperature for every section of the pipeline is determined as:

$$T_m = T_{in} + \Delta T_{s,pipe} \tag{3.15}$$

where T_{in} is the intake seawater temperature.

The overall heat transfer coefficient:

$$U = 1/R \tag{3.16}$$

The thermal resistance, R, to heat transfer through the seawater supply pipeline, can be found as:

$$R = \frac{1}{h_i A_i} + \frac{ln\frac{r_o}{r_i}}{2\pi L k_p} + \frac{1}{h_0 A_0} \tag{3.17}$$

Where h_i is the convective heat transfer coefficient of the seawater flowing inside the pipe, h_o is the convective heat transfer coefficient of the seawater flowing outside the line, r_i is the inside radius of the pipe, r_o is the outside radius of the pipe and k_p is the thermal conductivity of the pipe. For HPDE pipe the thermal conductivity can be assumed as k_p=0.465 W/m K.

The convective heat transfer coefficient of the seawater outside the pipe:

$$h_0 = k_s Nu_o / D_0 \tag{3.18}$$

Where k_s is the seawater thermal conductivity, Nu_o is the Nusselt number for conditions outside the pipe and D_o is the outside pipe diameter.

The Nusselt Number for conditions outside the pipe is determined by the Dittus-Boulter equation:

$$Nu_o = 0.023(Re^{0.8} \cdot Pr^{0.4}) \tag{3.19}$$

$$Re = VD/\nu \tag{3.20}$$

Where *Re* is the Reynold's Number of the flow outside the pipe, ν is the seawater kinematic viscosity and *Pr* is the Prandtl Number of conditions outside the pipe.

The scheme of finding the convective heat transfer coefficient for water flowing inside the pipeline is the same as it is for seawater outside the pipe. All seawater physical properties can be defined from Table E.1 - Table E.5 for corresponding salinity and temperature values.

Based on previous design experiences, the heat gain due to the friction is relatively small and can be neglected.

3.2.5. Seawater Intake Pump

To select a suitable pump for the SWAC system the flow and the pumping head have to be known. The flow rate is set by the heat exchanger requirements. The pumping head can be estimated from the energy equation applied between the seawater intake structure and the exit of the heat exchanger:

$$(P/\gamma + V^2/2g + Z)_1 = (P/\gamma + V^2/2g + Z)_2 + h_L \quad (3.21)$$

Where h_L is the total head loss, P_1 and P_2 are absolute pressures of seawater at the intake location and at the outlet of the intake pipeline respectively, Z_1 is the elevation of the intake location from the datum, Z_2 is the elevation onshore cooling facilities from the datum, V_1 is the seawater intake velocity and V_2 is the final seawater velocity in the pipe, g is the gravitational acceleration and γ is the specific weight of water.

The absolute pressure of seawater at the outlet of the intake pipeline is assumed to be equal to the atmospheric pressure since the seawater in the discharge line can flow gradually back to the sea under the effect of gravity and fluid momentum.

The flow inside the pipe is assumed to be incompressible and completely bounded, so the flow velocity is the same over the entire length of the pipe.

The total pumping head, h, can be expressed as follows:

$$h = P_1 - P_2 = \gamma[(Z_2 - Z_1) + (V_2^2 - V_1^2)/2g + h_L] \quad (3.22)$$

Where the total head loss results from the minor and major losses. The major loss is the frictional head loss, h_f, arising from the pipe wall friction and the viscous dissipation on flowing water. This loss is the primary concern for the long pipeline. The frictional head loss is found as:

$$h_f = fLV^2/2Dg \quad (3.23)$$

Where f is the friction factor, L is the pipeline length, D is the inside pipe diameter and V is the flow velocity.

The head losses must be calculated differently depending on whether the flow is laminar or turbulent. The flow type depends on its Reynolds Number that can be found from equation (3.20).

If the Reynolds Number is less than 2300, the flow in the pipe is considered to be laminar, and the friction factor can be found from the equation:

$$f = 64/Re \tag{3.24}$$

In the laminar flow, the pressure loss is dependent only on the Reynolds Number. For Reynolds Number larger than 2300, the flow is assumed to be turbulent. As the flow becomes turbulent, the friction factor depends on the relative roughness of the pipe surface rather than the Reynolds Number. The relative roughness of the pipe is determined from the pipe characteristics and is expressed as ε/D, where ε is the roughness height. And D is the pipe diameter. Roughness values for some common materials are given in Table F.2 in Appendix F. Using the relative roughness, the friction factor can be found from the Moody diagram (Figure F.1).

Minor losses are related to valves, tees, elbows and entrances. Changes in the pipe cross-section or the flow direction causes energy loss, and therefore should be taken into account in the hydraulic design.

Minor losses:

$$h_m = \sum k\, v^2/2g \tag{3.25}$$

where k is the minor loss coefficient.

The minor loss coefficient is different for each component of the pipe, and it is typically provided by the manufacturer or can be taken from generic tables (Table F.1).

Finally, the total head loss can be found as the sum of the frictional loss and minor losses:

$$h_L = h_f + h_m \tag{3.26}$$

A large range of marine water pumps is available on the market. Aczue manufactures cooling sea water pumps with frequency converter that adjusts the motor according to the water temperature. The maximum flow rate of the pump can is 4000 m^3/h with a maximum pressure head of 225 meters of water column.

3.3. Analysis of Energy Consumption and Carbon Emission

The seawater pump and the chiller consume most of the electricity within the SWAC system.

To evaluate the chiller efficiency, the most commonly used metrics are the full load and the part-load efficiencies. The full-load efficiency is defined by the coefficient of performance (*COP*) or energy efficiency ratio (EER). *COP* is based on the amount of power consumed by a system, compared to its power output. The EER is calculated as the rated capacity of the system divided by its rated total power input, including the total energy consumed by fans, pumps and controls. The higher the *COP* and the EER value the more efficient is the system.

At the part-load, the efficiency of the chiller is measured by integrated part-load value (IPLV) or by nonstandard part-load value (NPLV), depending on particular part-load test conditions. Both factors express the efficiency of the chiller using a weighted average referencing four operation load points (100%, 75%, 50% and 25%).

Chiller's performance coefficients depend on the maximum cooling capacity of the chiller and its work principle. All values for full and partial load operation usually are provided by the manufacturers.

For the air and seawater-cooled chiller units, the maximum capacity of the chiller should match the full cooling load requirements. Then the electrical power, W_c^w, required to operate the unit can be found as:

$$W_c^w = \dot{Q}_{load}/COP \tag{3.27}$$

However, in the hybrid system, part of the load is rejected to the seawater in the heat exchanger, so the chiller unit has to provide only the remaining cooling. In this case, the gross cooling power required for cooling can be represented as the sum of individual power contributions from each unit involved in the system [28]:

$$\dot{Q}_{load} = \dot{Q}_{HE} + \dot{Q}_c^w \tag{3.28}$$

Then the power required to run the water-cooled chiller, W_c^w, can be found as:

$$W_c^w = (\dot{Q}_{load} - \dot{Q}_{HE})\ /COP \tag{3.29}$$

In terms of temperatures at the heat exchanger, equation (3.29) can be expressed as:

$$W_c^w = (\dot{Q}_{load} - \dot{m}_f C_{pf}\ (T_{HE,in}^f - T_{HE,in}^s + \delta T_{f-s}^{HE} + \Delta T_{s,pipe})/COP \tag{3.30}$$

The final SWAC power requirement can be estimated from the sum of the power required for the water-cooled chiller unit operation and the pumping power.

In the case when the water-cooled chiller is directly cooled by the seawater, its internal piping system is usually made of copper nickel or titanium that are corrosion resistant materials with a long life expectancy. Such chillers are approximately 6% less efficient than fresh water-cooled units with copper heat exchanger tubes inside the condenser [30].

The power required to pump seawater from the intake depth to the heat exchanger can be found as follows:

$$W_p = \rho\ g\ h\ q/\eta \tag{3.31}$$

Where W_p is the pumping power, ρ is the seawater density, h is the pumping head, q is the flow rate and η is the pump efficiency, assumed 80%.

The greenhouse gas footprint of the SWAC system is defined by its electricity use. Since coal and natural gas are dominant sources of electrical power in Europe, SWAC application may result in significant reduction of carbon dioxide (CO_2) emission. To evaluate carbon footprint of cooling system the emission rate factor assigned by U.S. Environmental Protection Agency in 2015 can be used. It assumes 0.7 kg of CO_2 equivalent per one kilowatt-hour of electricity.

4. ECONOMIC ANALYSIS

Economic analysis chapter provides a guideline for the comparison of SWAC and conventional air-conditioning regarding capital and operating costs. For this analysis, it is assumed that the cooling system operates continuously (24/7) for four months during the summer, from June to September.

4.1. Capital Cost

There are a few key components of the capital cost of the SWAC system: intake and discharge pipelines, seawater pump, heat exchanger and optionally chiller unit. For the comparison to the conventional air-conditioning, the cost of the only air-cooled chiller in it should be assumed. The capital costs of all system elements can be obtained from manufacturers, modeled by software or defined from reference values from the current mechanical equipment price book.

The common way to estimate the equipment cost is by using the thumb rule of the *N* exponent and the use of cost indices to adjust costs to current prices. This rule approximates the cost of the item if the cost of a similar item of different size or capacity is known, and can be expressed as:

$$C_B = C_A \left({S_B}/{S_A} \right)^N \tag{3.32}$$

Where C_B is the cost of equipment of the size or capacity S_B, C_A is the known cost of the reference equipment with the size S_A and *N* is the empirical exponent.

The exponent factor value varies from 0.3 to 1 with the average near to 0.6. The use of the average value provides satisfactory price estimation with 20% approximation. For more accurate cost estimation, the *N* factor value can be set according to the equipment type (Table G.1).

If the known cost of equipment is based on the old price, the current cost of the piece can be approximated using a cost index that reflects the current cost compared to the baseline:

$$C_r = C_o \left({}^{I}/_{I_o} \right) \tag{3.33}$$

Where C_r is the current reference cost, C_o is the base cost, I is the current index and I_o is the reference index. There are many cost indices available on the market. The widely used one in the construction industry is the Marshall and Swift Equipment Cost Index.

4.2. Energy Cost

The largest savings from SWAC systems are expected to come from the reduction in energy use which primarily depends on the local electrical price and the efficiency of the equipment used. For the analysis, it is assumed that the cooling system operates 24 hours on a hot summer day. Present electricity prices in coastal communities around the Black Sea are given in Table 4.1.

Table 4.1. Electricity Prices in Countries around the Black Sea.

Country	**Electricity price, USD per kWh**
Turkey	0.132
Romania	0.131
Bulgaria	0.100
Georgia	0.094
Russia	0.062
Ukraine	0.062

4.3. Life-Cycle Cost

A final comparison of cooling systems to determine the most cost-effective alternative to conventional cooling in the Black Sea region is based on the life-cycle cost analysis.

In order to estimate the total cost of the ownership, few assumptions have to be made [2]:

- The entire capital cost of the system is spent in the first year;
- All systems have a life-cycle of 30 years;
- Energy costs are uniform series of payments with one year interval with the present value at interest rate of 7% common on electricity suppliers market;
- The cost of system maintenance is not considered for the calculations since it is assumed to be equal for all system configurations.

The present value *P* of a uniform series of yearly payment of amount *A* over *n* year at interest rate i can be found as:

$$P = A\left({(1+i)^n - 1}\big/{i(1+i)^n}\right) \tag{3.34}$$

5. CASE STUDY: BOĞAZİÇİ UNIVERSITY SARITEPE CAMPUS

Boğaziçi University Sarıtepe Campus locate at the Black Sea coast of Istanbul serves as a good example for the feasibility assessment of the SWAC system application in the Black Sea region. It is located in an area with a large cooling demand due to the high summer air temperature, and the electricity price of Turkey is the highest in the region.

Boğaziçi University is one of the leading science organizations in Turkey. A considerable amount of research on the topic of renewable energy and energy efficient technologies happen at the institution. Recently one of the most outstanding projects of Boğaziçi University is the development of the completely self-sufficient Zero Net Energy Campus at Sarıtepe Campus, the youngest campus of the University, located on the Black Sea coast of Istanbul. The campus operates a 1-MW Wind Energy Converter (WEC) and pursues research for several other renewable energy options, such as solar, biomass and wave energy. The WEC supplies yearly 1.5 million kWh, which covers the entire electricity demand of the campus and more. It also saves 1000 tons of carbon dioxide emission and approximately 200.000 USD on energy cost per year. Along with the wind turbine, the research on a new seawater treatment facility involving desalination, on algal biotechnology center and on heat conversion technologies is conducted at the campus. However, ample room remains for new renewable technologies at the shore, taking the advantageous of the campus location, its close proximity to the cold waters of the Black Sea. Since freshman students regularly live and study at the campus throughout the year, Sarıtepe Campus can be considered as a small-scale example of a green city. Dormitories, an indoor sports complex, hotel for 88 guests, the language school facilities and three laboratories are the main air-conditioning consumers of the campus (Figure 5.1).

5.1. Meteorologic and Oceanographic Analysis

Sarıtepe Campus is situated on the Black Sea coast of Istanbul, 9 kilometers west of the Strait of Istanbul. The mild bottom slopes of the near-shore zone increase the distance to the depths with sufficiently cold seawater, and consequently, high capital and operating costs of the system. Therefore, the application of SWAC system here becomes an example of the “worst case scenario” and reflects the feasibility of SWAC for the entire Black Sea region.

Figure 5.1. Boğaziçi University Sarıtepe Campus.

The continental shelf zone of this area is characterized with a mildly sloped bathymetry (approximately 1:9) up to 50 meters of depth. It is followed by the broad valley area with almost horizontal bottom, which it abruptly ends at 100 meters of depth (Figure 5.2, Figure 5.3). The shelf zone creates a boundary for the SWAC system’s deepest intake location.

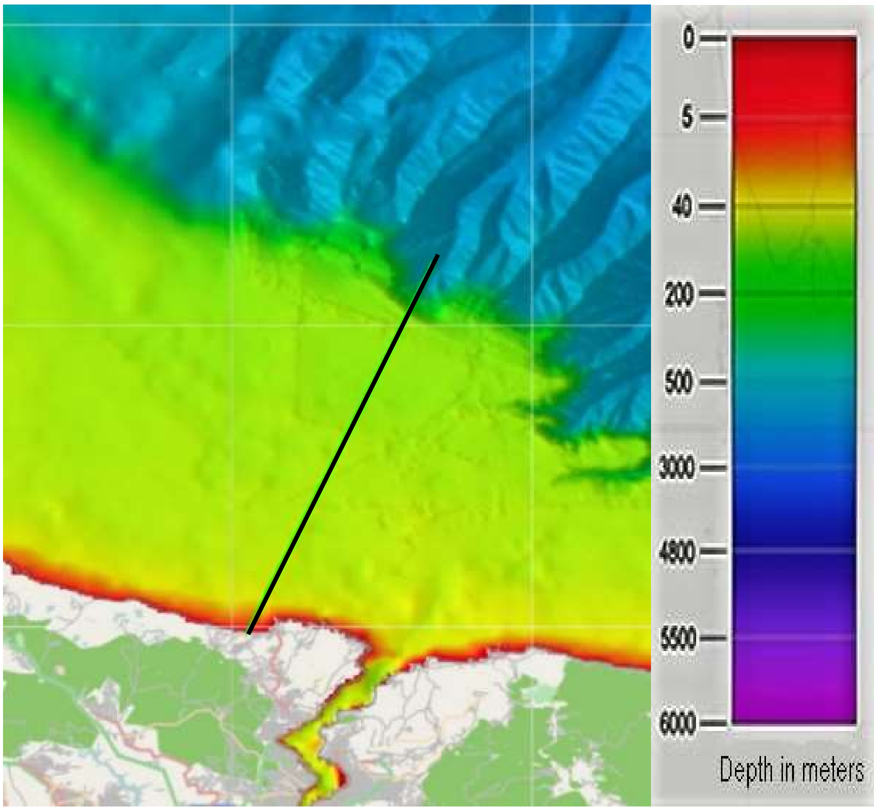

Figure 5.2. Black Sea Bathymetry Map [31].

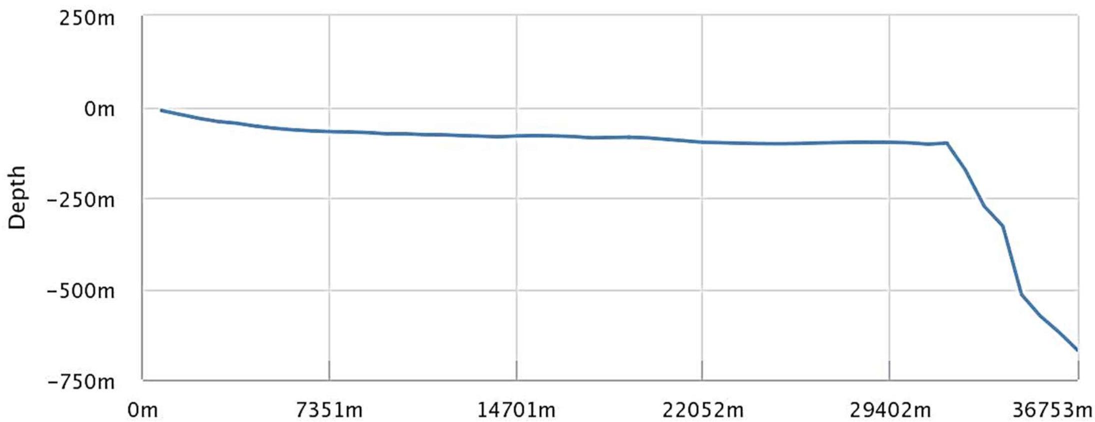

Figure 5.3. Depth Profile [31].

Seawater temperature fluctuations at seven depths available in Operational Mercator global ocean model from the sea surface up to 110 meters were examined in the study (Figure 5.4). The seasonal effect strongly influences the thermal variability of the sea upper layer up to 30 meters depth. This effect diminishes for deeper layers and is almost not observed at a depth of 65 meters, which can be assumed to be CIL based on previous studies. The water temperature here is mostly stable at 8ºC throughout all seasons with occasional fluctuations to 10-11ºC.

To evaluate the stability of cold seawater production at various depths, the probability density function together with the cumulative distribution function (Figure 5.5 - Figure 5.9) of water temperatures and of the temperature difference between the surface and the particular depth at each depth were examined.

In the upper 20 meters of the sea, water temperature fluctuates in the range of 20- 27ºC. The typical temperature difference between the bottom and the surface water is less than 3ºC. These depths cannot provide stable cold seawater to the SWAC system. Therefore, they are not considered as the seawater intake location. The final decision will be made based on heat exchanger modeling and hydraulic design.

For the estimation of the discharge location, the closure depth was calculated based on Hallermeir's formula. In Kilyos Beach, the extreme wave height is calculated as 3.8 meters with an exceedance probability of 12 hours per year. The corresponding wave period is 11 seconds and the closure depth here is 7.8 meters [32]. Taking into account a possible additional height of the outlet structure over the sea bottom, the minimum depth of the SWAC water discharge is set to 10 meters depth. The design temperature for the seawater discharge is assumed to be 24ºC which is the measured temperature at 10 meters depth. With a 2ºC tolerance, this temperature satisfies the environmental requirement at least in 80% of times (Figure 5.7).

Cumulative distribution function of temperature difference between a particular depth and the depth of discharge is shown in Figure 5.9. In most cases, the discharge will be in shallow water which is characterized as the surface water. Therefore the surface water temperature serves as a measure for which the system is designed to still operate safely. The optimum temperature change in the heat exchanger will be determined accordingly.

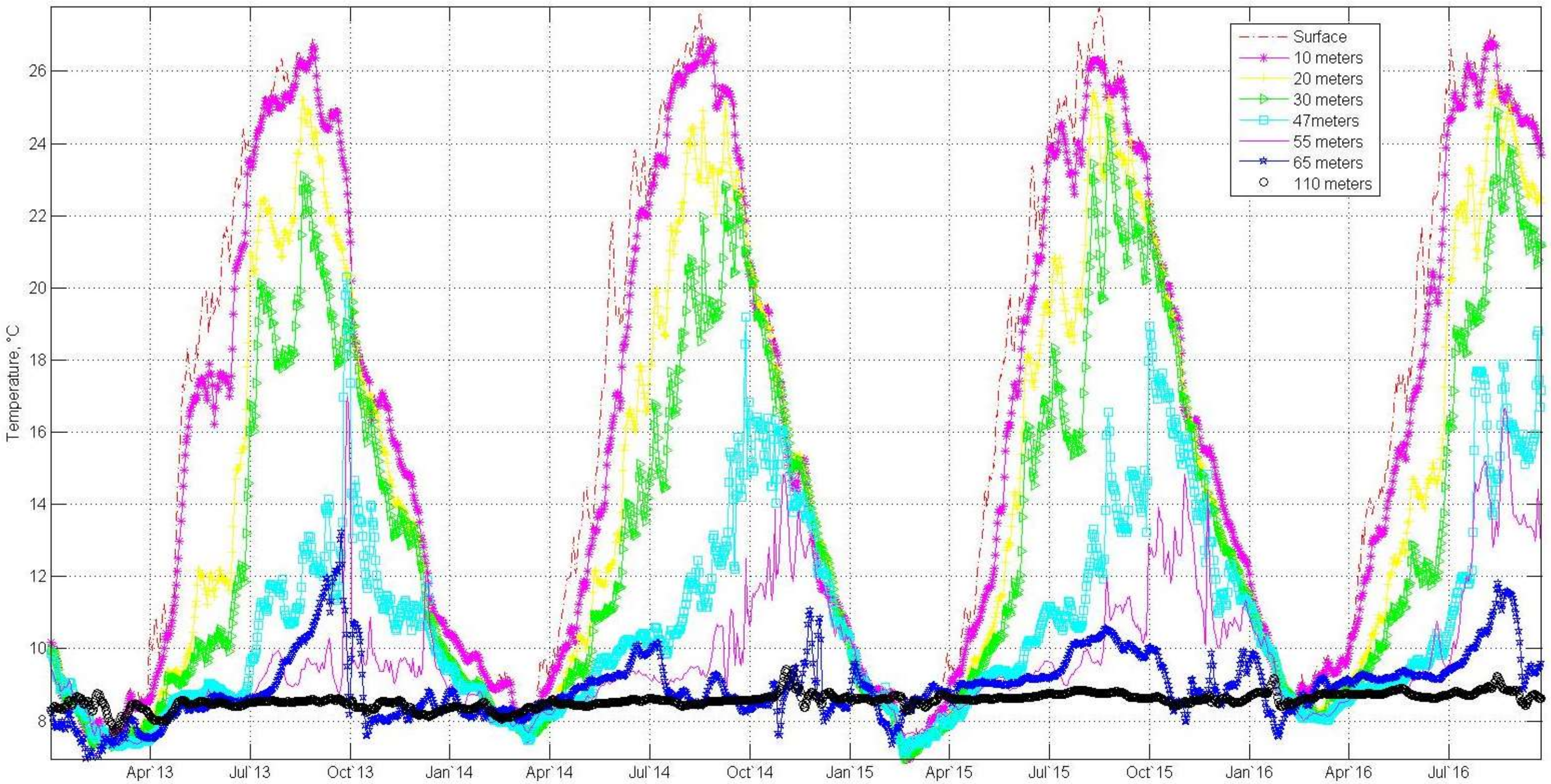

Figure 5.4. Seawater Temperature Fluctuation at Different Depths.

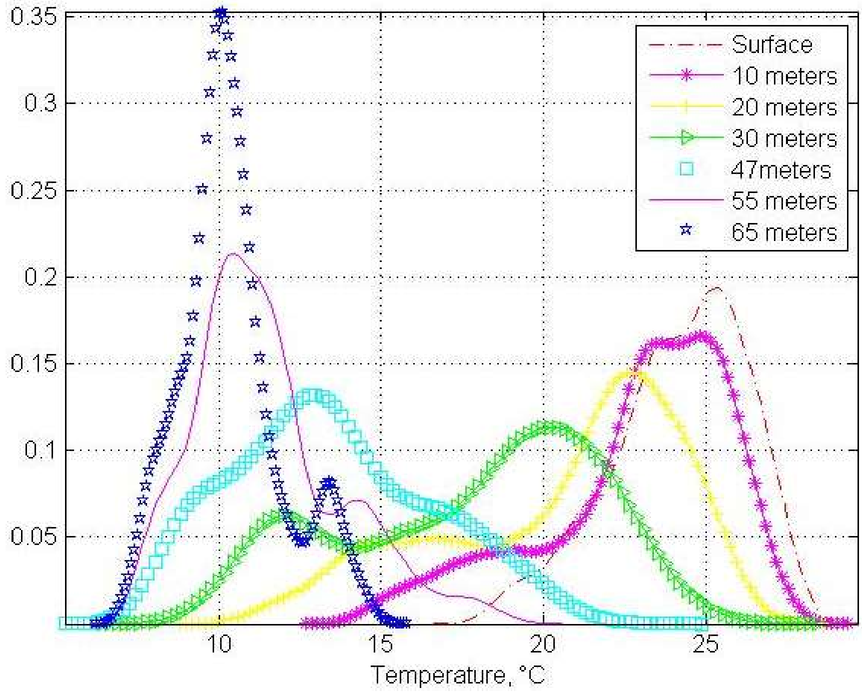

Figure 5.5. Probability Density Function of Seawater Temperature at Different Depths.

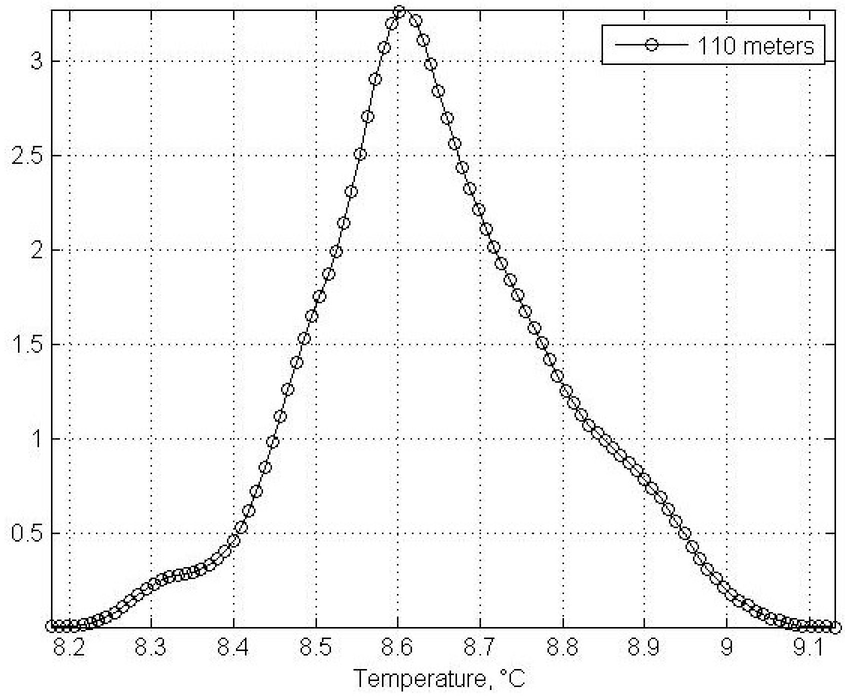

Figure 5.6. Probability Density Function of Seawater Temperature at 110 Meters of Depth.

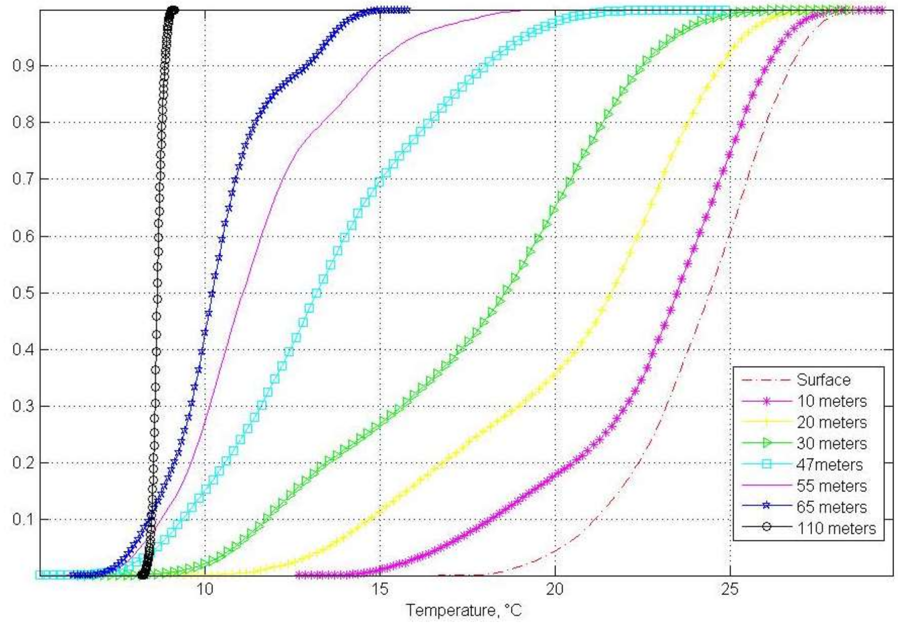

Figure 5.7. Cumulative Distribution Function of Seawater Temperature at Different Depths.

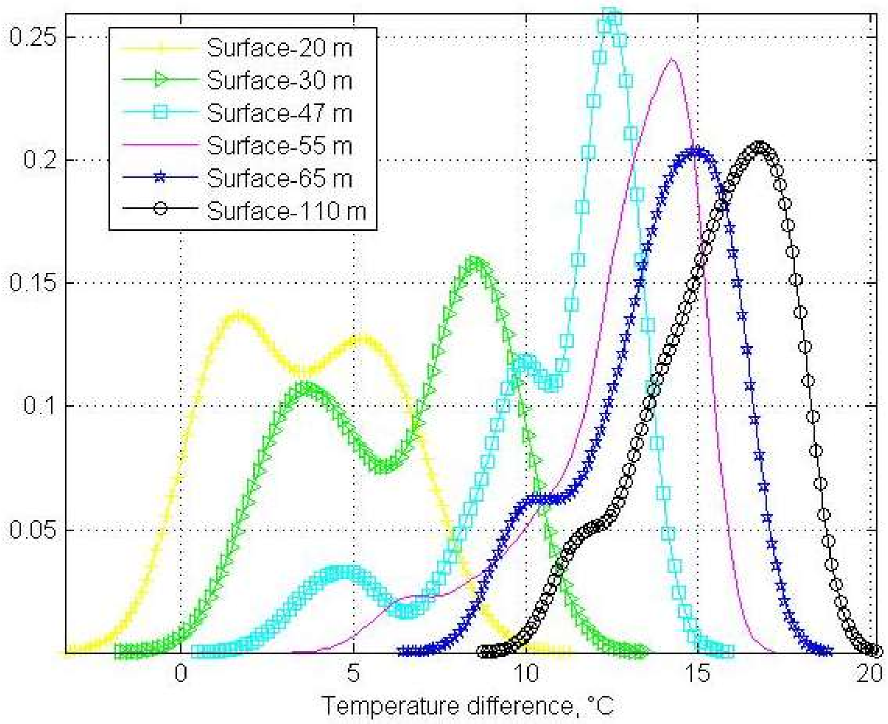

Figure 5.8. Probability Density Function of Temperature Difference for Different Depths.

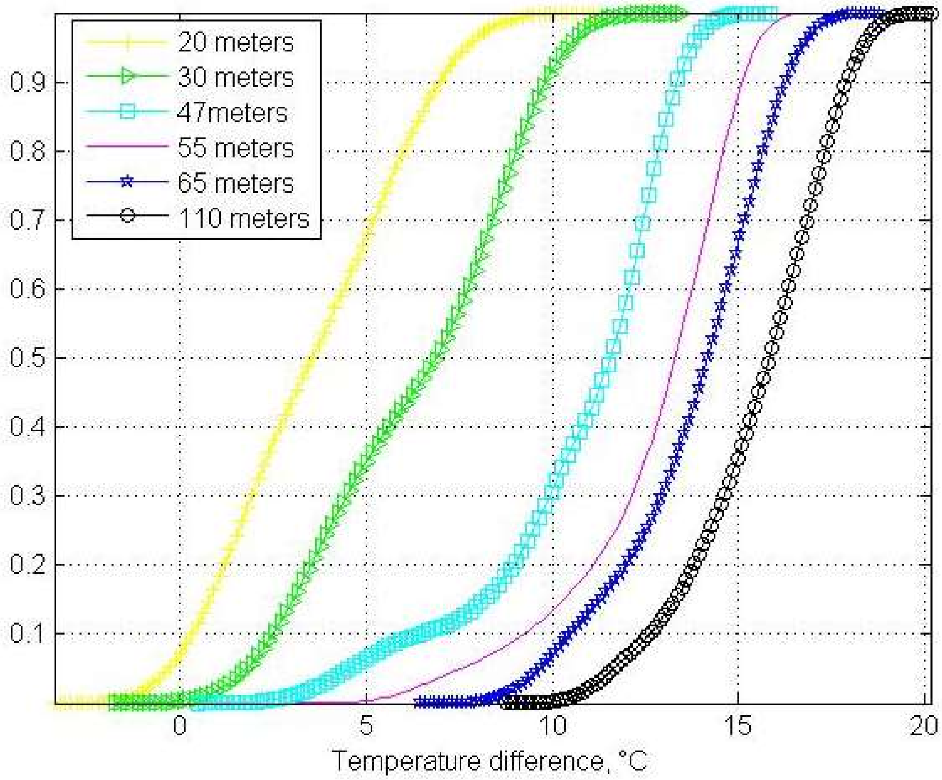

Figure 5.9. Cumulative Distribution Function of Temperature Difference for Different Depths.

5.2. Engineering Analysis

The engineering analysis chapter of the SWAC case study provides the detailed design and modeling of system components. It includes a comparison of SWAC with the conventional system in terms of energy consumption and carbon dioxide emission.

5.2.1. Air-Conditioning Demand Estimation

In this study linear GmbH Building software was used for the cooling demand calculation. Each building of the campus was modeled room-by-room, based on the volume, orientation, use schedule, envelope U-values, room types and occupancy rates. Detailed modeling results of cooling demand for every building are attached in the Appendix (Figure H.1 – Figure H.7). Outdoor design conditions assumed for Istanbul were taken from 2005 ASHRAE Handbook –Fundamentals (Figure A.2). Spatial geometries of all analyzed buildings were imported from the AutoCAD files. As a result, the peak cooling demand of the entire campus is calculated as 1011 kW occurring at 4 PM in summer with the assumption of continuous HVAC system operation. (Figure 5.10).

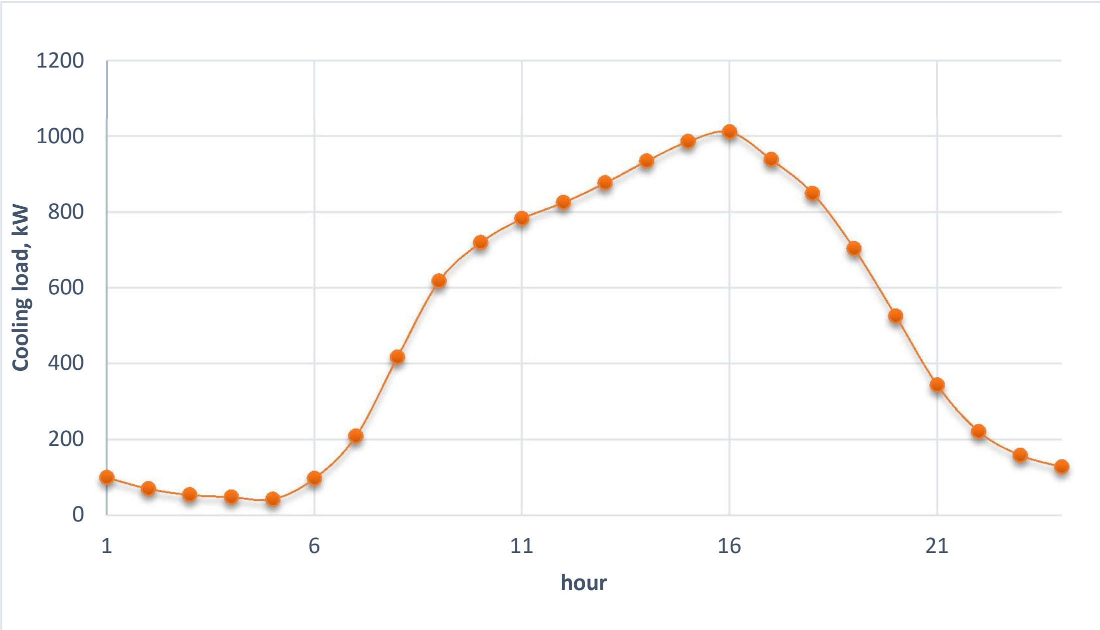

Figure 5.10. Campus Cooling Demand.

5.2.2. Selection of System Configuration

Currently, 1200 students live on the campus. Due to the future plans for campus expansion, the number of students may increase up to 2000 in the next five years and potentially reaching with a maximum number of 3000 students by the year of 2030s. Campus cooling demand needs to be increased accordingly. Therefore, cooling loads of 1000 kW, 1500 kW and 2000 kW are considered for the research to evaluate future scenarios.

For the SWAC assessment of the present university campus, the deepest intake location is limited because of a broad underwater valley at the seabed starting after 50 meters depth. This horizontal zone of the sea floor economically is not feasible for intake, since the average temperature change per kilometer is extremely low here (Figure 5.11). Therefore, only two possible depths of 30 and 47 meters will be analyzed as the intake locations.

Since the water temperature at the seafloor in the Black Sea is not cold enough for standalone SWAC systems, a hybrid system or a seawater-cooled chiller unit has to be considered for the campus. On the other hand, the mean water temperature 13°C at 47 meters depth is not enough for primary cooling of water returning from the building. Therefore, a hybrid SWAC system cannot be used either.

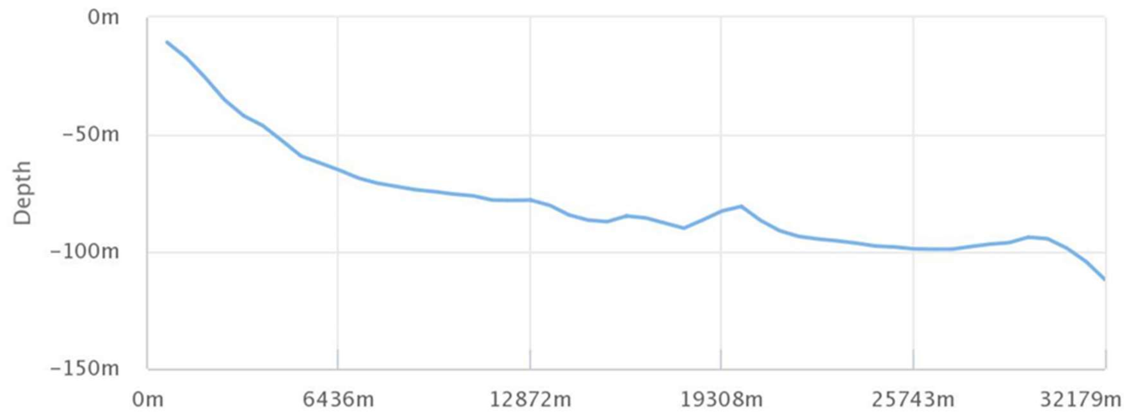

Figure 5.11. Bathymetry Profile in the Area of the University Campus [31].

Different configurations of direct and indirect seawater-cooled chiller units are analyzed. Operational properties of chiller units of two HVAC equipment manufacturers, YORK and Carrier, were used in the model. Their products comply with the current Turkish energy standards and achieve good efficiencies at true operating conditions without compromising the environment.

5.2.3. Heat Exchanger Design

The heat exchanger was modeled with the Aspen Exchanger Design and Rating V 8.8 to find the optimum solution in the range of available temperatures. Model outcomes include required mass flow rate on the cold side of the heat exchanger and equipment cost associated with various temperature for three cooling load scenarios (1000 kW, 1500 kW, 2000 kW) demanded by the campus.

The values of cold side inlet and outlet temperatures for the heat exchanger model were chosen based on the statistical analysis of seawater temperature in the Black Sea. The range of outlet temperature on the seaside of the exchanger corresponds to temperatures at shallow waters which is usually set as a discharge depth. The heat exchanger outlet temperatures were assumed to be 20 - 27ºC. Temperatures between 8ºC and 26ºC were selected as cold side inlet temperatures since they occur at potential intake depths analyzed in this study.

Deposits contaminate a heat exchanger surface and create an insulating layer that reduces heat transfer rate in time. Fouling occurs due to algae growth, salt deposition or unfiltered dirt. Typical fouling factor for fresh or seawater was assumed 0.0001 m^2 K/W.

The fluid properties on the hot side of the heat exchanger were constant and specified by chiller unit requirements. High efficiency variable speed screw chiller 23 XRV with possible cooling capacity range 879 – 2110 kW is assumed for modeling. Its entering/leaving chilled water temperatures are 12/7ºC and entering/leaving condenser water temperatures (consequently, inlet and outlet temperatures on the hot side of the heat exchanger) are 30/35ºC. Required pressure and flow rate for every cooling capacity of the chiller unit are given in Table I.1 in Appendix I.

From the model results (Appendix J), it was found that it is economically viable to design the heat exchanger assuming the temperature difference on the cold side, not less than 4ºC (Figure 5.12 - Figure 5.14).

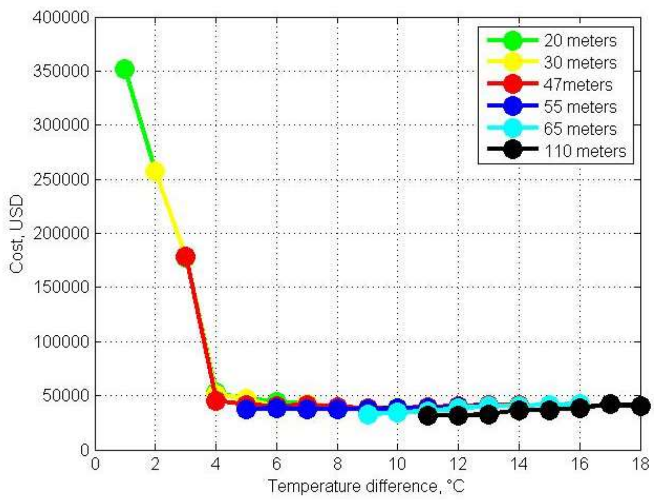

Figure 5.12. Heat Exchanger Cost Dependence on Temperature Difference at Cold Side (1000 kW).

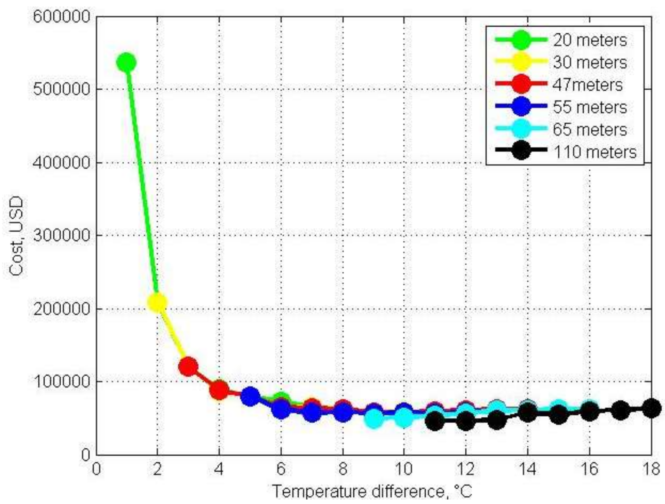

Figure 5.13. Heat Exchanger Cost Dependence on Temperature Difference at Cold Side (1500 kW).

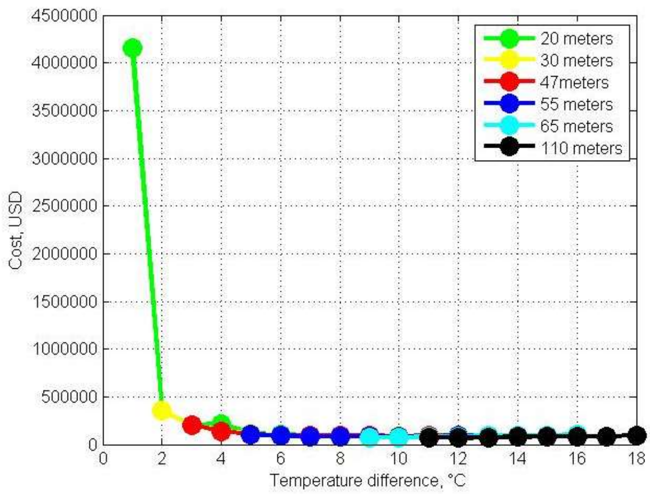

Figure 5.14. Heat Exchanger Cost Dependence on Temperature Difference at Cold Side (2000 kW).

If the working fluid temperature is too close to seawater temperature on the cold side, a very efficient and expensive heat exchanger is required. The probability of occurrence of temperature difference higher than 4 degrees at depths of 30 and 47 meters are 80% and 98% respectively (Figure 5.9). Therefore, these depths are two optimal locations of seawater intake for the university campus SWAC system.

5.2.4. Design of Seawater Intake and Discharge Pipes

The size of the intake pipe primarily depends on the required flow rate and velocity, defined by the heat exchanger, the flow type and associated heat and head losses.

Seawater properties were taken for an average seawater temperature of 16ºC between 30 and 47 meters depth and average salinity of 18 ppt at the Black Sea and were defined from Seawater Property Tables (Appendix E) and given in Table 5.1.

Table 5.1. Intake Seawater Properties.

Property	Value
Specific Heat Capacity at Constant Pressure, c_p, J/ kg K	4089
Density of Seawater, ρ, kg/m^3	1010.78
Prandtl Number, Pr	9.16
Kinematic Viscosity, μ x10^{-7}, μ, m^2/s	11.44
Dynamic Viscosity,v x 10^3, kg/s	1.2
Thermal Conductivity, k_s, W/m K	0.589

As it was previously stated, the average seawater velocity in the pipe should not exceed 2.4 m/s. Required flow rate is specified by heat exchanger characteristics. The optimum choice of pipe size may need a few iterations. Based on all these criteria, pipe with 250 mm diameter is an optimum size for the SWAC intake pipeline (Table 5.2). Flow characteristics of both water-cooled chillers are based on the same pipe diameter (Table I.1).

Temperature rise inside the selected intake pipeline and final seawater temperatures supplied to the heat exchanger are shown in Table 5.3 for different cooling load and intake locations considered in the study. Intake pipe lengths are 2400 meters and 3725 meters for the intake location at 30 and 47 meter depths respectively. The highest heat loss of 2ºC occurs when the seawater is taken at 47 m depth with the lowest flow rate.

Table 5.2. Seawater Intake Flow Characteristics.

Cooling Demand, kW	Pipe diameter, m	Flow rate, kg/s (m^3/s)		Velocity, m/s	
		30 meters	47 meters	30 meters	47 meters
1000	0.25	64.75 (0.06)	23.52 (0.02)	1.22	0.4
1500	0.25	92.05 (0.09)	33.45 (0.03)	1.83	0.61
2000	0.25	122.76 (0.12)	44.6 (0.04)	2.33	0.81

Table 5.3. Seawater Temperature Rise Inside the Intake Pipeline.

	30 meters			47 meters		
	1000 kW	1500 kW	2000 kW	1000 kW	1500 kW	2000 kW
Initial temperature, °C	20	20	20	13	13	13
Temperature rise, °C	0.52	0.37	0.28	2.11	1.52	1.16
Final temperature, °C	20.52	20.37	20.28	15.11	14.52	14.16

For the pumping head estimation, the elevation of the SWAC facility is assumed to be 8 meters above the sea level. The Reynolds Number exceeds 2300, and the flow is considered to be turbulent inside the pipe. The friction factor is determined from the Moody diagram.

Minor losses coefficient are as follows:

- Entrance loss: k=0,50;
- Exit loss: k=1,00;
- 90° elbow loss at velocity head: k= 0,3.

Varying pipeline lengths causes different amount of head loss which range 3.65 meters to 34.50 meters. Even though the pipeline up to 30 meters water depth is 1325 meters shorter than the one that goes to 47 meters, the head loss due to friction in the shorter pipeline is significantly higher due to the high flow rate required to provide the necessary cooling (Table 5.4).

Table 5.4. Pumping Head.

	30 meters			47 meters		
	1000 kW	**1500 kW**	**2000 kW**	**1000 kW**	**1500 kW**	**2000 kW**
Re	$2.48*10^5$	$3.5*10^5$	$4.3*10^5$	$2.48*10^5$	$3.5*10^5$	$4.3*10^5$
ε/D	$6*10^{-6}$	$6*10^{-6}$	$6*10^{-6}$	$6*10^{-6}$	$6*10^{-6}$	$6*10^{-6}$
f	0.013	0.013	0.013	0.013	0.013	0.013
h_f, m	9.46	21.29	34.5	1.57	3.67	6.47
h_m, m	0.15	0.3	0.46	0.15	0.3	0.46
h_L, m	9.61	21.59	34.96	1.72	3.97	6.93
h, m	39.61	51.59	64.96	48.72	50.97	53.93

The discharge pipeline brings the return water to the depth of 10 meters and was assumed to be 777 meters long with an inner diameter of 250 mm.

5.2.5. Electricity Consumption and Carbon Emissions

All *COP* values of air- and water-cooled chiller were taken from the chiller units specifications provided by the manufacturer (Appendix I). The efficiency of a directly seawater cooled chiller can be assumed 6% lower than the efficiency of chiller operating with fresh water [30]. The final annual electrical power consumption is found with the assumption that air cooling system operates only in hot season from June to September. For modeling of the future scenarios of cooling demand, a combination of two complementary air-cooled chiller units was assumed. Final annual power input required by the conventional air-conditioning system is shown in Table 5.5.

Table 5.5. Conventional Chiller's Power Consumption for Various Cooling Loads.

	1000 kW	**1500 kW**	**2000 kW**
Chiller capacity, kW	1000	1000+600	1000+1000
EER, BTU/Wh	3.1	3.1+3.09	3.1+3.1
Power input, kWh (per season)	464,343	696,515	928,687

Electricity consumption of the water-cooled chillers is the sum of power required by the chiller for heat transfer and the pumping power supply the necessary flow rate (Table 5.6 - Table 5.8).

Table 5.6. Indirectly Cooled Chiller's Power Consumption for Various Cooling Loads.

	1000 kW	**1500 kW**	**2000 kW**
Chiller capacity, kW	1055	1583	2110
COP	5.95	6.17	6.13
Power input, kWh (per season)	78,041	349,951	469,646

Table 5.7. Directly Cooled Chiller's Power Consumption for Various Cooling Loads.

	1000 kW	**1500 kW**	**2000 kW**
Chiller capacity, **kW**	1055	1000+600	2110
COP	5.65	5.86	5.82
Power input, kWh (per season)	82,148	368,369	494,364

Table 5.8. Pumping Power.

	30 meters			**47 meters**		
	1000 kW	**1500 kW**	**2000 kW**	**1000 kW**	**1500 kW**	**2000 kW**
Pumping power requirement, kW	29.68	57.56	96.64	12.67	18.9	26.74
Power input, kWh (per season)	92,717	179,778	303,959	37,090	55,483	78,305

For the case when water is taken from 30 meters depth, the pumping power should be found with the assumption of temperature difference between the intake and discharge of 3°C in 20% of times. The mass flow rate has to be increased respectively in order to provide enough of cooling. The final seasonal energy consumption of all systems is given in Figure 5.15.

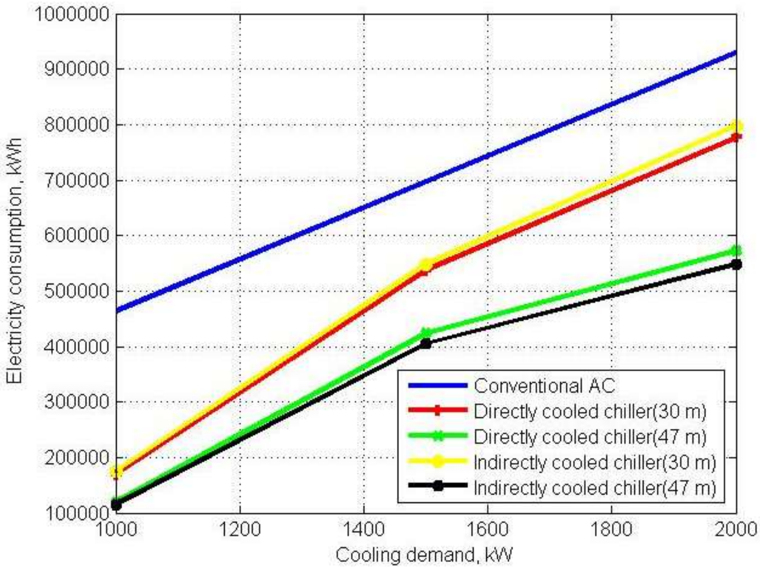

Figure 5.15. Annual Electricity Consumption.

The carbon footprint of examined systems was estimated using the emission rate factor of 0.7 kg of carbon dioxide equivalent per one kilowatt-hour of electricity (Table 5.9, Table 5.10, Figure 5.16). The amount of emission is given for one season from June to August.

Table 5.9. Carbon Emission from Conventional Air-Conditioning.

Cooling load, kW	**Carbon emission, tons of CO_2**
1000	325.0
1500	487.5
2000	650.0

Table 5.10. Carbon Emission from Water-Cooled Chiller Units.

Intake depth, m	**Cooling demand, kW**	**Indirectly cooled chiller, tons of CO_2**	**Directly cooled chiller, tons of CO_2**
30	**1000**	119.5	122.4
	1500	370.8	383.7
	2000	541.5	558.8
47	**1000**	80.5	83.4
	1500	296.6	296.6
	2000	383.5	400.8

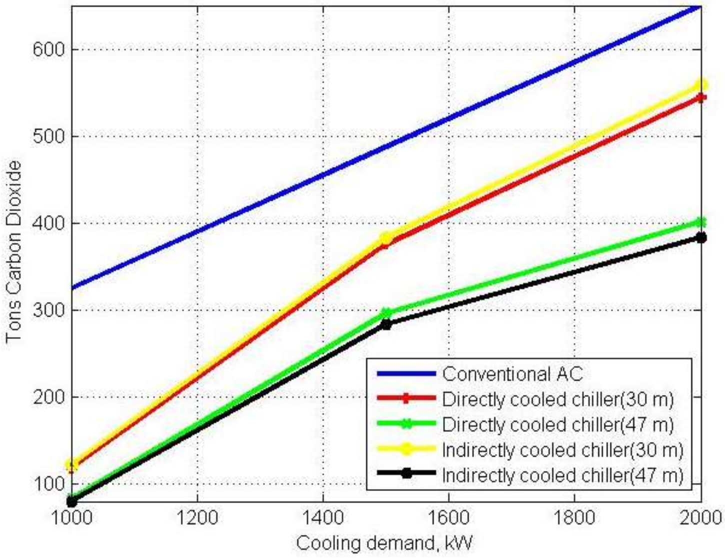

Figure 5.16. Annual Carbon Dioxide Emission.

5.3. Economic Analysis

This chapter includes final results of the economic comparison of SWAC systems to conventional air cooling regarding their capital, operational and life-cycle costs. Capital costs were found for each examined intake depth and cooling demand scenario. The values are expressed in USD with the prices in December 2016.

5.3.1. Capital Cost

The capital cost of every system configuration was found using the guideline from chapter 4.1 as the sum of capital costs of their components. The cost of the conventional system is merged into the air-cooled chiller cost only.

The cost of the pipeline was estimated based on the price list of local HDPE pipe manufacturer PETEK BORU (Table K.1). The price was assumed 23.8 TL per meter of pipe with 250 mm diameter. The construction cost (labor and equipment) can be assumed 2.5 times more than the total pipe cost [27]. The final capital cost of the pipeline takes into account both intake and discharge pipeline lengths (Table 5.11).

All chillers' capital costs were approximated by using the reference cost of the same type equipment from the current mechanical and electrical service price book [33]. The cost of a directly cooled chiller unit is assumed to be 1.5 times higher than the cost of the indirectly cooled unit due to the high price of corrosion resistant piping system inside the condenser [30]. Capital costs of all chiller units examined in this study are shown in Table 5.12 –Table 5.14.

The capital cost of the titanium heat exchanger unit was found using the Aspen Exchanger Design and Rating (Table I.1 – Table I.6). The reference intake and discharge temperatures were respectively assumed as 20ºC and 24ºC for the intake location at 30 meter depth and 13ºC and 24ºC for 47 meter depth (Table 5.15).

The pump cost was approximated using the N exponent rule and equation (3.32). The *N* value, taken as 0.67 (Table. G.1) and the reference equipment costs were taken from the mechanical and electrical service price book (Table 5.16) [33]. Final capital costs of all three systems are given in Table 5.17 and Table 5.18.

Table 5.11. Pipeline Capital Cost.

	30 meters			**47 meters**		
	1000 kW	**1500 kW**	**2000 kW**	**1000 kW**	**1500 kW**	**2000 kW**
Pipe diameter, mm	250	250	250	250	250	250
Intake pipe length, m	2400	2400	2400	3725	3725	3725
Discharge pipe length, m	777	777	777	777	777	777
Pipe price, TL/m	23.8	23.8	23.8	23.8	23.8	23.8
Intake pipe cost, TL	57,120	57,120	57,120	88,655	88,655	88,655
Discharge pipe cost, TL	18,492	18,492	18,492	18,492	18,492	18,492
Pipeline cost, TL	75,512	75,512	75,512	107,147	107,147	107,147
Construction cost, TL	188,780	188,780	188,780	267,897	267,897	267,897
Total pipeline cost, USD	69,594	69,594	69,594	98,758	98,758	98,758

Table 5.12. Air-Cooled Chiller's Capital Cost.

	1000 kW	1500 kW	2000 kW
Chiller capacity, kW	1000	1000 + 600	1000 + 1000
Chiller reference price, GBP	113,170	113,170 + 80,346	113,170 + 113,170
Total cost, USD	139,199	169,755	278,399

Table 5.13. Indirectly Cooled Chiller's Capital Cost.

	1000 kW	1500 kW	2000 kW
Chiller reference price, GBP	90,490	139,797	200,495
Total cost, USD	111,846	172,789	247,812

Table 5.14. Directly Cooled Chiller Capital Cost.

	1000 kW	1500 kW	2000 kW
Chiller reference price, GBP	135,743	209,696	300,742
Total cost, USD	167,769	259,184	371,718

Table 5.15. Heat Exchanger Unit's Capital Cost.

	30 meters			47 meters		
	1000 kW	**1500 kW**	**2000 kW**	**1000 kW**	**1500 kW**	**2000 kW**
Heat exchanger cost, USD	49,843	87,898	122,841	41,906	61,078	83,882

Table 5.16. Seawater Pump's Capital Cost.

	30 meters			47 meters		
	1000 kW	**1500 kW**	**2000 kW**	**1000 kW**	**1500 kW**	**2000 kW**
Pump cost, USD	75,933	101,163	122,841	39,961	50,896	61,716

Table 5.17. Conventional Air-Conditioning Capital Cost.

	1000 kW	1500 kW	2000 kW
Capital cost, USD	139,199	169,755	278,399

Table 5.18. SWAC Systems' Capital Cost.

Intake depth, m	Cooling load, kW	Indirectly cooled chiller, USD	Directly cooled chiller, USD
30	1000	307,217	419,063
	1500	431,445	604,235
	2000	579,193	827,005
47	1000	292,472	404,318
	1500	383,522	556,312
	2000	492,168	739,981

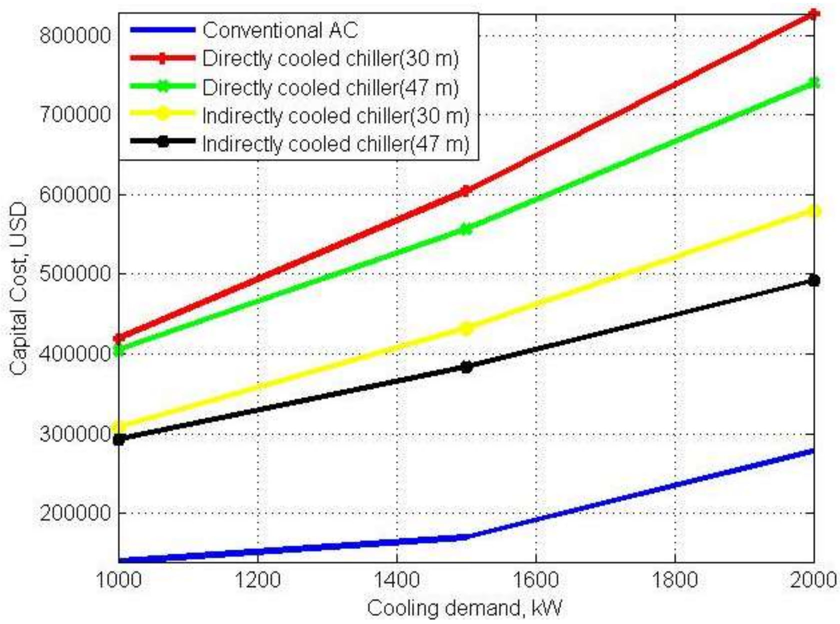

Figure 5.17. Capital Costs of Conventional Air-Conditioning System and Seawater Cooled Chillers.

5.3.2. Electrical and Life-Cycle Costs

The current electricity rate in Turkey is 0.132 USD for one kilowatt-hour. Using previous results of yearly power consumption cost (Table 5.5 – Table 5.8), the present values of electrical costs during 30 years systems' life-cycle are shown in Table 5.19 - Table 5.21 and Figure 5.18 with an interest rate of 7%.

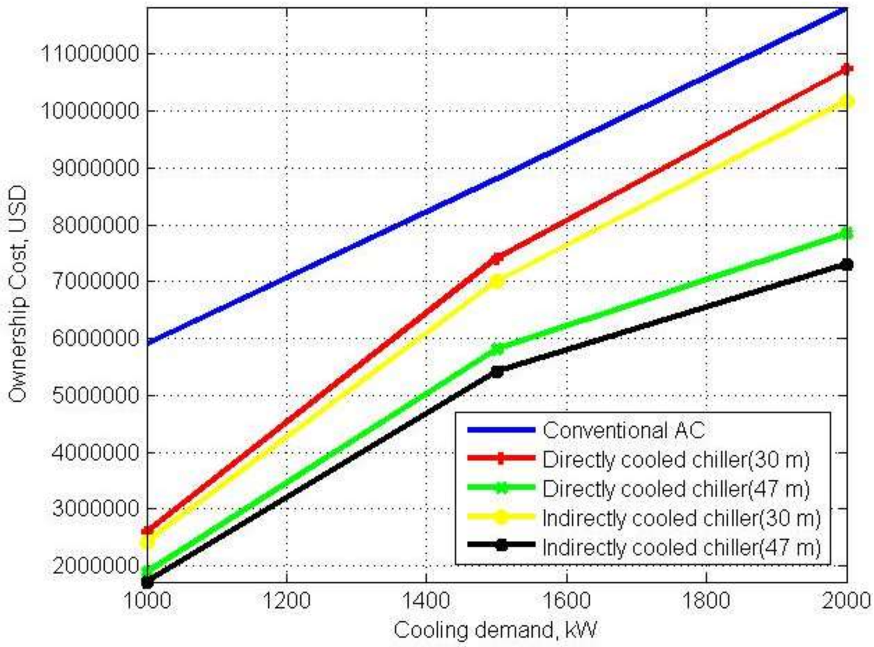

Figure 5.18. Total Ownership Cost.

Table 5.19. Conventional Air-Conditioning Total Ownership Cost.

Cooling capacity, kW	Capital cost, USD	Yearly energy cost, USD	Energy cost present value, USD	Total ownership, USD
1000	139,199	464,343	5,762,059	5,901,259
1500	169,755	696,515	8,643,090	8,812,846
2000	278,399	928,687	11,524,119	11,802,519

Table 5.20. Directly Cooled Chiller Unit's Total Ownership Cost.

Intake depth, m	Cooling capacity, kW	Capital cost, USD	Yearly energy cost, USD	Energy cost present value, USD	Total ownership, USD
30	**1000**	419,063	174,865	2,169,912	2,588,975
	1500	604,235	548,148	6,801,986	7,406,220
	2000	827,005	798,323	9,906,427	10,733,433
47	**1000**	404,318	119,239	1,479,645	1,883,963
	1500	556,312	423,853	5,259,615	5,815,927
	2000	739,981	572,670	7,106,283	7,846,264

Table 5.21. Indirectly Cooled Chiller Unit's Total Ownership Cost.

Intake depth, m	**Cooling capacity, kW**	**Capital cost, USD**	**Yearly energy cost, USD**	**Energy cost present value, USD**	**Total ownership, USD**
30	**1000**	307,217	170,758	2,118,943	2,426,160
	1500	431,445	529,729	6,573,430	7,004,875
	2000	579,193	773,605	9,599,698	10,178,891
47	**1000**	292,472	115,132	1,428,676	1,721,147
	1500	383,522	405,435	5,031,059	5,414,581
	2000	492,169	547,952	6,799,553	7,291,722

6. DISCUSSION

Previous studies have shown that SWAC is technically and economically feasible technology for air cooling and has been successfully applied to coastal communities in several places around the world. Even though there are several existing SWAC plant in Europe, the Black Sea cold waters remain unused. The present thesis gives the first evaluation of energy potential of cold seawater from the Black Sea to air condition indoor spaces and defines system configurations feasible for the application in this region. The Black Sea has the high potential to be used for the SWAC application since it has the lowest water temperature at the seafloor in the entire Mediterranean basin.

It is important to fully understand the oceanographic nature of water temperatures in the Black Sea to effectively evaluate the feasibility of SWAC in the region. The Black Sea is a large land-locked sea basin, and due to the weak water exchange with the global ocean, it is remarkable for its unique environment. Under the effect of regional climate, winds, currents, fresh water inflow from rivers and high density water flux from the Mediterranean Sea, the water of the Black Sea has a distinct vertical stratification with permanent halocline and stable thermal characteristics of each layer across the basin. The surface water is exposed to a significant influence from the atmosphere. Its temperature fluctuates between 6ºC and 28ºC depending on the season. The underlying Cold Intermediate Layer (CIL) is on the contrary very stable with year round water temperatures of 8-9ºC at the upper part and 6ºC occasionally observed in the core. The CIL is formed due to the upwelling of cold deep water in the northern part of the central basin and winter formation of cold dense surface water in the northwestern part of the sea, that after sinks to the depths of 50 -180 meters where CIL is usually found. The deep water of the Black Sea is an oxygen free water body with stagnant water temperature slightly warmer than the CIL. Its anoxic nature becomes challenging for the cooling application and may not satisfy environmental requirements for SWAC. Therefore, CIL is the most favorable source of cold seawater in the Black Sea for the cooling application. At a depth of 50 meters, cold water of 8ºC is available throughout the year, except the coastal zone of Istanbul, where warm Mediterranean influx affects the water temperature. Therefore, a standalone SWAC system cannot be used at the Black Sea coast of Istanbul. The coldest possible water temperature stable throughout the year is 8ºC, whereas the required temperature value in chilled water loop is required to be 6-7°C for proper heat removal. Three other SWAC system configurations can be considered for the application at the Black Sea: hybrid SWAC system and directly and indirectly seawater-cooled chiller units. The seawater temperature supplied to the hybrid SWAC system has to be lower than the temperature of chilled water returned from the building, which is typically 12-13°C. The efficiency of the hybrid SWAC system mainly depends on of the temperature change that can occur in the heat exchanger since the remaining cooling has to be provided by a chiller unit. Seawater-cooled chiller units are less dependent on the availability of cold seawater since the required inlet temperature for condenser cooling is usually in the range of 20-30°C and set by the manufacturer.

Another factor that influences the SWAC system configuration and feasibility is the distance to the cold seawater at the desired temperature. In the Black Sea, the distance to the 50 meter depth contour varies from 150 meters up to five kilometers everywhere except the northwestern part of the sea. There, the distance is increased up to 150 kilometers near Odessa due to the flat bathymetry. Seawater intake and discharge locations have to be seaward of the closure depth to avoid the wave damage on the intake and discharge structures. In the Black Sea, the closure depth is in the range of 5-8 meters across the basin. Therefore, the area for possible seawater intake and discharge location is limited by the closure depth at 7 meters depth and the outer edge of the shelf zone that can be traced along 100-150 meters depth contour in the Black Sea. From the economical point of view, the most economically feasible solution for the seawater intake is found below 50 meter depth to ensure stable operation of the system. Shallower depths can also be considered, with an additional statistical analysis of seawater temperatures.

All components of SWAC system are interrelated. The heat exchanger together with the chiller unit are the "heart" of the SWAC system. The cost of the heat exchanger primarily depends on the allowable temperature difference between the inlet and outlet water temperatures on the cold side. The outlet temperature is specified by the average ambient temperature at the discharge location, which is usually few meters below of the closure depth to guarantee the outlet structure safety. To obey environmental constraints and avoid negative effect to the marine organisms, the temperature of the seawater returned from the cooling system should not deviate from the ambient water temperature more than in 2°C.

The heat exchanger size and the final cost are also dependent on the associated chiller unit requirements and specification. It has to ensure that required flow rate and temperatures are supplied to the chiller for its proper work. Typically the water temperature difference between the inlet and outlet of the water-cooled condenser is about 5ºC and it is economically feasible to design the heat exchanger for a seawater temperature difference between the inlet and outlet of more than 4ºC. Using the water-cooled chiller unit with high condenser cooling water temperatures will allow to use warmer seawater temperatures in the heat exchanger and consequently, decrease the length of the offshore pipe and pump energy consumption due to the pumping head reduction. In the case of the hybrid system, the amount of cooling provided by the exchanger depends on the temperature difference between the seawater intake and fresh water returned from the building.

The feasibility of the SWAC system is evaluated through the comparison of life-cycle costs and energy consumption to the conventional air-conditioning system. For the present research, the site for the case study was selected at Boğaziçi University Sarıtepe Campus located on the Black Sea coast of Istanbul. The mildly sloped bathymetry increases the distance to the depths with sufficiently cold seawater. Consequently, the capital and operating costs of the system becomes relatively high. Compared to other Black Sea towns, the university campus has highest maximum monthly average summer temperature in the region. It is located just 9 kilometers west of the Strait of Istanbul, which brings warm Mediterranean water to the Black Sea. As a result, the water in the upper layer of the sea is slightly warmer compared to other coasts of the Black Sea. Together with the highest electricity price in the region, the application of SWAC system at the selected test case is an example of the “worst case scenario” and is a good feasibility test for the rest of the Black Sea.

Depths of 30 and 47 meters were considered for seawater intake location with average seawater temperatures of 20ºC and 13ºC respectively. It is technically not feasible to locate the intake structure deeper than 50 meters in this region, due to the broad flat valley that starts at this depth and extends up to the end of the shelf zone. The temperature of 13ºC is not cold enough for the primary cooling of water returning from the building and makes the use of hybrid SWAC system not possible. Therefore, two SWAC system configurations were tested in the case study: directly and indirectly cooled chillers both using seawater as coolant fluid.

Comparison of electrical demands of SWAC and conventional air-conditioning showed a drastic energy reduction in favour of SWAC. Performances of directly and indirectly cooled chillers are very similar as long as the intake depths are the same. However, systems with the seawater intake at 30 meter depth consume 45% more electrical energy than the ones at the deeper location. The reason is that the flow rate has to be significantly increased to compensate for the reduced cooling available as the seawater temperature increases from 13ºC to 20ºC. As a result, the pumping power and the overall energy requirement of the system increases. Compared to the conventional system, SWAC systems can be 75% and 60% more efficient at 47 and 30 meters depths respectively. By using SWAC, the carbon footprints of cooling systems are also reduced proportionally. With the growth of the cooling, SWAC systems become less efficient compared to the conventional units.

Even though the capital cost of conventional air-conditioning is significantly lower than the cost of SWAC, the final total system ownership cost over 30 years shows that the use of directly and indirectly seawater-cooled chiller units in the Black Sea can be economically 60% more feasible than the conventional cooling.

Design recommendations and most feasible system configuration for present size of the university campus (1000 kW) are given in Table 6.1 and Figure 6.1.

Table 6.1. SWAC Design Recommendations for Sarıtepe Campus.

Intake / discharge depth	47 m / 10 m
Intake / discharge pipeline length	3725 m / 777 m
Intake seawater temperature	13ºC
Discharge seawater temperature	24ºC
Ambient seawater temperature at a discharge location	19-27 ºC
Annual electricity consumption	115,132 kWh
Annual electricity savings	343,216 kWh
Annual carbon emission reduction	247.4 tons
Capital cost	292,471 USD
Total ownership cost	1,721,147 USD
Total ownership savings	4,180,113 USD
System life period	30 years
Cost efficiency	60 %
Energy efficiency	75 %

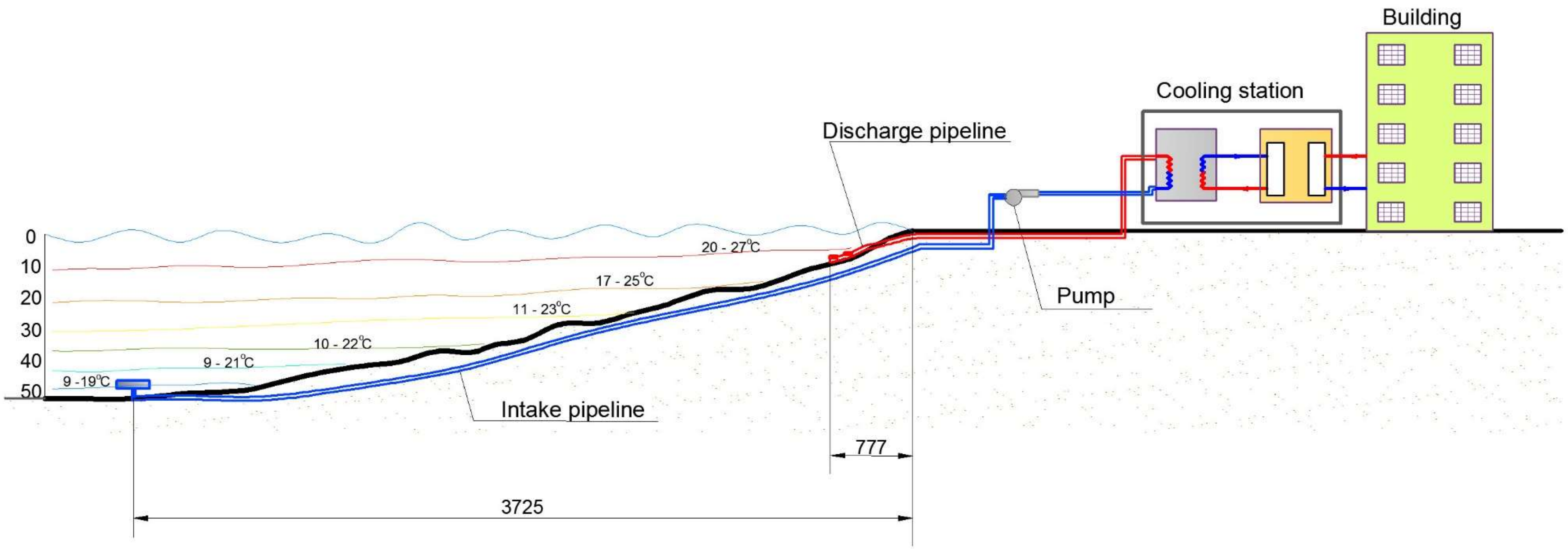

Figure 6.1. Sketch of SWAC System for Boğaziçi University Sarıtepe Campus with the Seawater Intake at 47 Meter Depth.

7. CONCLUSION

The present research showed that the seawater air-conditioning (SWAC) can successfully be used by the coastal communities around the Black Sea. A unique thermal structure of the Black Sea with a Cold Intermediate Layer (CIL) makes seawater available at relatively shallow depths and creates ample room for the SWAC application in the region.

The availability of cold water temperatures at changing depths cannot guarantee the stable operation of the SWAC system since it may be influenced by currents and seasonal atmospheric changes. Therefore, it is important to choose the proper location for the seawater intake based on a statistical analysis of temperature fluctuations. In the Black Sea, the stable source of sufficiently cold seawater for SWAC can be found at 50 meters depth with the temperature of 8ºC over the entire basin. This depth corresponds to the upper boundary of the CIL, which is the rare phenomenon characterized by the temperatures that are slightly lower than the deep water and does not change throughout the year.

Despite the advantages of CIL, coastal seawater temperatures in the Black Sea are still not sufficient for standalone SWAC. However, the technical investigation carried out in this research has shown that system configurations supported with seawater-cooled chillers may be feasible with up to 75% of electricity savings and greenhouse gas emission reduction as well as up to 60% of life-cycle cost reduction. Therefore, SWAC can be an energy and cost-effective alternative to conventional cooling systems to be used around the Black Sea coast including Turkey, Georgia, Russia, Ukraine, Romania and Bulgaria. in the Black Sea.

The final feasibility of SWAC is site specific as it depends on local bathymetry, cooling demand and electricity price. A case study for the Boğaziçi University Sarıtepe Campus showed that SWAC is a feasible solution for cooling the campus buildings despite of disadvantages of warmer Mediterranean influx from the nearby Strait, flat nearshore bathymetry and relatively high air temperature compared to the rest of the Black Sea.

REREFENCES

1. Wang, S. K., *Handbook of Air Conditioning and Refrigeration*, McGraw-Hill, New York, NY, USA, 2000.

2. Bimpong, H., *A Technical and Economic Investigation of the Use of Deep Cold Seawater for Air Conditioning in Coastal Communities in Ghana*, M.S. Thesis, Kwame Nkrumah University of Science and Technology, 2012.

3. Makai Ocean Engineering, Inc., *Seawater Air Conditioning: A Basic Understanding,* 2004, http://www.makai.com, accessed at December 2016.

4. Hirshman, J., Whithaus, D. A., & Brooks, I. H., *Feasibility of a District Cooling System Utilizing Cold Seawater*, Phase I: Final report (No. TID-28034), Physical Oceanographic Lab., Tracor Marine, Port Everglades, FL, USA; Nova Univ., Dania, FL, USA, 1975.

5. War, J. C., "Seawater Air Conditioning (SWAC) a Renewable Energy Alternative", *Oceans, MTS/IEEE KONA*, pp. 1-9, IEEE, 2011.

6. Fermbäck, G., "District Cooling in Stockholm Using Sea Water", No. CONF-9510169, *International District Energy Association*, Washington, DC, USA, 1995.

7. Kershaw, S., & Liu, M., "Modern Black Sea Oceanography Applied to the End-Permian Extinction Event", *Journal of Palaeogeography*, 4(1), pp. 52-62, 2015.

8. Capet, A., Barth, A., Beckers, J. M., Marilaure, G., "Interannual Variability of Black Sea's Hydrodynamics and Connection to Atmospheric Patterns", *Deep Sea Research Part II: Topical Studies in Oceanography*, 77, pp. 128-142, 2012.

9. Özsoy, E., & Ünlüata, Ü., "Oceanography of the Black Sea: A Review of Some Recent Results", *Earth-Science Reviews*, 42(4), 231-272, 1997.

10. Stanev, E., Staneva, J., & Roussenov, V., "On the Black Sea Water Mass Formation. Model Sensitivity Study to Atmospheric Forcing and Parameterizations of Physical Processes", *Journal of Marine Systems*, 13(1-4), pp. 245-272, 1997.

11. Ovchinikov I.M., Popov Yu.1., *On the Problem of the Cold Intermediate Layer Formation in the Black Sea*, Doklady Akademiy Nauk SSSR, 279(4), pp. 986-990, 1984.

12. Blatov, A. S., Bulgakov, N. P., Ivanov, V. A., Kosarev, A. N., & Tujilkin, V. S., "Variability of Hydrophysical Fields in the Black Sea"*, Gidrometeoizdat, Leningrad*, 239, 1984.

13. Kosnyrev, V. N., Mikhailova, E. N., & Stanichny, S. V., "Upwelling in the Black Sea by the Results of Numerical Experiments and Satellite Data", *Physical Oceanography*, 8(5), pp. 329-340, 1997.

14. Trukhchev, D. I., & Ibrayev, R. A., "Seasonal Variability of the Black Sea Climatic Circulation", *Sensitivity to Change: Black Sea, Baltic Sea and North Sea*, pp. 365-374, Springer Netherlands, 1997.

15. Maderich, V., Ilyin, Y., & Lemeshko, E., "Seasonal and Interannual Variability of the Water Exchange in the Turkish Straits System Estimated by Modelling", *Mediterranean Marine Science*, 16(2), pp. 444-459, 2015.

16. *Global Ocean Currents*, 2013, https://www.crd.bc.ca, accessed at December 2016.

17. Missimer, T. M., Jones, B. H., & Maliva, R. G., *Intakes and Outfalls for Seawater Reverse-Osmosis Desalination Facilities: Innovations and Environmental Impacts*, Heidelberg: Springer Verlag, 2015.

18. Koon, C. H., Sing, S. J., Soon, N. Y., Chua, T. L., & Boon, N. C., "Indirect Seawater Cooling and Thermal Storage System in Changi Naval Base", n.d., *DSTA Horizons*, pp. 46-55, https://www.dsta.gov.sg/, accessed at December 2016.

19. Pelc, R., & Fujita, R. M., *Renewable Energy from the Ocean*, Marine Policy, 26(6), pp. 471-479, 2002.

20. U.S. Environmental Protection Agency, *Water Quality Standards Criteria Summaries: A Compilation of State/Federal Criteria: Temperature,* Office of Water Regulations and Standards, 1998.

21. South East European Climate Change Center, *Climate Monitoring*, 2016, http://www.seevccc.rs, accessed at December 2016.

22. GEOHIVE, *Global Population Statistics*, 2016, http://www.geohive.com/cntry, accessed at December 2016.

23. Navionics, *Navionics Webapp.Sonar Chart,* 2016, http://webapp.navionics.com, accessed at December 2016.

24. Soomere, T., Viška, M., & Eelsalu, M., "Spatial Variations of Wave Loads and Closure Depths along the Coast of the Eastern Baltic Sea", *Estonian Journal of Engineering*, 19(2), 93, 2013.

25. Galabov, V., *The Black Sea Wave Energy: The Present State and the Twentieth Century Changes*, National Institute of Meteorology and Hydrology, Bulgarian Academy of Sciences, 2015.

26. GreenBuildingAdvisor.com, *Calculating Cooling Loads*, 2012, http://www.greenbuildingadvisor.com, accessed at December 2016.

27. Williams, M., *Use of Seawater for Air Conditioning at Waikiki Convention Center*, M.S. Thesis, Naval Postgraduate School, Monterey, California, 1994.

28. Porak, D. N., Van Zwieten, J. H., & Rauchenstein, L. T., “Florida's Sea Water Cooling Resource: An Updated Assessment”, *Oceans*, pp. 1-10, IEEE, 2012.

29. Jones W.P., *Air Conditioning Applications and Design*, 2nd Edition, New York, NY, USA, 1997.

30. Farjo, A., *Sea Water Cooled Chillers*, Johnson Controls, n.d., http://www.districtenergy.org, accessed at December 2016.

31. EMODnet, *Bathymetry Portal,* European Marine Observation and Data Network, n.d., http://www.emodnet.eu, accessed at December 2016.

32. BERKÜN, U., *Wind and Swell Wave Climate For The Southern Part Of Black Sea*, Ph. D. Thesis, Middle East Technical University, 2007.

33. AECOM, *Spon’s Mechanical and Electrical Services Price Book*, 46th Edition, CRC Press, 2015.

34. Handbook, A. S. H. R. A. E., *Fundamentals. American Society of Heating, Refrigerating and Air Conditioning Engineers*, Atlanta, USA, 2005.

35. Sharqawy, M. H., Lienhard, J. H., & Zubair, S. M., “Thermophysical Properties of Seawater: a Review of Existing Correlations and Data”*, Desalination and Water Treatment*, 16(1-3), pp. 354-380, 2010.

36. Whitesides, R. W., *Process Equipment Cost Estimation by Ratio and Proportion*, Course notes, PDH Course G, 2005.

37. Carrier Building, *23 XRV. High-Efficiency Variable Speed Screw Chiller*, 2013, Carrier United Technologies, http://www.carrier.com, accessed at December 2016.

38. YORK Chiller Solutions, *Industrial & Commercial HVAC Chillers for Sustainable Solutions*, Johnson Controls, n.d., http://www.johnsoncontrols.com, accessed at December 2016.

39. PETEK BORU, *HDPE Boru Fiyat Listesi*, 2012, http://petekboru.com.tr, accessed at December 2016.

APPENDIX A: AIR-CONDITIONING SYSTEM DESIGN CONDITIONS

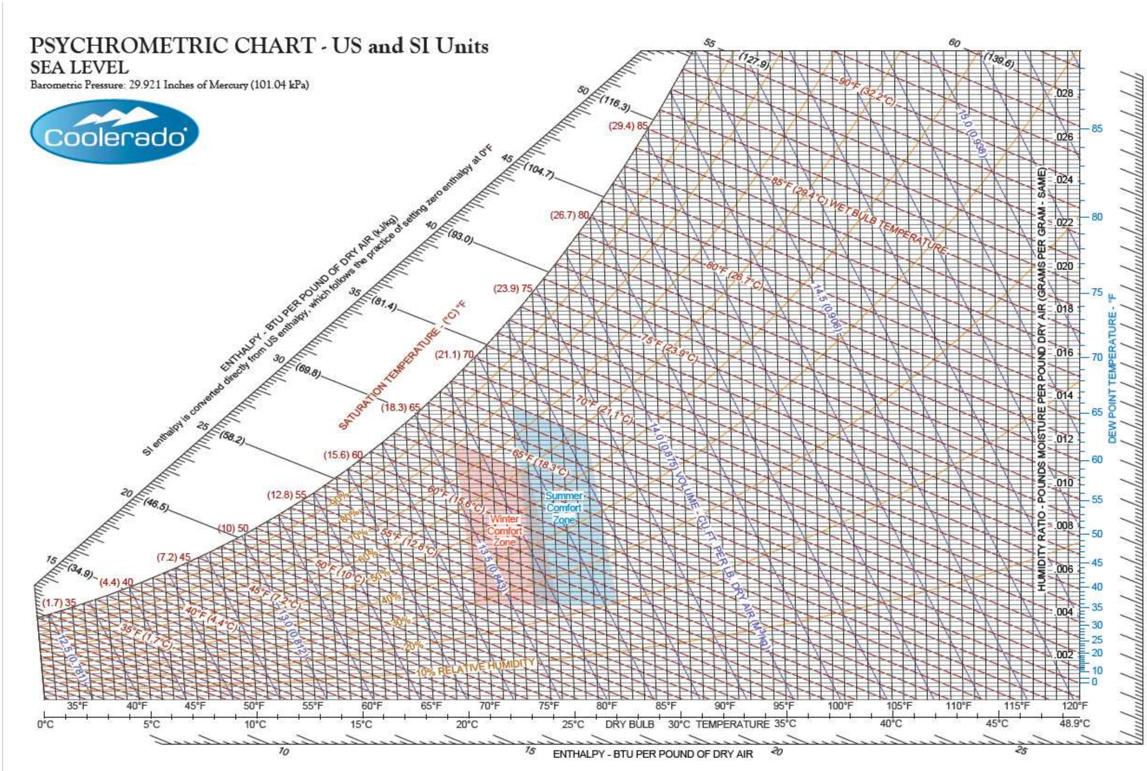

Figure A.1. Psychrometric Chart.

Design conditions for ISTANBUL/ATATURK AB, Turkey

Station Information

Station name	WMO#	Lat	Long	Elev	StdP	Hours +/- UTC	Time zone code	Period
1a	*1b*	*1c*	*1d*	*1e*	*1f*	*1g*	*1h*	*1i*
ISTANBUL/ATATURK AB	**170600**	**40.97N**	**28.82E**	**37**	**100.88**	**2.00**	**GTB**	**8201**

Annual Heating and Humidification Design Conditions

Coldest month	Heating DB		Humidification DP/MCDB and HR						Coldest month WS/MCDB				MCWS/PCWD to 99.6% DB	
			99.6%			99%			0.4%		1%			
	99.6%	99%	DP	HR	MCDB	DP	HR	MCDB	WS	MCDB	WS	MCDB	MCWS	PCWD
2	*3a*	*3b*	*4a*	*4b*	*4c*	*4d*	*4e*	*4f*	*5a*	*5b*	*5c*	*5d*	*6a*	*6b*
2	**-2.5**	**-0.9**	**-7.2**	**2.0**	**0.3**	**-5.7**	**2.3**	**1.7**	**12.8**	**1.3**	**11.3**	**2.0**	**5.7**	**0**

Annual Cooling, Dehumidification, and Enthalpy Design Conditions

Hottest month	Hottest month DB range	Cooling DB/MCWB						Evaporation WB/MCDB						MCWS/PCWD to 0.4% DB	
		0.4%		1%		2%		0.4%		1%		2%			
		DB	MCWB	DB	MCWB	DB	MCWB	WB	MCDB	WB	MCDB	WB	MCDB	MCWS	PCWD
7	*8*	*9a*	*9b*	*9c*	*9d*	*9e*	*9f*	*10a*	*10b*	*10c*	*10d*	*10e*	*10f*	*11a*	*11b*
8	**7.9**	**31.1**	**21.5**	**29.9**	**21.4**	**28.8**	**20.9**	**24.3**	**27.6**	**23.3**	**27.0**	**22.5**	**26.3**	**6.0**	**30**

Dehumidification DP/MCDB and HR									Enthalpy/MCDB					
0.4%			1%			2%			0.4%		1%		2%	
DP	HR	MCDB	DP	HR	MCDB	DP	HR	MCDB	Enth	MCDB	Enth	MCDB	Enth	MCDB
12a	*12b*	*12c*	*12d*	*12e*	*12f*	*12g*	*12h*	*12i*	*13a*	*13b*	*13c*	*13d*	*13e*	*13f*
23.1	**18.0**	**26.3**	**22.1**	**16.8**	**25.4**	**21.2**	**15.9**	**24.8**	**73.4**	**27.7**	**69.6**	**27.2**	**66.6**	**26.2**

Extreme Annual Design Conditions

Extreme Annual WS			Extreme Max WB	Extreme Annual DB				n-Year Return Period Values of Extreme DB							
				Mean		Standard deviation		n=5 years		n=10 years		n=20 years		n=50 years	
1%	2.5%	5%	WB	Max	Min	Max	Min	Max	Min	Max	Min	Max	Min	Max	Min
14a	*14b*	*14c*	*15*	*16a*	*16b*	*16c*	*16d*	*17a*	*17b*	*17c*	*17d*	*17e*	*17f*	*17g*	*17h*
10.9	**9.8**	**9.1**	**27.0**	**34.5**	**-5.0**	**1.9**	**3.5**	**35.9**	**-7.5**	**37.0**	**-9.6**	**38.0**	**-11.5**	**39.4**	**-14.1**

Monthly Design Dry Bulb and Mean Coincident Wet Bulb Temperatures

%	Jan		Feb		Mar		Apr		May		Jun	
	DB	MCWB	DB	MCWB	DB	MCWB	DB	MCWB	DB	MCWB	DB	MCWB
	18a	*18b*	*18c*	*18d*	*18e*	*18f*	*18g*	*18h*	*18i*	*18j*	*18k*	*18l*
0.4%	**14.9**	**10.6**	**16.1**	**10.2**	**20.1**	**12.9**	**24.6**	**16.3**	**28.0**	**18.3**	**31.1**	**20.3**
1%	**14.1**	**10.4**	**15.0**	**10.0**	**18.9**	**12.5**	**23.0**	**15.0**	**26.5**	**17.7**	**30.1**	**20.2**
2%	**13.2**	**9.9**	**14.0**	**10.1**	**17.3**	**11.6**	**21.8**	**14.7**	**25.2**	**17.6**	**29.1**	**20.0**

%	Jul		Aug		Sep		Oct		Nov		Dec	
	DB	MCWB	DB	MCWB	DB	MCWB	DB	MCWB	DB	MCWB	DB	MCWB
	18m	*18n*	*18o*	*18p*	*18q*	*18r*	*18s*	*18t*	*18u*	*18v*	*18w*	*18x*
0.4%	**33.2**	**21.0**	**32.7**	**23.1**	**30.1**	**19.9**	**27.0**	**19.1**	**21.1**	**15.6**	**16.1**	**12.3**
1%	**32.2**	**21.6**	**31.8**	**22.3**	**29.1**	**19.9**	**25.2**	**18.9**	**19.9**	**15.4**	**15.2**	**11.9**
2%	**31.2**	**21.6**	**31.0**	**22.0**	**28.1**	**19.8**	**24.1**	**18.6**	**18.9**	**14.9**	**14.8**	**11.7**

Monthly Design Wet Bulb and Mean Coincident Dry Bulb Temperatures

%	Jan		Feb		Mar		Apr		May		Jun	
	WB	MCDB	WB	MCDB	WB	MCDB	WB	MCDB	WB	MCDB	WB	MCDB
	19a	*19b*	*19c*	*19d*	*19e*	*19f*	*19g*	*19h*	*19i*	*19j*	*19k*	*19l*
0.4%	**11.7**	**13.9**	**11.6**	**14.2**	**13.6**	**18.6**	**17.2**	**23.0**	**20.1**	**25.6**	**23.1**	**27.1**
1%	**10.9**	**13.3**	**10.9**	**13.9**	**12.9**	**17.4**	**16.1**	**21.1**	**19.4**	**24.4**	**22.5**	**26.3**
2%	**10.4**	**12.5**	**10.3**	**13.2**	**12.2**	**16.5**	**15.2**	**19.9**	**18.7**	**23.4**	**22.0**	**25.7**

%	Jul		Aug		Sep		Oct		Nov		Dec	
	WB	MCDB	WB	MCDB	WB	MCDB	WB	MCDB	WB	MCDB	WB	MCDB
	19m	*19n*	*19o*	*19p*	*19q*	*19r*	*19s*	*19t*	*19u*	*19v*	*19w*	*19x*
0.4%	**25.3**	**28.3**	**25.7**	**28.5**	**22.6**	**25.7**	**21.0**	**24.3**	**17.1**	**19.5**	**13.0**	**15.1**
1%	**24.7**	**27.7**	**25.2**	**28.3**	**22.1**	**25.4**	**20.3**	**23.4**	**16.5**	**18.7**	**12.5**	**14.6**
2%	**24.2**	**27.4**	**24.6**	**27.9**	**21.7**	**25.2**	**19.6**	**22.5**	**15.7**	**17.8**	**12.1**	**14.2**

Monthly Mean Daily Temperature Range

Jan	Feb	Mar	Apr	May	Jun	Jul	Aug	Sep	Oct	Nov	Dec
20a	*20b*	*20c*	*20d*	*20e*	*20f*	*20g*	*20h*	*20i*	*20j*	*20k*	*20l*
4.7	**5.4**	**6.1**	**7.4**	**7.8**	**8.2**	**8.2**	**7.9**	**7.8**	**6.2**	**5.3**	**4.4**

WMO#	World Meteorological Organization number	Lat	Latitude, °	Long	Longitude, °
Elev	Elevation, m	StdP	Standard pressure at station elevation, kPa		
DB	Dry bulb temperature, °C	DP	Dew point temperature, °C	WB	Wet bulb temperature, °C
WS	Wind speed, m/s	Enth	Enthalpy, kJ/kg	HR	Humidity ratio, grams of moisture per kilogram of dry air
MCDB	Mean coincident dry bulb temperature, °C	MCWB	Mean coincident wet bulb temperature, °C	MCWS	Mean coincident wind speed, m/s
PCWD	Prevailing coincident wind direction, °, 0 = North, 90 = East				

Figure A.2. Outdoor Design Conditions for Istanbul, Turkey [34].

APPENDIX B: FIELD MEASUREMENT RESULTS

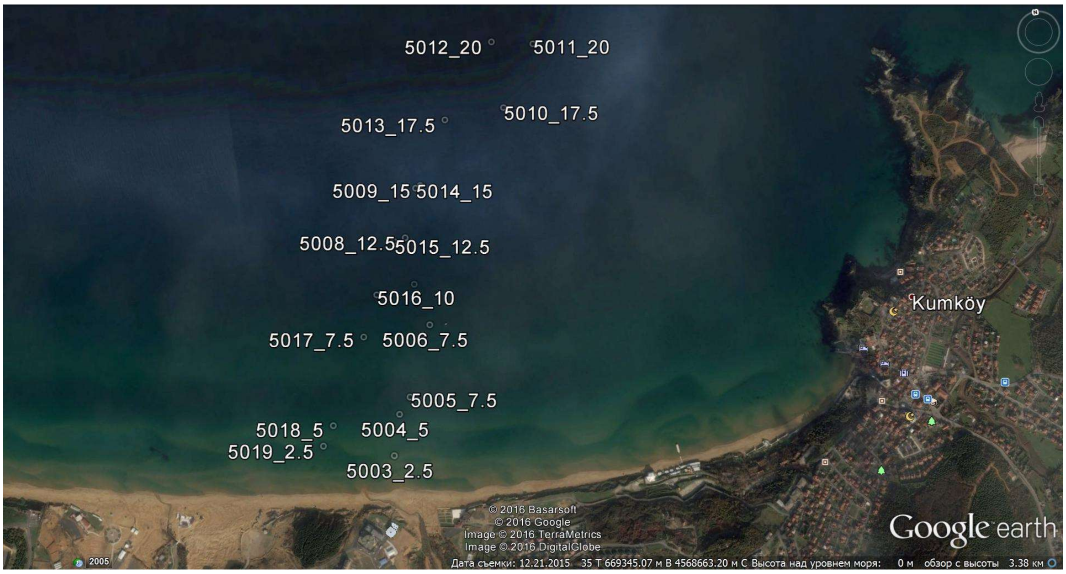

Figure B.1. Locations of CTD Measurements (April 16, 2016).

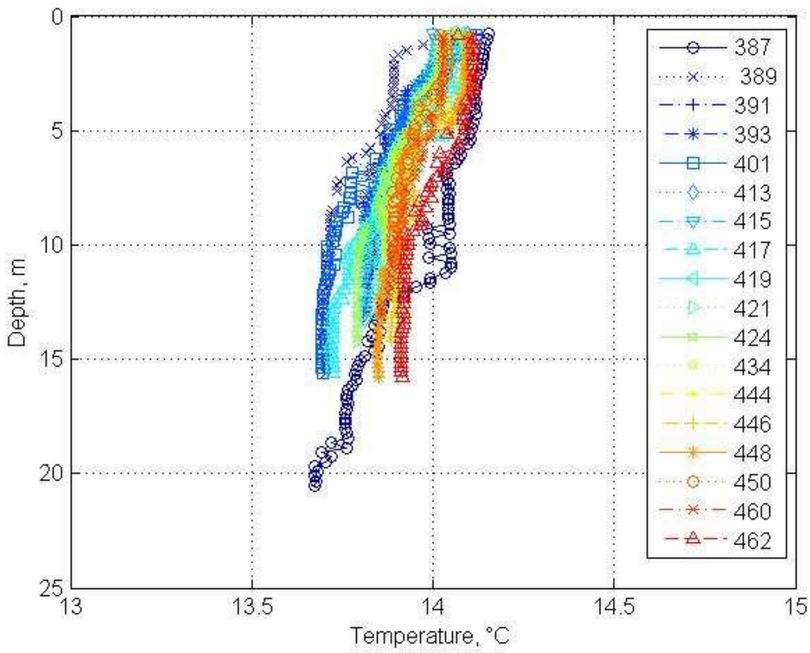

Figure B.2. Temperature Profile Measurements Results (December 7, 2015).

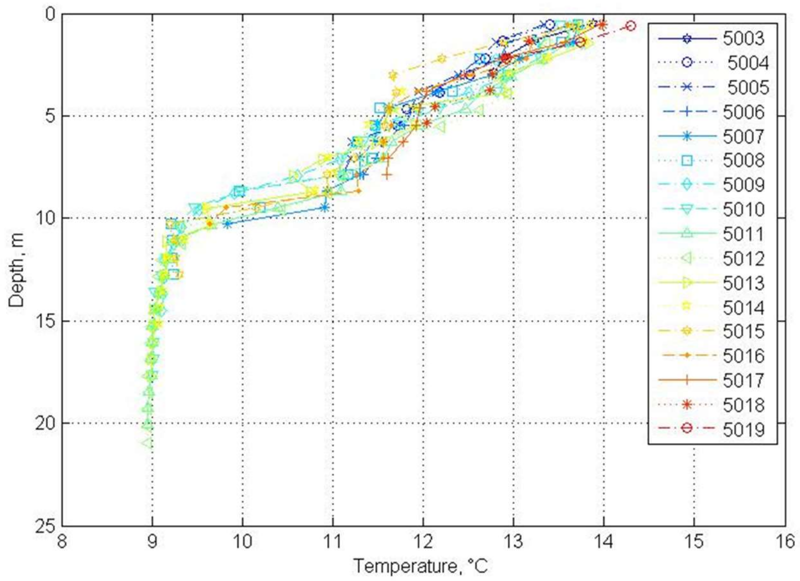

Figure B.3. Temperature Profile Measurements Results (April 16, 2016).

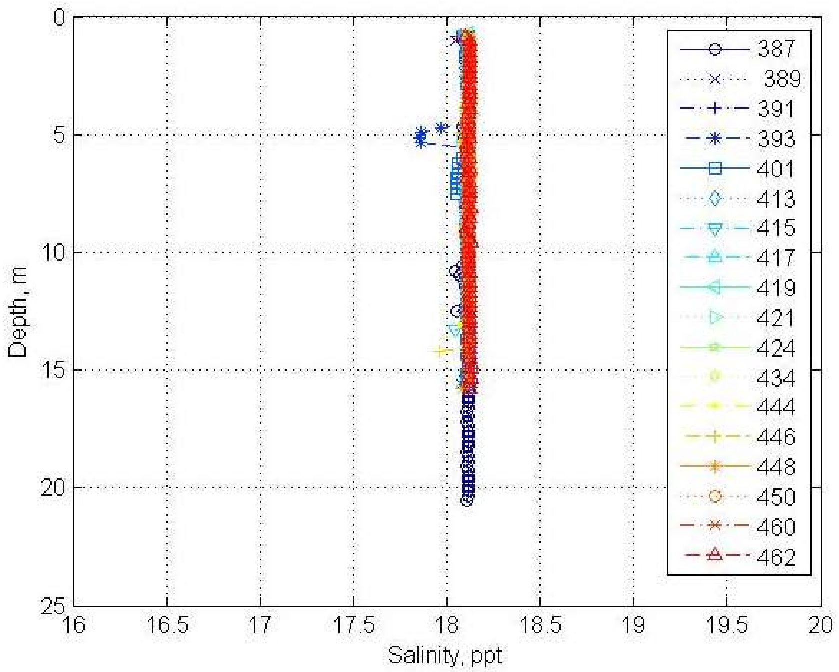

Figure B.4. Salinity Profile Measurements Results (December 7, 2015).

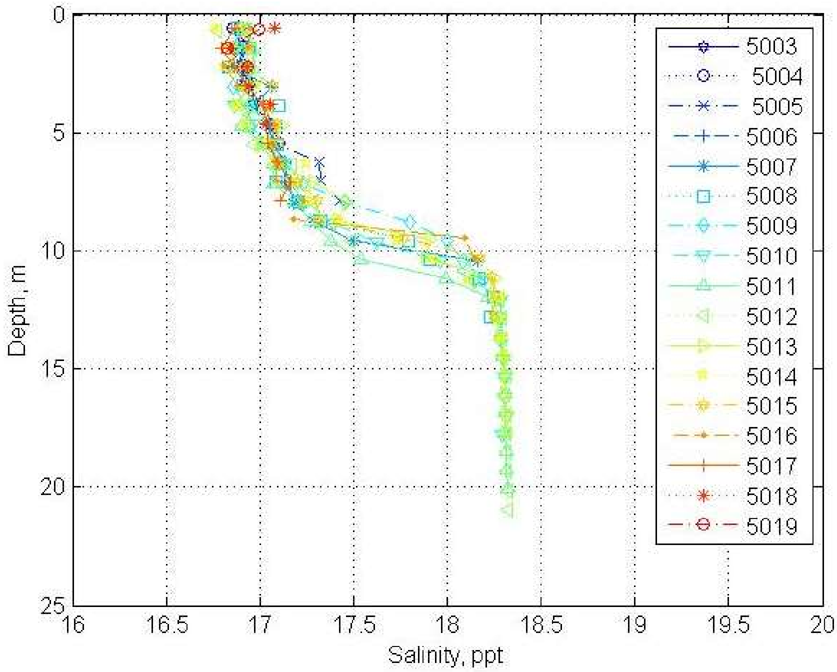

Figure B.5. Salinity Profile Measurements Results (April 16, 2016).

APPENDIX C: STATISTICAL ANALYSIS OF SEAWATER TEMPERATURE IN THE BLACK SEA

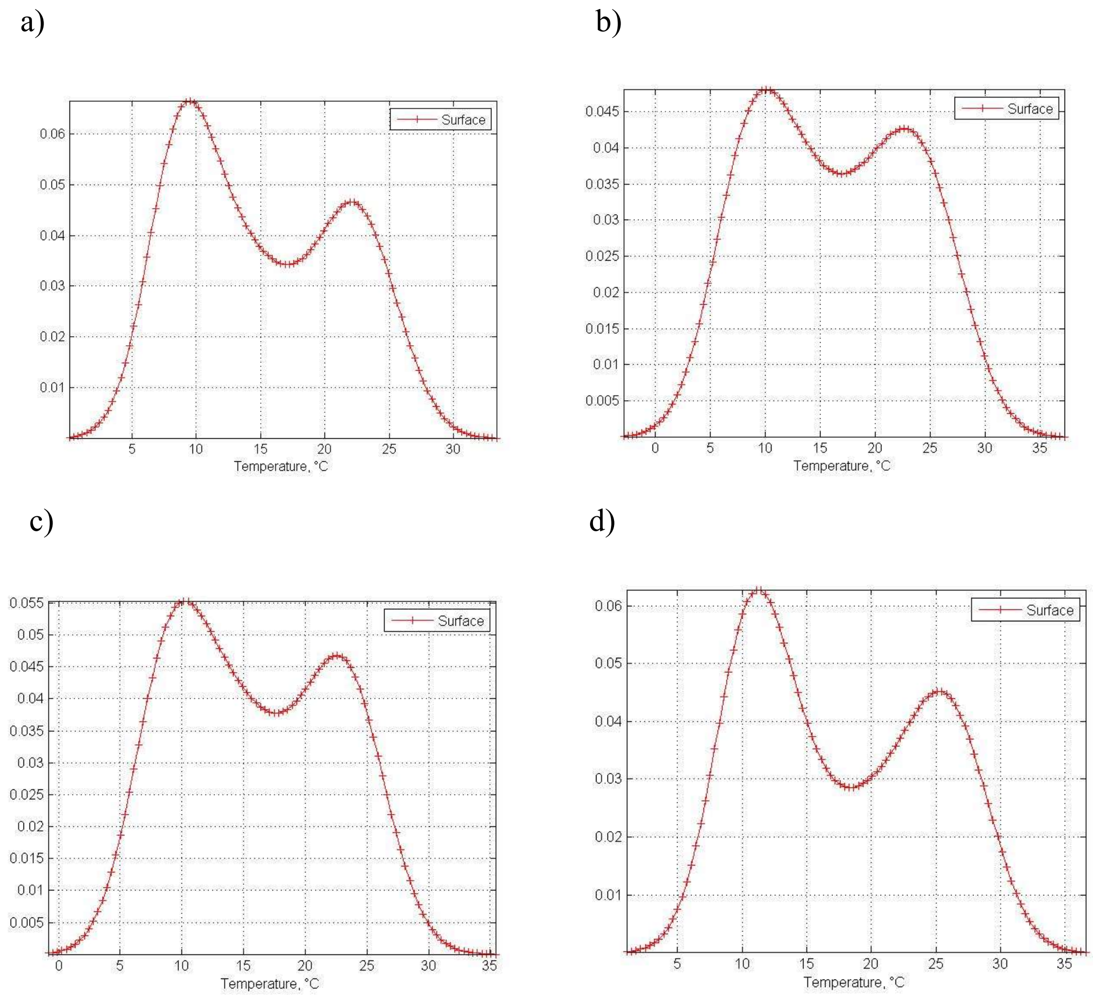

Figure C.1. Probability Distribution of Annual Seawater Surface Temperature Records in a) Northern, b) Western, c) Southern and d) Eastern Black Sea.

a) b) c) d)

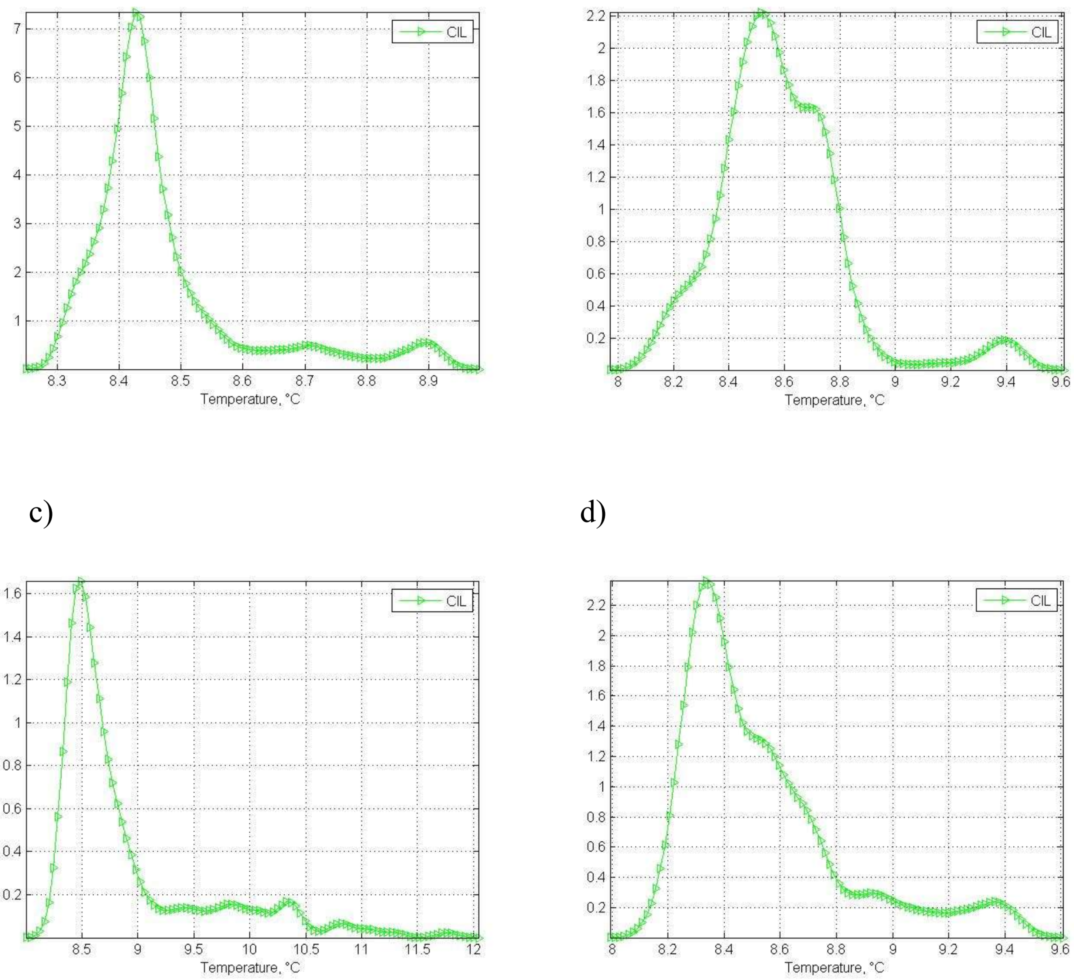

Figure C.2. Probability Distribution of Annual Seawater CIL temperature Records in a) Northern, b) Western, c) Southern and d) Eastern Black Sea.

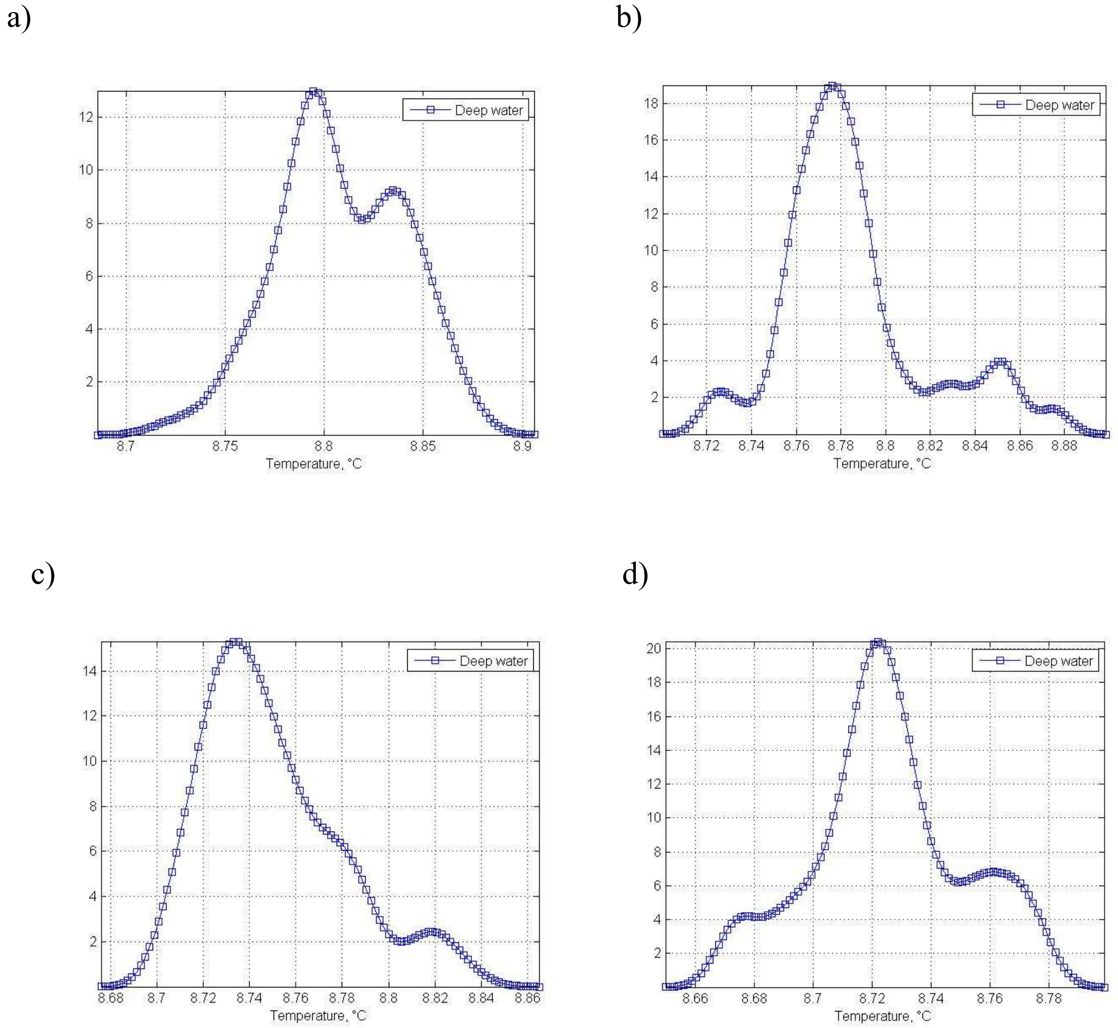

Figure C.3. Probability Distribution of Annual Deep Seawater Temperature Records in a) Northern, b) Western, c) Southern and d) Eastern Black Sea.

APPENDIX D: SUMMER TEMPERATURE PROFILES AT LARGE COASTAL COMMUNITIES AROUND THE BLACK SEA

a) Batumi

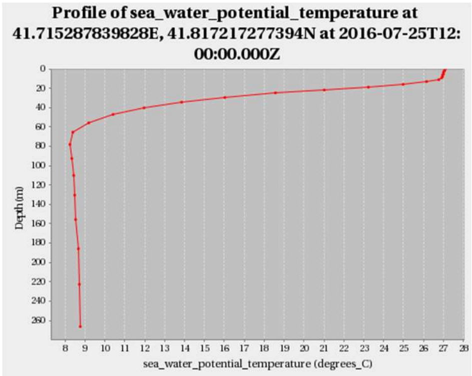

b) Istanbul

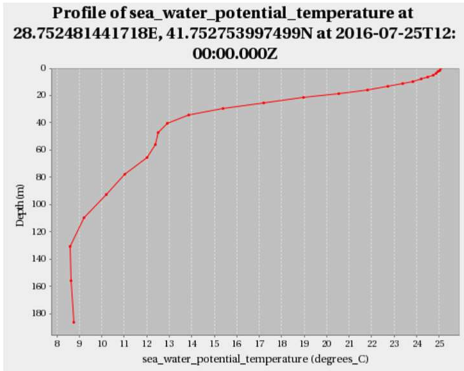

c) Novorossiysk

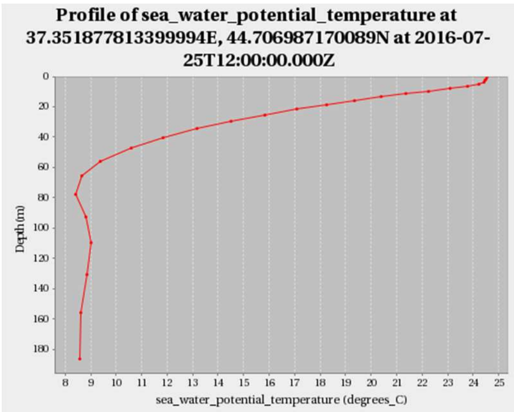

d) Odessa

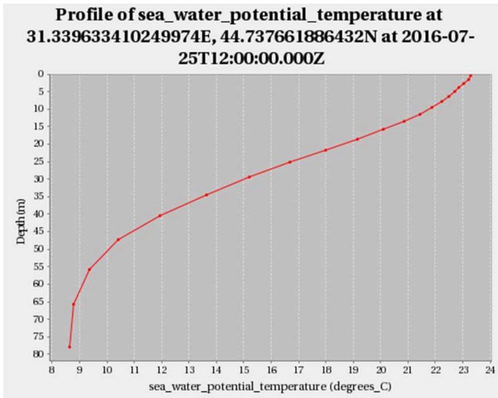

Figure D.1. Modeled Seawater Temperature Profile on 25.07.2016 near a) Batumi, b) Istanbul, c) Novorossiysk, d) Odessa, e) Samsun, f) Varna, g) Yalta.

e) Samsun

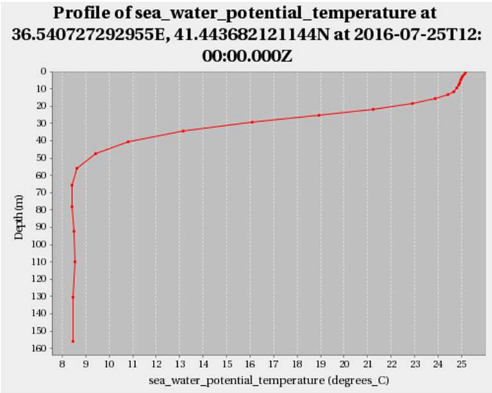

f) Varna

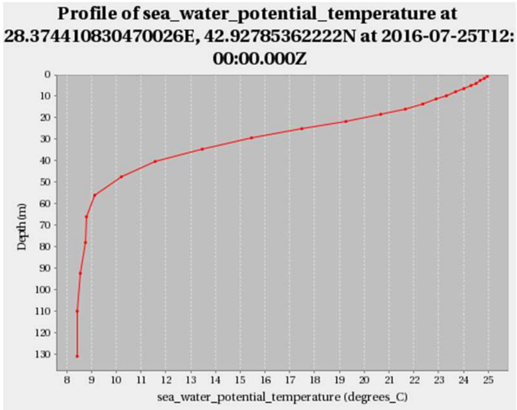

g) Yalta

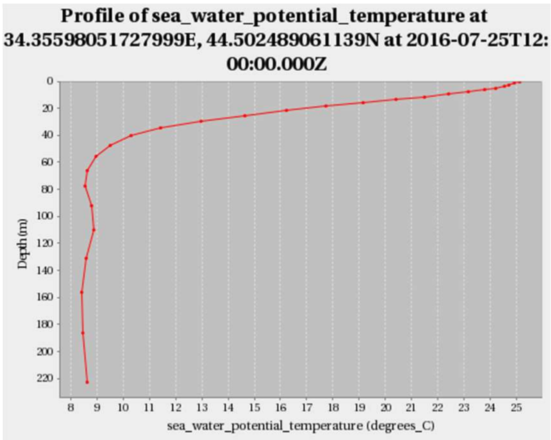

Figure D.1. Modeled Seawater Temperature Profile on 25.07.2016 near a) Batumi, b) Istanbul, c) Novorossiysk, d) Odessa, e) Samsun, f) Varna, g) Yalta (cont.).

APPENDIX E: SEAWATER PHYSICAL PROPERTIES

Table E.1. Density of Seawater at Varying Temperature and Salinity [35].

Density, kg/m^3

	Salinity, g/kg												
Temp, °C	0	10	20	30	40	50	60	70	80	90	100	110	120
0	999.8	1007.9	1016.0	1024.0	1032.0	1040.0	1048.0	1056.1	1064.1	1072.1	1080.1	1088.1	1096.2
10	999.7	1007.4	1015.2	1023.0	1030.9	1038.7	1046.6	1054.4	1062.2	1070.1	1077.9	1085.7	1093.6
20	998.2	1005.7	1013.4	1021.1	1028.8	1036.5	1044.1	1051.8	1059.5	1067.2	1074.9	1082.6	1090.3
30	995.7	1003.1	1010.7	1018.2	1025.8	1033.4	1040.9	1048.5	1056.1	1063.6	1071.2	1078.7	1086.3
40	992.2	999.7	1007.1	1014.6	1022.1	1029.5	1037.0	1044.5	1052.0	1059.4	1066.9	1074.4	1081.8
50	988.0	995.5	1002.9	1010.3	1017.7	1025.1	1032.5	1039.9	1047.3	1054.7	1062.1	1069.5	1076.9
60	983.2	990.6	998.0	1005.3	1012.7	1020.0	1027.4	1034.7	1042.1	1049.5	1056.8	1064.2	1071.5
70	977.8	985.1	992.5	999.8	1007.1	1014.5	1021.8	1029.1	1036.5	1043.8	1051.2	1058.5	1065.8
80	971.8	979.1	986.5	993.8	1001.1	1008.5	1015.8	1023.1	1030.5	1037.8	1045.1	1052.5	1059.8
90	965.3	972.6	980.0	987.3	994.7	1002.0	1009.4	1016.8	1024.1	1031.5	1038.8	1046.2	1053.5
100	958.4	965.7	973.1	980.5	987.9	995.2	1002.6	1010.0	1017.4	1024.8	1032.2	1039.6	1047.0
110	950.9	958.3	965.8	973.2	980.6	988.1	995.5	1003.0	1010.4	1017.8	1025.3	1032.7	1040.2
120	943.1	950.6	958.1	965.6	973.1	980.6	988.1	995.6	1003.1	1010.6	1018.1	1025.6	1033.1

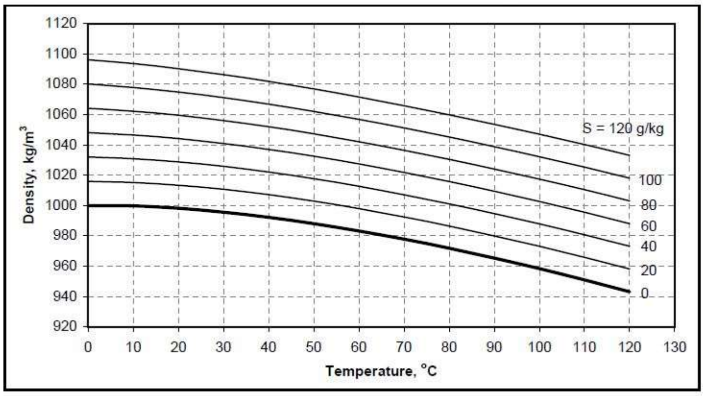

Accuracy ±0.1%

Table E.2. Dynamic Viscosity of Seawater at Varying Temperature and Salinity [35].

Dynamic viscosity x 10^3, kg/m s

	Salinity, g/kg												
Temp, °C	0	10	20	30	40	50	60	70	80	90	100	110	120
0	1.791	1.820	1.852	1.887	1.925	1.965	2.008	2.055	2.104	2.156	2.210	2.268	2.328
10	1.306	1.330	1.355	1.382	1.412	1.443	1.476	1.511	1.548	1.586	1.627	1.669	1.714
20	1.002	1.021	1.043	1.065	1.089	1.114	1.140	1.168	1.197	1.227	1.259	1.292	1.326
30	0.797	0.814	0.832	0.851	0.871	0.891	0.913	0.936	0.960	0.984	1.010	1.037	1.064
40	0.653	0.667	0.683	0.699	0.716	0.734	0.752	0.771	0.791	0.812	0.833	0.855	0.878
50	0.547	0.560	0.573	0.587	0.602	0.617	0.633	0.649	0.666	0.684	0.702	0.721	0.740
60	0.466	0.478	0.490	0.502	0.515	0.528	0.542	0.556	0.571	0.586	0.602	0.618	0.635
70	0.404	0.414	0.425	0.436	0.447	0.459	0.471	0.484	0.497	0.510	0.524	0.538	0.553
80	0.354	0.364	0.373	0.383	0.393	0.404	0.415	0.426	0.437	0.449	0.462	0.474	0.487
90	0.315	0.323	0.331	0.340	0.349	0.359	0.369	0.379	0.389	0.400	0.411	0.422	0.434
100	0.282	0.289	0.297	0.305	0.313	0.322	0.331	0.340	0.350	0.359	0.369	0.380	0.390
110	0.255	0.262	0.269	0.276	0.283	0.291	0.299	0.308	0.316	0.325	0.334	0.344	0.354
120	0.232	0.238	0.245	0.251	0.258	0.265	0.273	0.280	0.288	0.297	0.305	0.314	0.323

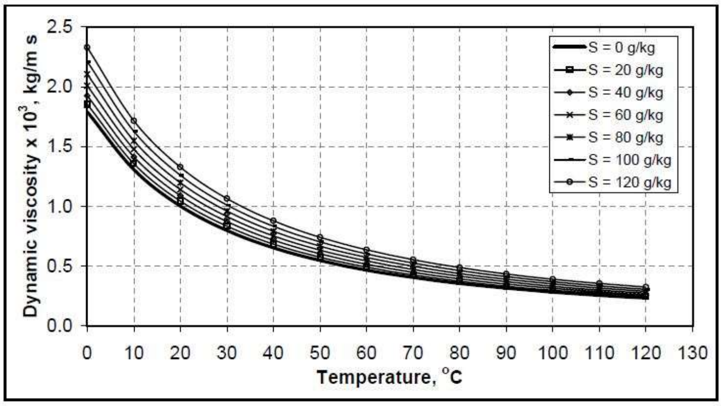

Accuracy ±1.5%

Table E.3. Kinematic Viscosity of Seawater at Varying Temperature and Salinity [35].

Kinematic viscosity x 10^7, m^2/s

	Salinity, g/kg												
Temp, °C	**0**	**10**	**20**	**30**	**40**	**50**	**60**	**70**	**80**	**90**	**100**	**110**	**120**
0	17.92	18.06	18.23	18.43	18.65	18.90	19.16	19.46	19.77	20.11	20.46	20.84	21.24
10	13.07	13.20	13.35	13.51	13.69	13.89	14.10	14.33	14.57	14.82	15.09	15.38	15.67
20	10.04	10.16	10.29	10.43	10.58	10.75	10.92	11.10	11.30	11.50	11.71	11.93	12.17
30	8.01	8.12	8.23	8.36	8.49	8.63	8.77	8.93	9.09	9.26	9.43	9.61	9.80
40	6.58	6.68	6.78	6.89	7.00	7.13	7.25	7.38	7.52	7.66	7.81	7.96	8.11
50	5.53	5.62	5.71	5.81	5.91	6.02	6.13	6.24	6.36	6.48	6.61	6.74	6.87
60	4.74	4.82	4.91	4.99	5.08	5.18	5.28	5.38	5.48	5.59	5.70	5.81	5.93
70	4.13	4.20	4.28	4.36	4.44	4.52	4.61	4.70	4.79	4.89	4.98	5.08	5.19
80	3.65	3.71	3.78	3.85	3.93	4.00	4.08	4.16	4.25	4.33	4.42	4.51	4.60
90	3.26	3.32	3.38	3.45	3.51	3.58	3.65	3.73	3.80	3.88	3.96	4.04	4.12
100	2.94	3.00	3.05	3.11	3.17	3.24	3.30	3.37	3.44	3.51	3.58	3.65	3.73
110	2.68	2.73	2.78	2.84	2.89	2.95	3.01	3.07	3.13	3.20	3.26	3.33	3.40
120	2.46	2.51	2.55	2.60	2.65	2.71	2.76	2.82	2.88	2.93	3.00	3.06	3.12

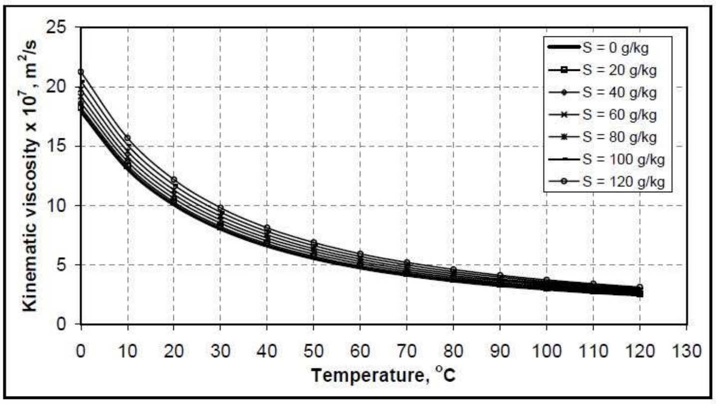

Accuracy ±1.5%

Table E.4. Prandtl Number of Seawater at Varying Temperature and Salinity [35].

Prandtl number

	Salinity, g/kg												
Temp, °C	**0**	**10**	**20**	**30**	**40**	**50**	**60**	**70**	**80**	**90**	**100**	**110**	**120**
0	13.18	13.21	13.25	13.31	13.40	13.50	13.63	13.78	13.94	14.13	14.34	14.56	14.81
10	9.32	9.36	9.41	9.48	9.56	9.65	9.76	9.87	10.00	10.14	10.30	10.46	10.64
20	6.95	7.00	7.06	7.12	7.19	7.27	7.36	7.46	7.56	7.67	7.79	7.92	8.05
30	5.40	5.45	5.51	5.57	5.63	5.70	5.78	5.86	5.94	6.03	6.13	6.23	6.33
40	4.34	4.38	4.43	4.49	4.54	4.60	4.67	4.74	4.81	4.88	4.96	5.04	5.13
50	3.57	3.61	3.66	3.71	3.76	3.81	3.87	3.93	3.99	4.05	4.12	4.18	4.25
60	3.00	3.04	3.08	3.12	3.17	3.22	3.27	3.32	3.37	3.42	3.48	3.54	3.60
70	2.57	2.60	2.64	2.68	2.72	2.76	2.81	2.85	2.90	2.94	2.99	3.04	3.09
80	2.23	2.27	2.30	2.33	2.37	2.41	2.45	2.49	2.53	2.57	2.61	2.66	2.70
90	1.97	2.00	2.03	2.06	2.09	2.13	2.16	2.20	2.23	2.27	2.31	2.35	2.39
100	1.76	1.78	1.81	1.84	1.87	1.90	1.93	1.96	1.99	2.03	2.06	2.10	2.13
110	1.59	1.61	1.63	1.66	1.69	1.71	1.74	1.77	1.80	1.83	1.86	1.89	1.93
120	1.45	1.47	1.49	1.51	1.54	1.56	1.59	1.61	1.64	1.67	1.70	1.73	1.76

Accuracy ±3.3%

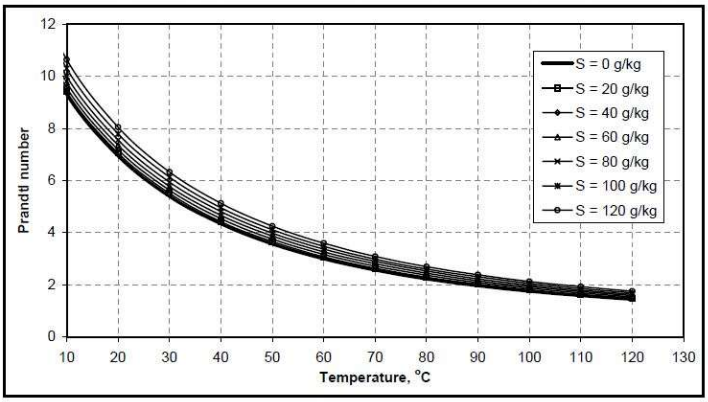

Table E.5. Specific Heat of Seawater at Varying Temperature and Salinity [35].

Specific heat at constant pressure, J/kg K

	Salinity, g/kg												
Temp, °C	**0**	**10**	**20**	**30**	**40**	**50**	**60**	**70**	**80**	**90**	**100**	**110**	**120**
0	4206.8	4142.1	4079.9	4020.1	3962.7	3907.8	3855.3	3805.2	3757.6	3712.4	3669.7	3629.3	3591.5
10	4196.7	4136.7	4078.8	4022.8	3968.9	3916.9	3867.1	3819.2	3773.3	3729.5	3687.7	3647.9	3610.1
20	4189.1	4132.8	4078.2	4025.3	3974.1	3924.5	3876.6	3830.4	3785.9	3743.0	3701.8	3662.3	3624.5
30	4183.9	4130.5	4078.5	4027.8	3978.6	3930.8	3884.4	3839.4	3795.8	3753.6	3712.7	3673.3	3635.3
40	4181.0	4129.7	4079.6	4030.7	3982.9	3936.4	3891.0	3846.7	3803.7	3761.8	3721.1	3681.6	3643.2
50	4180.6	4130.8	4081.9	4034.1	3987.3	3941.5	3896.6	3852.9	3810.1	3768.3	3727.5	3687.8	3649.0
60	4182.7	4133.7	4085.5	4038.3	3992.0	3946.5	3902.0	3858.3	3815.5	3773.7	3732.7	3692.6	3653.4
70	4187.1	4138.5	4090.6	4043.6	3997.3	3951.9	3907.4	3863.6	3820.6	3778.5	3737.2	3696.7	3657.0
80	4194.0	4145.3	4097.3	4050.1	4003.7	3958.1	3913.3	3869.2	3825.9	3783.5	3741.7	3700.8	3660.7
90	4203.4	4154.2	4105.9	4058.3	4011.5	3965.4	3920.2	3875.7	3832.0	3789.1	3746.9	3705.6	3665.0
100	4215.2	4165.4	4116.4	4068.2	4020.9	3974.3	3928.5	3883.6	3839.4	3796.0	3753.5	3711.7	3670.8
110	4229.4	4178.8	4129.1	4080.2	4032.2	3985.1	3938.7	3893.3	3848.6	3804.9	3761.9	3719.9	3678.6
120	4246.1	4194.7	4144.2	4094.6	4045.9	3998.2	3951.3	3905.4	3860.3	3816.2	3773.0	3730.7	3689.4

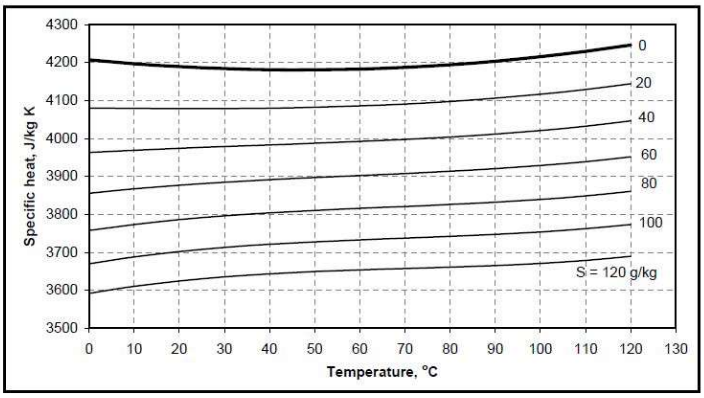

Accuracy ±1%

Table E.6. Thermal Conductivity of Seawater at Varying Temperature and Salinity [35].

Thermal conductivity, W/m K

	Salinity, g/kg												
Temp, °C	0	10	20	30	40	50	60	70	80	90	100	110	120
0	0.572	0.571	0.570	0.570	0.569	0.569	0.568	0.568	0.567	0.566	0.566	0.565	0.565
10	0.588	0.588	0.587	0.587	0.586	0.585	0.585	0.584	0.584	0.583	0.583	0.582	0.582
20	0.604	0.603	0.602	0.602	0.601	0.601	0.600	0.600	0.599	0.599	0.598	0.598	0.597
30	0.617	0.617	0.616	0.616	0.615	0.615	0.614	0.614	0.613	0.613	0.612	0.612	0.611
40	0.630	0.629	0.629	0.628	0.628	0.627	0.627	0.626	0.626	0.625	0.625	0.624	0.624
50	0.641	0.640	0.640	0.639	0.639	0.638	0.638	0.637	0.637	0.636	0.636	0.635	0.635
60	0.650	0.650	0.649	0.649	0.648	0.648	0.647	0.647	0.647	0.646	0.646	0.645	0.645
70	0.658	0.658	0.658	0.657	0.657	0.656	0.656	0.655	0.655	0.655	0.654	0.654	0.653
80	0.665	0.665	0.665	0.664	0.664	0.663	0.663	0.663	0.662	0.662	0.661	0.661	0.661
90	0.671	0.671	0.670	0.670	0.670	0.669	0.669	0.669	0.668	0.668	0.667	0.667	0.667
100	0.676	0.675	0.675	0.675	0.674	0.674	0.674	0.673	0.673	0.673	0.672	0.672	0.672
110	0.679	0.679	0.679	0.678	0.678	0.678	0.677	0.677	0.677	0.676	0.676	0.676	0.675
120	0.682	0.681	0.681	0.681	0.680	0.680	0.680	0.679	0.679	0.679	0.679	0.678	0.678

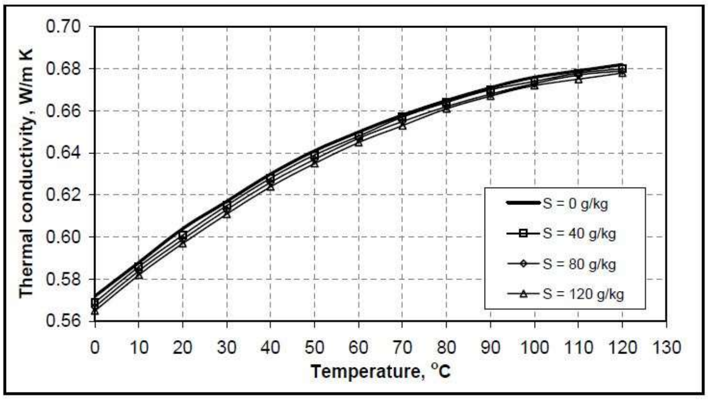

Accuracy ±3.0%

APPENDIX F: PIPE AND FLOW CHARACTERISTICS

Table F.1. Minor Loss Coefficients for Pipes.

FITTING TYPE	PROPERTY	PRESSURE LOSS COEFFICIENT		FLOW DIRECTION
90° ELBOW	R=1.0xd	0.51		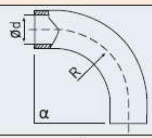
	1.5xd	0.41		
	2.0xd	0.34		
	4.0xd	0.23		
45° ELBOW	R = 1.0xd	0.34		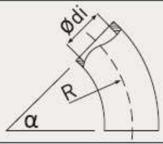
	1.5xd	0.27		
	2.0xd	0.20		
	4.0xd	0.15		
ELBOW	$a = 45°$	0.30		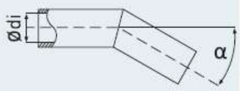
	30°	0.14		
	20°	0.05		
	15°	0.05		
	20°	0.04		
	V_z / V_s	ζ_z	ζ_c	
TEE PART	0.0	-1.2	0.06	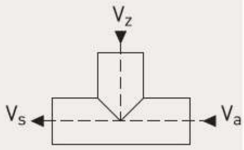
(COLLECTION BRANCH 90°)	0.2	0.40	0.20	
$V_s = V_a + V_d$	0.3	0.10	0.30	
	0.6	0.50	0.40	
	0.8	0.70	0.50	
	1.0	0.90	1.60	
	V_a / V_s	ζ_a	ζ_s	
TEE PART	0.0	0.97	0.10	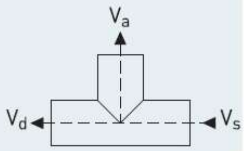
(DISTRIBUTION BRANCH 90°)	0.2	0.90	0.10	
$V_s = V_a + V_d$	0.4	0.10	0.05	
	0.6	0.90	0.10	
	0.8	1.10	0.20	
	1.0	1.30	0.35	
	a	ζ_s		
REDUCER	30°	0.60		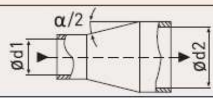
(EXPANDING OUTPUT)	45°	0.80		
ζ = value $\lambda_R = 0.025$	60°	1.00		
REDUCER	30°	0.02		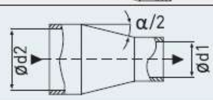
(TAPERING OUTPUT)	45°	0.02		
ζ = value $\lambda_R = 0.025$	60°	1.07		

Table F.2. Pipe Roughness.

Pipe Material	e (mm)	e (ft)
Brass	0.0015	0.000005
Concrete		
Steel forms, smooth	0.18	0.0006
Good joints, average	0.36	0.0012
Rough, visible form marks	0.60	0.002
Copper	0.0015	0.000005
Corrugated metal (CMP)	45	0.15
Iron (common in older water lines, except ductile or DIP, which is widely used today)		
Asphalt lined	0.12	0.0004
Cast	0.26	0.00085
Ductile; DIP—cement mortar lined	0.12	0.0004
Galvanized	0.15	0.0005
Wrought	0.045	0.00015
Polyvinyl chloride (PVC)	0.0015	0.000005
Polyethylene, high density (HDPE)	0.0015	0.000005
Steel		
Enamel coated	0.0048	0.000016
Riveted	0.9 ~ 9.0	0.003–0.03
Seamless	0.004	0.000013
Commercial	0.045	0.00015

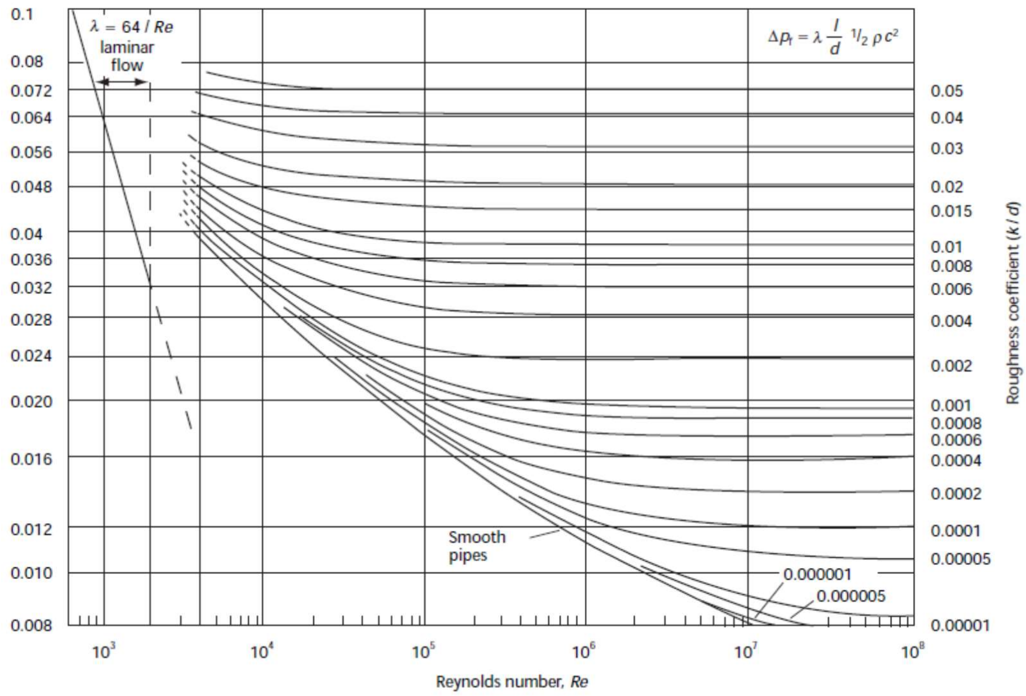

Figure F.1. Moody Diagram.

APPENDIX G: PROCESS EQUIPMENT SIZE EXPONENT

Table G.1. Process Equipment Size Exponent [36].

PROCESS EQUIPMENT SIZE EXPONENT (N) - TABLE 1		
EQUIPMENT NAME	UNIT	SIZE EXPONENT (N)
Agitator, propeller	Hp	0.50
Agitator, turbine	Hp	0.30
Air compressor, single stage	cfm	0.67
Air compressor, multiple stage	cfm	0.75
Air dryer	cfm	0.56
Boiler, industrial, all sizes	lb/hr	0.50
Boiler, package	lb/hr	0.72
Centrifuge, horizontal basket	dia (inches)	1.72
Centrifuge, solid bowl	dia (inches)	1.00
Conveyor, belt	feet	0.65
Conveyor, bucket	feet	0.77
Conveyor, screw	feet	0.76
Conveyor, vibrating	feet	0.87
Crystallizer, growth	ton/day	0.65
Crystallizer, forced circulation	ton/day	0.55
Crystallizer, batch	gallons	0.70

Table G.1. Process Equipment Size Exponent (cont.) [36].

PROCESS EQUIPMENT SIZE EXPONENT (N) - TABLE 1		
EQUIPMENT NAME	UNIT	SIZE EXPONENT (N)
Dryer, drum and rotatory	sq. ft.	0.45
Dust collector, cyclone	cfm	0.80
Dust collector, cloth filter	cfm	0.68
Dust collector, precipitator	cfm	0.75
Evaporator, forced circulation	sq. ft.	0.70
Evaporator, vertical and horizontal tube	sq. ft.	0.53
Fan	Hp	0.66
Filter, plate and press	sq. ft.	0.58
Filter, pressure leaf	sq. ft.	0.55
Heat exchanger, fixed tube	sq. ft.	0.62
Heat exchanger, U-tube	sq. ft.	0.53
Mill, ball and roller	ton/hr	0.65
Mill, hammer	ton/hr	0.85
Pump, centrifugal carbon steel	Hp	0.67
Pump, centrifugal stainless steel	Hp	0.70
Tanks and vessels, pressure, carbon steel	gallons	0.60
Tanks and vessels, horizontal, carbon steel	gallons	0.50
Tanks and vessels, stainless steel	gallons	0.68

APPENDIX H: BOĞAZİÇİ UNIVERSITY SARITEPE CAMPUS COOLING DEMAND MODEL RESULTS

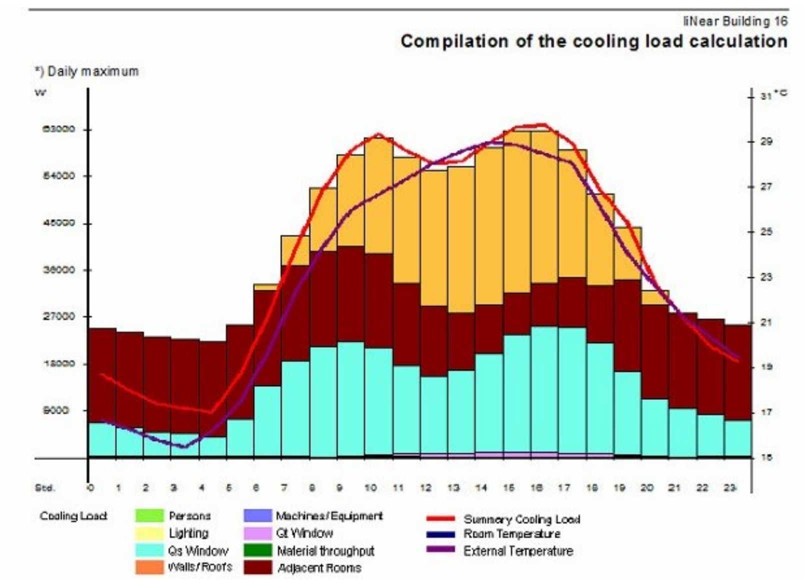

Figure H.1. First Female Dormitory Daily Cooling Load Variation.

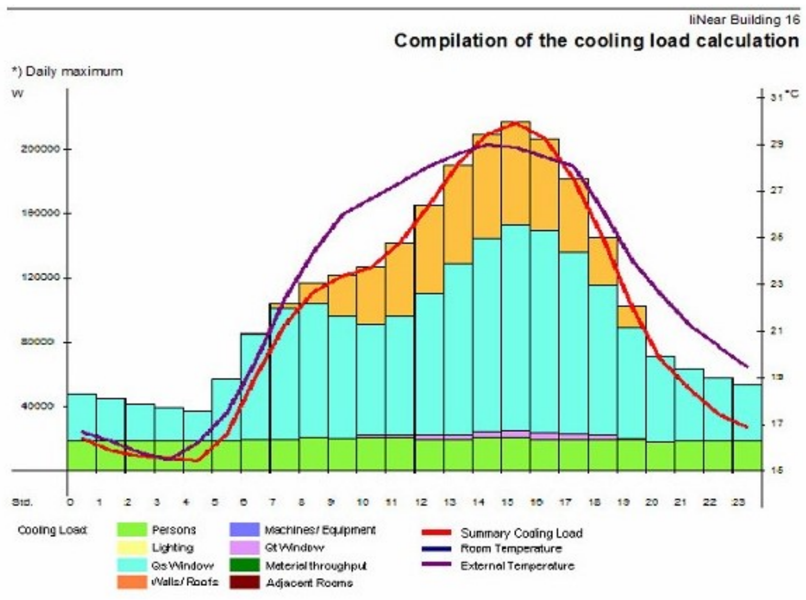

Figure H.2. Second Male Dormitory Daily Cooling Load Variation.

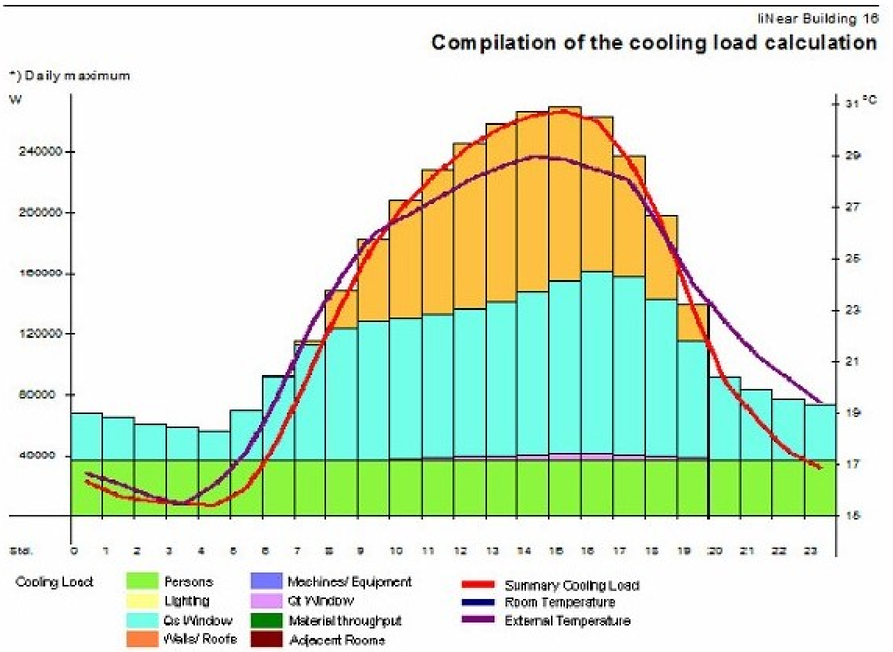

Figure H.3. Third Dormitory Daily Cooling Load Variation.

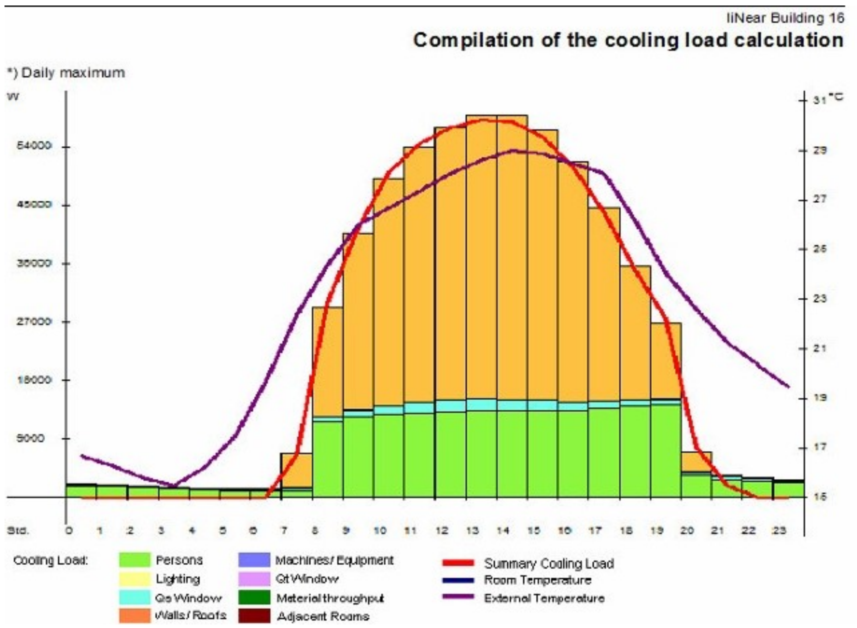

Figure H.4. Sports Complex Daily Cooling Load Variation.

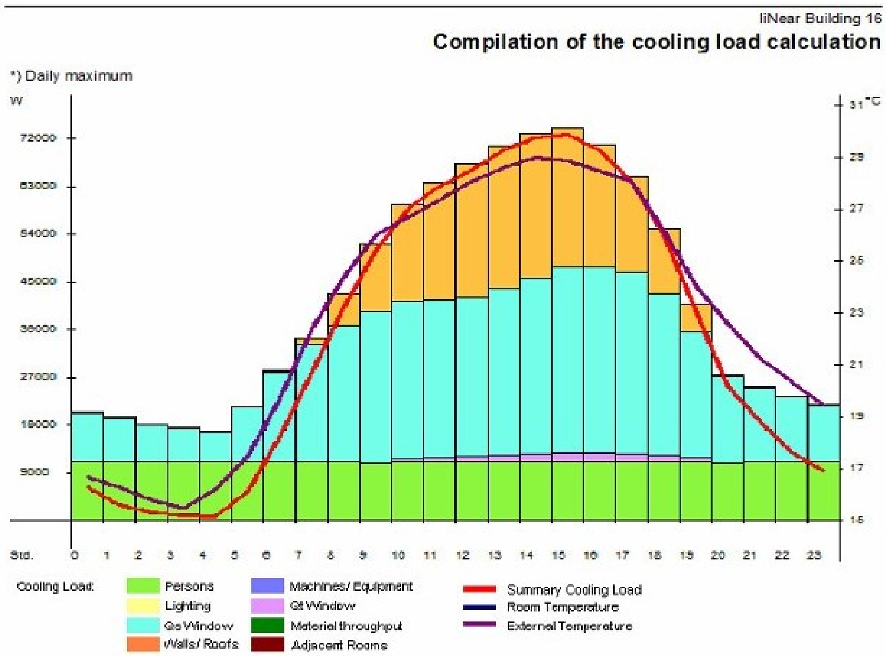

Figure H.5. Hotel Daily Cooling Load Variation.

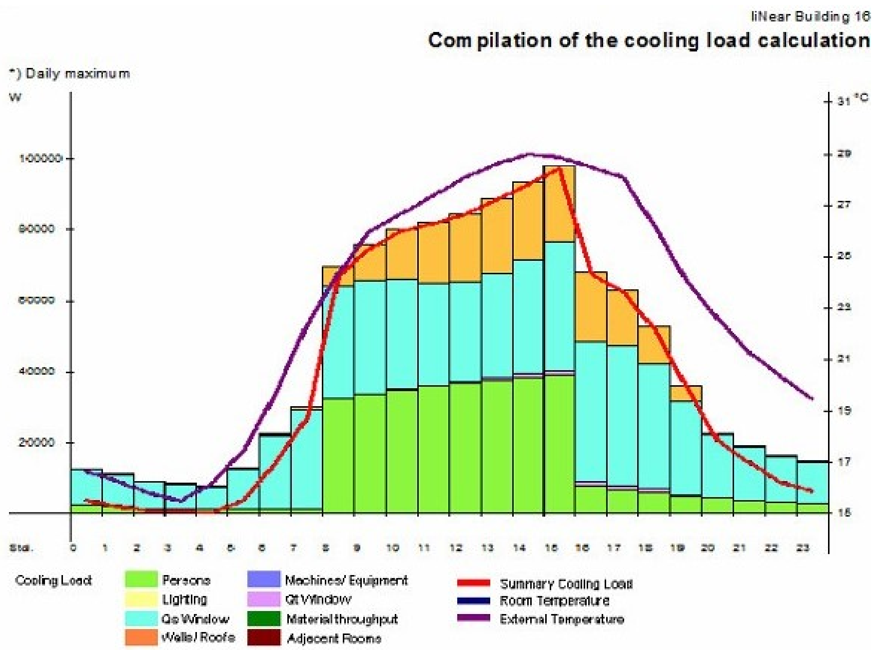

Figure H.6. Language School Building 1 Daily Cooling Load Variation.

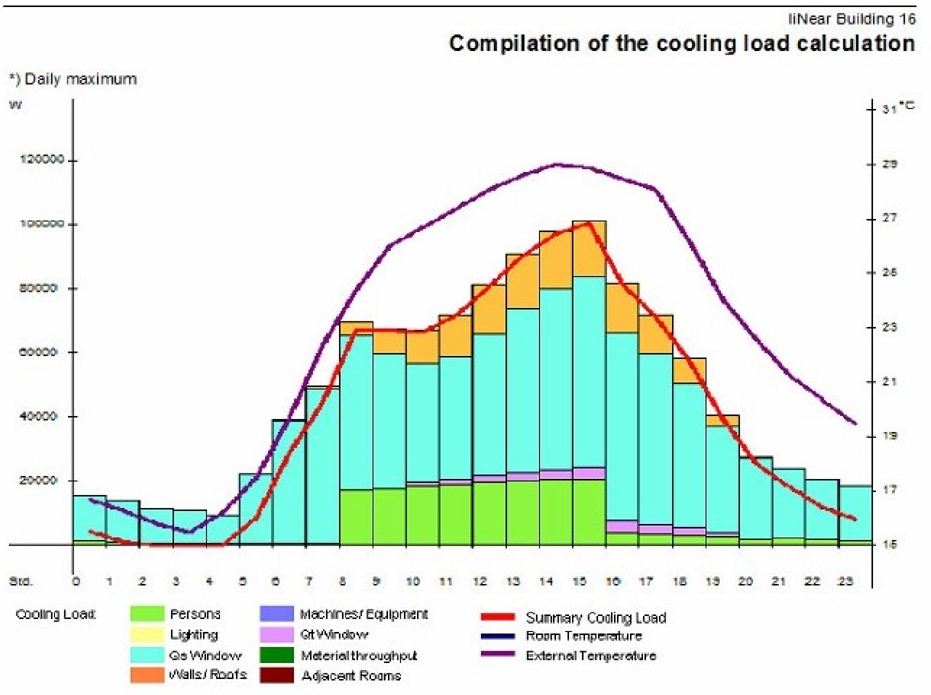

Figure H.7. Language School Building 2 Daily Cooling Load Variation.

APPENDIX I: CHILLER UNITS' SPECIFICATIONS

Table I.1. Water-Cooled Chiller Unit 23 XRV [37].

Model			23XRV3030 NQVAA90	23XRV3232 NQVAA90	23XRV4041 EQVAA90	23XRV4041 NRVAA90	23XRV4142 NRVAA90	23XRV4747 ERVBA90	23XRV5657 ERXCC90
Chiller	Cooling Capacity	kW	1055	1231	1407	1583	1758	1913	2110
		Tons	300	350	400	450	500	544	600
	Full Load COP	ikW/kW	0.168	0.161	0.158	0.162	0.167	0.163	0.163
	NPLV	ikW/kW	0.097	0.093	0.093	0.095	0.095	0.094	0.092
	Input Power	kW	177	198	223	256	293	313	343
Motor	RLA	A	269	299	337	387	443	472	520
	Inrush Amps	A	269	299	337	387	443	472	520
	Flow Rate	l/s	50.4	58.8	67.2	75.6	84	91.4	100.8
Condenser	Water Connection	mm	DN200						
	Flow Rate	l/s	59.1	68.6	78.2	88.2	98.3	106.5	117.7
Cooler	Water Connection	mm	DN200						DN250
Dimensions	Length	mm	4172	4172	4347	4347	4347	4867	4902
	Width	mm	1930	1930	2045	2045	2045	2127	2127
	Height	mm	2200	2200	2299	2299	2299	2305	2305
Weight	Rigging (w/Refrigerant)	kg	6953	7310	8404	8594	8759	9705	10791
	Operating	kg	7374	7864	9247	9437	9668	10731	12070
	Refrigerant	kg	295	295	408	340	340	460	649

Table I.2. Air-Cooled VSD Screw Chiller Unit [38].

Air-cooled VSD screw chiller

YVAA 0543 to 1700

Application flexibility (*) example of selections

YVAA	0543	0565	0588	0643	0665	0688	0700	0743	0765	0788	0843	0865	0888	0943	0963
Cooling capacity (kW)	471	549	569	573	588	639	614	658	698	738	748	768	808	812	867
Full Load Efficiency (EER)	3.04	3.13	3.22	3.07	3.09	3.17	2.78	3.11	3.16	3.13	3	3.08	3.15	3.06	3.14
Part Load Efficiency (ESEER)	4.2	4.26	4.39	4.27	4.26	4.34	3.8	4.29	4.31	4.29	4.22	4.34	4.32	4.25	4.32
Sound power level (dBA)	95	97	94	96	94	95	95	97	97	95	97	95	96	98	98

YVAA	0965	0988	1015	1065	1088	1093	1143	1188	1193	1215	1315	1343	1443	1700
Cooling capacity (kW)	898	933	948	971	997	964	1002	1022	1017	1047	1118	1077	1221	1455
Full Load Efficiency (EER)	3.02	3.13	3.05	3.03	3.12	3.06	3.1	3.18	3.06	3.14	3.14	3.07	3.12	3.03
Part Load Efficiency (ESEER)	4.31	4.38	4.37	4.29	4.47	4.3	4.38	4.34	4.3	4.43	4.37	4.27	4.31	4.17
Sound power level (dBA)	96	96	95	97	97	99	99	97	97	97	97	97	101	101

APPENDIX J: RESULTS OF HEAT EXCHANGER MODELING IN ASPEN EXCHANGER DESIGN AND RATING V 8.8

Table J.1. Heat Exchanger Cost for 1000 kW Heat Transfer Rate (USD).

		Outlet water temperature, °C							
		20	**21**	**22**	**23**	**24**	**25**	**26**	**27**
Inlet water temperature, °C	**8**	31,357	32,604	36,941	36,941	38,925	41,906	40,039	41,906
	9	31,357	32,604	38,925	36,941	40,918	41906	41,906	41,906
	10	31,357	32,604	35,082	38,925	40,918	41,906	41,906	41,906
	11	31,357	32,604	35,082	40,918	40,918	41,906	41,906	41,906
	12	32,604	32,604	35,082	37,561	40,918	41,906	41,906	41,906
	13	33,961	32,604	35,082	38,800	41,906	41,906	41,906	41,906
	14	33,961	36,322	35,082	38,800	41,906	41,906	41,906	41,906
	15	35,945	36,941	36,322	38,800	41,906	41,906	41,906	41,906
	16	45,875	36,941	39,922	38,800	42,518	41,906	41,906	42,902
	17	179,035	45,875	39,922	41,278	42,518	44,886	41,906	43,890
	18	257,174	179,035	44,886	44,886	42,518	47,467	44,886	44,886
	19	351,821	257,174	179,035	44,886	49,843	47,467	50,839	45,875
	20		351,821	257,174	177,320	49,843	49,937	54,878	50,839
	21			348,963	257,174	177,320	62,290	56,118	58,769
	22				348,963	257,174	177,320	62,290	64,761
	23					348,963	257,174	177,320	672,31
	24						368,340	257,174	177,320
	25							346,105	257,174
	26								346,105

Table J.2. Mass Flow Rate on a Seawater Side for 1000 kW Heat Transfer Rate (kg/s).

		Outlet water temperature, °C							
		20	**21**	**22**	**23**	**24**	**25**	**26**	**27**
Inlet water temperature, °C	**8**	21.54	19.88	18.47	17.24	16.16	15.21	14.37	13.61
	9	23.5	21.54	19.89	18.47	17.24	16.16	15.21	14.37
	10	25.46	23.51	21.55	19.89	18.47	17.24	16.17	15.22
	11	28.73	25.86	23.51	21.56	19.9	18.48	17.25	16.17
	12	32.33	28.74	25.86	23.52	21.56	19.9	18.48	17.25
	13	36.96	32.34	28.75	25.87	23.52	21.57	19.9	18.49
	14	43.13	36.96	32.34	28.75	25.88	23.53	21.57	19.9
	15	51.85	43.13	36.97	32.35	28.76	25.89	23.53	21.58
	16	64.7	51.76	43.14	36.98	32.36	28.77	25.89	23.54
	17	86.27	64.7	51.78	43.15	36.99	32.37	28.77	25.9
	18	129.4	86.29	64.7	51.79	43.16	36.99	32.37	28.78
	19	258.9	129.4	86.3	64.74	51.8	43.17	37	32.38
	20		258.9	129.48	86.33	64.75	51.81	43.17	37.01
	21			259.9	129.51	86.34	64.76	51.81	43.18
	22				259.9	129.54	86.36	64.78	51.82
	23					259.1	129.56	86.38	64.79
	24						259.1	129.58	86.39
	25							259.1	129.59
	26								259.1

Table J.3. Heat Exchanger Cost for 1500 kW Heat Transfer Rate (USD).

		Outlet water temperature, °C							
		20	**21**	**22**	**23**	**24**	**25**	**26**	**27**
Inlet water temperature, °C	**8**	45,267	48,158	56,997	54,682	59,706	61,078	62,780	62,780
	9	45,267	48,158	51,050	56,997	61,142	61,078	62,780	62,780
	10	45,267	48,158	51,050	62,780	61,142	61,078	62,780	62,780
	11	46,712	48,158	52,495	56,824	62,780	61,078	62,780	62,780
	12	51,205	48,158	52,495	56,824	62,780	61,078	62,780	62,780
	13	51,205	52,495	52,495	56,824	62,780	62,780	62,780	62,780
	14	51,205	55,835	52,495	56,824	61,078	62,780	62,780	62,780
	15	79,873	54,682	58,260	56,824	62,588	62,780	62,780	63,933
	16	87,898	79,873	69,790	58,260	62,588	65,095	62,780	63,933
	17	120,391	87,898	79,873	69,790	64,025	71,235	65,095	66,248
	18	208,637	120,391	87,898	79,873	69,790	71,235	73,184	67,401
	19	540,976	208,637	120,391	87,898	79,873	72,672	84,750	73,184
	20		537,042	208,637	120,391	87,898	79,873	97,277	80,999
	21			537,042	208,637	120,391	84,650	79,873	97,277
	22				537,042	206,495	120,391	87,898	79,873
	23					537,042	206,495	120,391	100,901
	24						533,107	206,495	118,762
	25							533,107	206,,495
	26								533,107

Table J.4. Mass Flow Rate on a Seawater Side for 1500 kW Heat Transfer Rate (kg/s).

		Outlet water temperature, °C							
		20	**21**	**22**	**23**	**24**	**25**	**26**	**27**
Inlet water temperature, °C	**8**	30.62	28.27	26.25	24.51	22.98	21.63	20.43	19.36
	9	33.41	30.63	28.28	26.26	24.51	22.98	21.63	20.44
	10	36.77	33.42	30.64	28.28	26.27	24.52	22.99	21.64
	11	40.85	36.77	33.43	30.65	28.29	26.28	24.53	23
	12	45.97	40.86	36.78	33.44	30.66	28.3	26.28	24.53
	13	52.54	45.98	40.87	36.79	33.45	30.66	28.31	26.29
	14	61.31	52.55	45.99	40.88	36.79	33.46	30.67	28.31
	15	73.66	61.31	52.57	46	40.88	36.8	33.46	30.68
	16	91.99	73.66	61.34	52.58	46	40.9	36.81	33.47
	17	122.67	92.01	73.66	61.35	52.58	46.02	40.91	36.82
	18	184.02	122.69	92.03	73.66	61.35	52.6	46.03	40.92
	19	368.1	184.07	122.72	92.05	73.66	61.38	52.61	46.04
	20		368.17	184.1	122.74	92.05	73.66	61.39	52.62
	21			368.22	184.13	122.77	92.08	73.66	61.4
	22				368.32	184.18	122.79	92.1	73.66
	23					368.39	184.21	122.82	92.12
	24						368.46	184.24	122.84
	25							368.52	184.27
	26								368.57

Table J.5. Heat Exchanger Cost for 2000 kW Heat Transfer Rate (USD).

		Outlet water temperature, °C							
		20	**21**	**22**	**23**	**24**	**25**	**26**	**27**
Inlet water temperature, °C	**8**	67,661	73,301	78,930	83,882	83,882	86,438	93,947	105,183
	9	67,661	73,301	78,930	83,882	83,882	93,947	93,947	105,183
	10	67,661	73,301	78,930	83,882	83,882	97,696	95,721	105,183
	11	67,661	73,301	78,930	83,882	83,882	88,614	97,696	107,559
	12	67,661	73,301	78,930	83,882	83,882	88,614	105,194	109,925
	13	75,181	73,301	78,930	83,882	83,882	90,990	112,702	109,925
	14	88,318	75,181	78,930	83,882	83,882	90,990	100,452	112,290
	15	107,073	88,318	78,930	88,318	83,882	90,990	100,452	118,320
	16	138,945	105,194	88,318	88,212	93,355	93,355	102,818	118,320
	17	206,195	138,945	105,194	88,318	97,696	93,355	105,183	118,320
	18	355,437	206,195	138,945	105,194	99,575	105,183	105,183	120,200
	19	4182085	355,437	206,195	138,945	105,194	112,702	107,559	124,108
	20		4173003	355,437	206,195	138,945	112,702	124,108	124,108
	21			4163921	352,311	203,724	138,945	131,447	128,839
	22				4154839	352,311	203,724	138,945	150,118
	23					4145757	352,311	203,724	774,300
	24						4145757	352,311	203,724
	25							4136674	352,311
	26								4127592

Table J.6. Mass Flow Rate on a Seawater Side for 2000 kW Heat Transfer Rate (kg/s).

		Outlet water temperature, °C							
		20	**21**	**22**	**23**	**24**	**25**	**26**	**27**
Inlet water temperature, °C	**8**	40.83	37.7	35.01	32.68	30.64	28.84	27.24	25.81
	9	44.55	40.85	37.71	35.02	32.69	30.65	28.85	27.25
	10	49.02	44.57	40.86	37.72	35.03	32.7	30.66	28.85
	11	54.47	49.03	44.58	40.87	37.73	35.04	32.71	30.66
	12	61.29	54.49	49.04	44.59	40.88	37.74	35.05	32.71
	13	70.06	61.31	54.5	49.05	44.6	40.89	37.75	35.05
	14	81.74	70.08	61.32	54.51	49.07	44.61	40.9	37.75
	15	98.11	81.77	70.09	61.34	54.53	49.08	44.62	40.91
	16	122.65	98.14	81.79	70.11	61.35	54.54	49.09	44.63
	17	163.56	122.68	98.16	81.8	70.12	61.36	54.55	49.1
	18	245.37	163.6	122.71	98.17	81.82	70.14	61.37	54.56
	19	490.8	245.43	163.63	122.73	98.19	81.84	70.15	61.39
	20		490.9	245.47	163.66	122.76	98.21	81.85	70.16
	21			490.97	245.51	163.69	122.78	98.23	81.87
	22				491.1	245.57	163.73	122.8	98.25
	23					491.19	245.64	163.76	122.82
	24						491.28	245.66	163.78
	25							491.36	245.7
	26								491.43

APPENDIX K: HDPE 100 PIPE PRICES

Table K.1. HDPE 100 Pipe Cost, Manufactured by PETEK BORU [39].

HDPE 100 BORULARI FİYAT LİSTESİ

01.08.2012

PU. KILIF BORUSU				SDR 41 - PN 4				SDR 33 - PN 5				SDR 26 - PN 6			
Çap DN	Et Kal.(mm)	Kg/mt	TL/mt	Çap DN	Et Kal.(mm)	Kg/mt	TL/mt	Çap DN	Et Kal.(mm)	Kg/mt	TL/mt	Çap DN	Et Kal.(mm)	Kg/mt	TL/mt
												50	2,0	0,31	1,55
								63	2,0	0,38	1,90	63	2,5	0,49	2,45
75	2,2	0,53	2,65	75	2,0	0,46	2,30	75	2,3	0,53	2,65	75	2,9	0,67	3,35
90	2,2	0,64	3,20	90	2,3	0,64	3,20	90	2,8	0,77	3,85	90	3,5	0,97	4,85
110	2,5	0,89	4,45	110	2,7	0,91	4,55	110	3,4	1,14	5,70	110	4,2	1,43	7,15
125	2,5	1,01	5,05	125	3,1	1,19	5,95	125	3,9	1,49	7,45	125	4,8	1,84	9,20
140	3,0	1,36	6,80	140	3,5	1,51	7,55	140	4,3	1,84	9,20	140	5,4	2,32	11,60
160	3,0	1,55	7,75	160	4,0	1,97	9,85	160	4,9	2,39	11,95	160	6,2	3,05	15,25
180	3,0	1,75	8,75	180	4,4	2,43	12,15	180	5,5	3,02	15,10	180	6,9	3,79	18,95
200	3,2	2,08	10,40	200	4,9	3,01	15,05	200	6,2	3,79	18,95	200	7,7	4,71	23,55
225	3,5	2,56	12,80	225	5,5	3,8	19,00	225	6,9	4,74	23,70	225	8,6	5,92	29,60
250	3,9	3,17	15,85	250	6,2	4,76	23,80	250	7,7	5,88	29,40	250	9,6	7,34	36,70

SDR 21 - PN 8				SDR 17 - PN 10				SDR 13,6 - PN 12,5				SDR 11 - PN 16			
Çap DN	Et Kal.(mm)	Kg/mt	TL/mt	Çap DN	Et Kal.(mm)	Kg/mt	TL/mt	Çap DN	Et Kal.(mm)	Kg/mt	TL/mt	Çap DN	Et Kal.(mm)	Kg/mt	TL/mt
50	2,4	0,36	1,80	50	3,0	0,44	2,20	50	3,7	0,54	2,70	50	4,6	0,66	3,30
63	3,0	0,57	2,85	63	3,8	0,71	3,55	63	4,7	0,86	4,30	63	5,8	1,05	5,25
75	3,6	0,81	4,05	75	4,5	1	5,00	75	5,6	1,22	6,10	75	6,8	1,46	7,30
90	4,3	1,16	5,80	90	5,4	1,44	7,20	90	6,7	1,76	8,80	90	8,2	2,11	10,55
110	5,3	1,75	8,75	110	6,6	2,15	10,75	110	8,1	2,6	13,00	110	10,0	3,15	15,75
125	6,0	2,25	11,25	125	7,4	2,74	13,70	125	9,2	3,36	16,80	125	11,4	4,08	20,40
140	6,7	2,81	14,05	140	8,3	3,44	17,20	140	10,3	4,21	21,05	140	12,7	5,09	25,45
160	7,7	3,69	18,45	160	9,5	4,5	22,50	160	11,8	5,51	27,55	160	14,6	6,69	33,45
180	8,6	4,64	23,20	180	10,7	5,71	28,55	180	13,3	6,98	34,90	180	16,4	8,45	42,25
200	9,6	5,76	28,80	200	11,9	7,05	35,25	200	14,7	8,58	42,90	200	18,2	10,42	52,10
225	10,8	7,29	36,45	225	13,4	8,93	44,65	225	16,6	10,9	54,50	225	20,5	13,21	66,05
250	11,9	8,93	44,65	250	14,8	10,97	54,85	250	18,4	13,42	67,10	250	22,7	16,25	81,25

SDR 9 - PN 20				SDR 7,4 - PN 25				SDR 6 - PN 32			
Çap DN	Et Kal.(mm)	Kg/mt	TL/mt	Çap DN	Et Kal.(mm)	Kg/mt	TL/mt	Çap DN	Et Kal.(mm)	Kg/mt	TL/mt
50	5,6	0,78	3,90	50	6,9	0,94	4,70	50	8,3	1,09	5,45
63	7,1	1,25	6,25	63	8,6	1,47	7,35	63	10,5	1,74	8,70
75	8,4	1,76	8,80	75	10,3	2,1	10,50	75	12,5	2,46	12,30
90	10,1	2,25	11,25	90	21,3	3,01	15,05	90	15,0	3,54	17,70
110	12,3	3,79	18,95	110	15,1	4,51	22,55	110	18,3	5,29	26,45
125	14,0	4,9	24,50	125	17,1	5,81	29,05	125	20,8	6,83	34,15
140	15,7	6,15	30,75	140	19,2	7,31	36,55	140	23,3	8,57	42,85
160	17,9	8,01	40,05	160	21,9	9,53	47,65	160	26,6	11,18	55,90
180	20,1	10,12	50,60	180	24,6	12,04	60,20	180	29,9	14,14	70,70
200	22,4	12,53	62,65	200	27,4	14,9	74,50	200	33,2	17,45	87,25
225	25,2	15,86	79,30	225	30,8	18,84	94,20	225	37,4	22,1	110,50
250	27,9	19,52	97,60	250	34,2	23,25	116,25	250	41,5	27,26	136,30